Network Modeling and Interference Analysis in Pervasive Technology

POLITECNICO DI TORINO

SCUOLA DI DOTTORATO

Dottorato in Ingegneria Informatica e dei Sistemi – XXIV ciclo

Tesi di Dottorato

Network Modeling and Interference Analysis in Pervasive Technology

Renato Ferrero, 160749

Tutore
Prof. M. Rebaudengo

Coordinatore del corso di dottorato
Prof. P. Laface

2012

Contents

Summary

Pervasive computing (also called ubiquitous computing) is a new paradigm for human-computer interaction. The word "pervasive" refers to the complete integration of the technology into the environment. As a result, pervasive application are transparent to the user, constantly available and completely connected. A ubiquitous communication system is a key enabler for pervasive computing, in order to share data and deliver information to anyone. Due to their flexibility, wireless networks are the natural support for pervasive applications. A wireless network consists of several electronic devices that communicate through wireless transmission, typically by means of radio waves. Each device is a node of the network. Cooperation among the nodes is the strength of a wireless network: a node relies on information exchanged with other nodes in order to perform its task. Communication occurs in a finite space: the signal broadcast by a node reaches only the nodes within a circle of radius r, called *neighborhood surface*. In a homogeneous network, each node has the same r.

A wireless homogeneous network deployed on a Euclidean plane can be modeled by a unit disk graph (UDG) [1]. Given N points in a Euclidean plane, a UDG is defined as a graph where each vertex corresponds to a point, and an edge connects two vertices if the distance between the corresponding points is below a threshold r [2]. An important aspect for investigating the behavior of a wireless network is the degree distribution of the corresponding UDG. It expresses the probability distribution of the vertex degrees over the whole graph. The *degree* of vertex v_i is the number of edges incident to v_i and is denoted as k_i. In a network, the degree of a node corresponds to the number of nodes within its neighborhood surface. The degree of a node depends on the number of nodes N, on the deployment surface S_d of area A_d and on the neighborhood surface S_n of area A_n. A_n is determined by the transmission range r: in a toroidal model, $A_n = \pi r^2$. However, in real cases, nodes are deployed on a Euclidean surface, and the toroidal model is not accurate, since it does not consider the *border effects*. In a Euclidean deployment surface, for nodes close to the brim A_n is smaller than πr^2, because S_n intersects S_d. A rectangular S_d is the most common analyzed case for evaluating border effects [3]. Although in some previous works the exact average node degree was computed,

the degree distribution was approximated, overlooking border effects and fitting it to a known discrete probability distribution (binomial or Poisson). The analysis conducted in Chapter 1 accurately describes the degree distribution of a UDG that can represent a wireless network of nodes randomly deployed on a rectangular S_d. Border effects are taken into account even for a small S_d. In order to characterize the discrete probability distribution of node degree, the probability mass function (pmf) is computed and the exact average node degree is derived. The results were presented in [4].

The UDG model is frequently used for the interference modeling in Radio Frequency IDentification (RFID) systems. RFID systems are composed by a large number of tags and at least one reader. Tags store relevant information about the items they are attached to (e.g. price, expiration date, etc.). Passive tags do not incorporate battery and feed their circuitries from the energy of the electromagnetic field emitted by the readers. Communication among readers and tags can only occur in a finite space, called the *interrogation zone*. Its range is affected by the transmission power, the on-board antennas, and the environmental conditions [5]. RFID technology is a key component in the implementation of pervasive computing: thanks to their automatic identification, physical objects can be easily mapped in an information system. RFID applications frequently consist of several readers in order to achieve complete interrogation coverage. RFID systems are subject to various interference problems. In particular, in UHF passive systems, readers can interfere together, leading to a *reader-to-reader* collision. It occurs when a reader is listening to the tag's reply, but receives a stronger field from one or more neighboring readers operating at the same frequency. Consequently, the reader can not successfully decode the tag's reply. The maximum distance at which the signal of a reader can disturb the communication of another reader is called *interference range*.

The UDG model is the most common reader-to-reader interference model. Its basic assumption is that all the reader-to-reader collisions are generated by the direct interference between two readers. The additive effect of the interferences produced by more than one reader is ignored. On the other hand, more realistic models [6, 7] consider the propagation loss and the sum of the interferences produced by all the readers. Chapter 2 evaluates the effectiveness of the UDG model for the study of reader-to-reader interference. The study will be presented in [8].

Chapter 3 describes the state-of-the-art solutions for the reader-to-reader collision problem. The European standard ETSI EN 302 208 [9] specifies a protocol, called Listen Before Talk (LBT), based on the Code Division Multiple Access (CSMA) scheme. However, its high collision probability and the delay embedded in CSMA handshake have been sensibly reduced by subsequent proposed protocols, like Distributed Color Selection (DCS) and Colorwave [10, 11], that exploit the Time Division Multiple Access (TDMA) scheme to better organize the communication. The transmissions are composed of rounds divided in timeslots called *colors*. In DCS,

after every collision, a reader randomly changes timeslot. DCS provides good performance without noteworthy additional requirements. Colorwave is more adaptable to the network configuration: each reader can vary the length of its round according to the quantity of collisions. DCS achieves a very good *fairness*, whereas Colorwave provides a higher *throughput*. Other protocols try to reach better performance using an additional control channel. However, they require additional resources. Among them, the highest throughput is attained by Neighbor Friendly Reader Anticollision (NFRA) [12]. In NFRA, the communication is synchronized by a polling server. The server determines the beginning of the rounds and the timeslots. Every reader randomly selects a timeslot, during which it exchanges control signals to determine if the channel is free.

According to the performance criterion that is improved and to the network requirements, different solutions for the reader-to-reader collisions are proposed in Chapters 4 and 5. Chapter 4 focuses on proposals that exploits only one or more data channels. The first suggested protocol is an enhancement of DCS, called Probabilistic Distributed Color Selection (PDCS). In DCS, after a collision, both the involved readers choose a new color. In case of an identical selection, a new collision between them will occur in the next round. In PDCS, each colliding reader may possibly change color, according to a defined probability. In this way, if only one of them change color, they certainly avoid a further collision. Experimental results show that the number of reader-to-reader collisions after a slot change decreases by over 30%. The probabilistic approach in the collision resolution was presented in [13] and a full version of the protocol was described in [14].

A second solution focuses on maximizing throughput in reader-to-reader anticollision protocols for low cost RFID readers. Two contributions are provided. Firstly, a new configuration for Colorwave, called the Killer configuration, is proposed. The Killer configuration generates a selfish behavior similar to the natural selection, where each node tries to obtain as much resources as possible. Secondly, a new protocol, called Distributed color natural selection (DCNS), is specifically designed to fully exploit the Killer configuration. DCNS uses the slot reservation system adopted by DCS and Colorwave, modifying the collision resolution subroutine, according to the priority parameter. A further novelty of the protocol is the dynamic priority management, which allows high priority readers to reach good performance even in densely deployed areas. Like Colorwave, the proposed protocol employs a routine for automatic parameter updating, but with a lower control overhead. DCNS is suitable both for single-channel and multi-channel data bands and it does not require any control channel. Since the proposed strategy is based on selfish behavior, it provides high throughput but it is not fair. The proposed solution is especially suitable to systems where readers with different priority levels operate in the same area. Experimental simulations have been performed in order to evaluate DCNS

and to observe the effects of the dynamic priority management. Moreover, the proposed protocol has been compared to state-of-the-art reader-to-reader anti-collision protocols. DCNS provides an outstanding throughput rise, representing not only the best cost-effective reader-to-reader anti-collision protocol, but also proving more efficient than high-cost protocols. This work was presented in [15].

The third approach evaluates the effects of the introduction of a probability parameter in the collision resolution of Colorwave. According to this proposal, denoted as Probabilistic Colorwave (PCW), the readers involved in a collision change color depending on a probability. PCW is tested with two different configurations: the first one is the same as proposed in [10, 11]; the second one is the Killer configuration. PCW can outperform Colorwave either in throughput or in fairness or in both of them: its performance varies according to the adopted configuration and to the deployment density of the network.

Chapter 5 presents two reader-to-reader anticollision protocols that exploits a control channel. As far as throughput is concerned, NFRA attains the best performance among the state-of-the-art protocols that require a control channel. It provides an efficient management of the readers within the interference range (*neighbors*). However, readers with few neighbors have a lower probability of colliding, so the throughput of the readers highly differ. Two approaches are proposed to increase the fairness of the protocol without penalizing the throughput. The first one, denoted as NFRA+, introduces the concept of dynamic priority. The readers are ordered according to the elapsed time from their request of transmission, and a higher probability of transmitting is reserved to readers with longer waiting time. Ideally, the throughput becomes independent from the size of the neighborhood. The experimental analysis shows that the introduction of the dynamic priority provides a very good fairness, but with a negative effect on the throughput. A second approach is proposed in order to compensate this reduction. The detection of reader-to-reader interference is improved by means of a second control signal, with a resulting throughput improvement. A preliminary version of the protocol was presented in [16] and the fully description was provided in [17].

The high network requirements of NFRA are reduced by another proposal, called Geometric Distribution Reader Anticollision (GDRA). GDRA improves the performance of NFRA by means of specific modifications in the contention algorithm. Moreover, it tunes some configuration parameters in order to fulfill the requirements of the European regulation [9] and the global standard [18]. The throughput improvement is provided by the use of the *Sift* geometric probability distribution function[19] in the contention procedure, instead of the uniform distribution function. The *Sift* distribution minimizes the collision probability among contending readers, as confirmed by the simulation results. Finally, the approach is well suited to make use of the classical centralized infrastructure of the DRE, which commonly

relies on a centralized server to store and process the upper-layer identification information. Therefore, the model suggests an implementation of the algorithm as a new process integrated in this existing central element, and thus eliminating the need of extra control channels or specific additional hardware to coordinate the readers.

Chapter 1

Wireless network modeling

Pervasive computing aims to create environments where the technology is invisibly integrated into. This vision is realized by means of wireless networks, i.e. cheap and small pervasively distributed devices which communicate wireless. Nowadays, these technologies are widely employed for several applications, such as accurate area monitoring and distributed information systems, where the information is directly matched to the items. Sections 1.1 and 1.2 introduces the basic concepts about pervasive computing and wireless networks.

The strength of a wireless network is the cooperation among nodes: in order to perform its task, a node relies on the information exchanged with other nodes. The nodes and the links of a wireless networks are easily modeled by a family of graphs called unit disk graph (UDG). The degree distribution of a unit disk graph is an important aspect for investigating the behavior of a wireless network. The formal definition of unit disk graph is provided in Section 1.3. The concept of the degree distribution is presented in Section 1.4. In the literature, several studies was focused on the degree distribution of unit disk graphs, but they lacked in precision. The main results achieved are reviewed in Section 1.5. In Section 1.6 the geometric model is presented. Section 1.7 describes the degree distribution and studies it with the inclusion of border effects. The achieved results are validated through simulations and compared to the state-of-the-art approaches in Section 1.8.

1.1 Pervasive computing

Pervasive computing (also called ubiquitous computing) refers to a new, advanced paradigm for human-computer interaction. The traditional planning and design of the interaction between people and computers relies on the desktop environment. It consists on a graphical user interface (GUI), provided with icons, windows, toolbars and other desktop widgets, in order to help the user in accessing, configuring and

utilizing the computer features. The desktop model requires an active and skilled involvement of the user. This kind of interaction is *explicit* and can easily distract and overwhelm users. On the contrary, the user of pervasive technology may exploit many computational devices at the same time, without necessarily being aware that these machines are working. The human-computer interaction becomes *implicit* and more complex tasks can be achieved, since the variety of devices increases and they interoperate automatically.

The words pervasive and ubiquitous mean "existing everywhere". As a matter of fact, the main features of pervasive computing devices are their complete connection and their constant availability. This approach aims for embedding microprocessors in everyday objects and activities, in order to process and share information. The integration into environments shows another core property of pervasive computing: the transparency. The access of the devices is hidden and they do not intrude into the workplace environment.

Context awareness is another important property of pervasive computing. The context knowledge refers not only to the user location, but also to its identity, activity and to the time. Pervasive computing devices can sense the environment and react based on it. The phases followed during the information processing are the acquisition of the context, its abstraction and understanding, and the execution of the rule based on the recognized context.

Pervasive computing is also described as ambient intelligence, Everyware (a pun with the word "everywhere" and the ending "ware", which is used in this context for the terms "software" and "hardware"), Internet of Things, haptic computing, things that think.

A ubiquitous communication system is a key enabler for pervasive computing. It is the task of the communication network to deliver any content to anyone, anywhere and anytime. In this sense, wired networks show hard limits for several reasons: the physical media depends strongly on the content, the access points are fixed and only static applications can be implemented. Instead, wireless networks support pervasive applications in a more natural way. They provide access everywhere and are available also to mobile users. Furthermore, the trend is toward the convergence of different networks content, such as VoIP and IPTV.

1.2 Wireless networks

A wireless network consists of several electronic devices that communicate through wireless transmission. On the contrary, the traditional systems based on cable connection are called wired. Generally a wireless communication exploits radio waves, although less frequent systems adopt infrared or laser transmission.

The main advantage of wireless networks is the minimization of the cable connection, with a drastic reduction of the installation cost. Moreover, they offer a greater mobility, without forcing people to use a device near a network socket. The user devices, such as laptops, mobile phones and Personal Digital Assistant, are usually linked to an *access point* via Wi-Fi, Bluetooth or other standards. The access point is then connected to a wired network (directly, through a *router*, or indirectly, via other access points). In this way, data can be transmitted between the wireless user devices and the wired ones. If this centralized infrastructure lacks, the wireless network is called *ad-hoc*. A wireless ad-hoc network is characterized by a decentralized architecture, in which all the devices have equal status and are called *node*. The nodes are actively responsible for the data routing: each node can forward data for the nodes it is linked to. The great advantage of ad-hoc network is the flexibility: the routing path is dynamically determined, according to the actual network connectivity, and the network is highly scalable. This technology is exploited in a large number of applications, ranging from military purposes to vehicular information services and from healthcare to emergency management [20, 21]. According to their application, wireless ad hoc networks can be classified into mobile ad-hoc networks (MANET), wireless sensor networks (WSN) and wireless mesh networks (WMN).

A MANET is an autonomous system of mobile devices, which are connect together through wireless ad-hoc links. The physical topology of a MANET varies dynamically: due to the mobility of the nodes, the links among them change frequently. If two nodes that wish to communicate are not located within a direct wireless range, they use multi-hop communication. Consequently, each node operates not only as a host but also as a router in order to forward data for other nodes. The nodes are often constrained by resources, such as low power, limited energy, bandwidth, CPU and memory capacity. MANETs are exploited in military area, vehicular communication, home automation.

A WSN consist of spatially distributed sensors to monitor physical or environmental conditions, such as temperature, humidity, pressure, vibration, sound and vital body functions. Each node is equipped with a radio transceiver, in order to cooperatively pass the acquired data through the network to a main location. WSNs have gained great importance because of sensor nodes characteristics such as low cost, low power, small size and unbounded communications. Important applications of WSNs are related to civil protection, environmental and agricultural monitoring, and medical supervision.

In a WMN, nodes are organized in a mesh topology. This kind of infrastructure is low cost, very adaptable and resistant, because each node is required to transmit data only to the next one. Moreover, the network is very reliable and fault tolerant: in the eventuality of a node fault, the neighboring nodes autonomously looks for other paths in order to maintain the mesh connectivity. With respect to MANET and WSN, usually a WMS is not limited in terms of resources and can be exploited

in military or civil fields when more resource intensive functions are required.

1.3 Unit Disk Graph (UDG)

Several definitions are applicable for a unit disk graph G_u [2]:

1. given N circles with radius $\frac{r}{2}$ in a Euclidean plane, their intersection is a unit disk graph. Each node of G_u corresponds to a circle, and two nodes are connected if their corresponding circles intersect.

2. given N circles with radius r in a Euclidean plane, a unit disk graph is a graph with N nodes corresponding to the N circles, and with an edge between two nodes if one of the corresponding circles contains the center of the other circle.

3. given N points in a Euclidean plane, a unit disk graph is a graph with N nodes corresponding to the N points, and with an edge between two nodes if the distance between the two corresponding points is below a threshold r.

The definitions are equivalent to each other up to a scale factor. Fig 1.1 shows a unit disk graph according to the second definition.

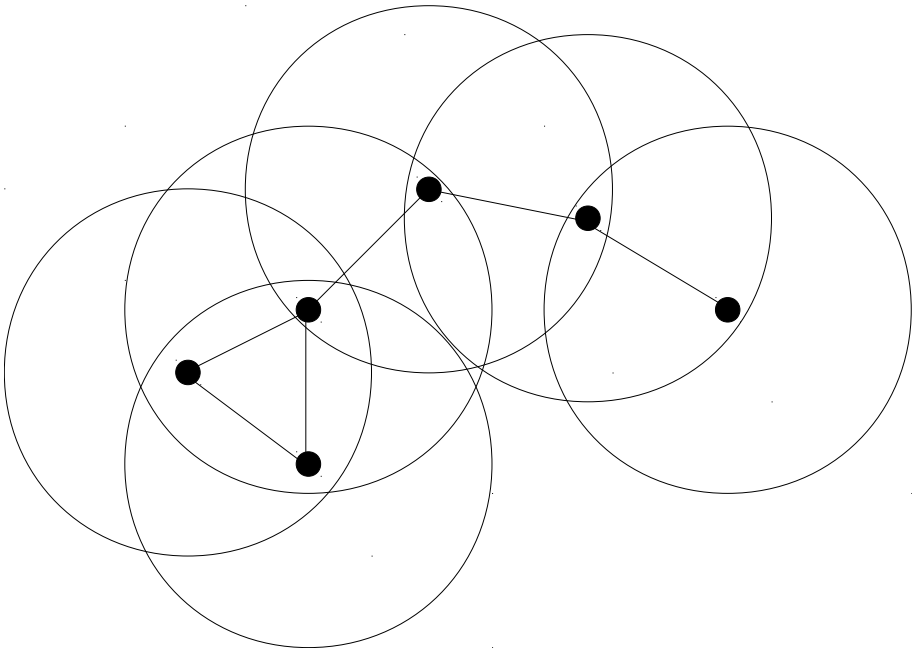

Figure 1.1. A unit disk graph

In a wireless network, the signal broadcast by a node reaches only the nodes within a circle of radius r, called *neighborhood surface*. In a homogeneous network,

each node has the same r. Therefore, unit disk graphs can model wireless homogeneous networks deployed on a Euclidean plane [1]. The geometric model of UDG is consistent with several theoretical results for wireless homogeneous networks, regarding topology control [22, 23, 24], transmission scheduling [25, 26, 27], network deployment [28], clustering [29], sensor localization [30] and routing [31, 32].

1.4 Degree distribution

In a graph, the *degree* of vertex v_i is the number of edges incident to v_i and is denoted as k_i. Since unit disk graphs are a simple model for wireless networks, the concept of the degree can be easily extended to a wireless network. In a network, the degree of a node corresponds to the number of nodes within its neighborhood surface.

The degree distribution of a graph expresses the probability distribution of the vertex degrees over the whole graph. The degree distribution of a UDG is a key feature for the study of the behavior of the corresponding wireless network. Indeed, the node degree affects the performance of the network in several ways:

- energy saving. The energy source of a node is often a battery cell. In order to prolong its lifetime, the node can be switched off, provided that the properties of the network (i.e., connectivity and coverage) are kept up by its neighbors. A high quantity of neighbors extends the idle time of the node.

- fault tolerance. The behavior of a wireless network does not suffer from the failure of a node if there are neighbors replacing it. The size of the neighborhood is an indicator of the level of fault tolerance of the network.

- interference reduction. In some types of networks, such as RFID, concomitant transmission of the nodes can disturb each other. A communication protocol is adopted in order to regulate interference among signals. In such a situation, a node with many neighbors usually has fewer opportunities to transmit.

- network security. Many networks exploit symmetric encryption, in order to protect privacy and to authenticate messages. The degree distribution strongly affects several characteristics of the security system (e.g., the number of keys to store [keyNumber]).

The degree of a node depends on the number of nodes N, on the deployment surface S_d of area A_d and on the neighborhood surface S_n of area A_n. A_n is determined by the transmission range r: in a toroidal model, $A_n = \pi r^2$. However, in real cases, nodes are deployed on a Euclidean surface, and the toroidal model

is not accurate, since it does not consider the *border effects*. In a Euclidean deployment surface, for nodes close to the brim A_n is smaller than πr^2, because S_n intersects S_d. A rectangular S_d is the most common analyzed case for evaluating border effects [3, 14]. The exact average node degree was computed in some previous works, which are described in Section 1.5, although the degree distribution was approximated, overlooking border effects and fitting it to a known discrete probability distribution (binomial or Poisson). On the contrary, Section 1.7 accurately describes the degree distribution of a UDG that can represent a wireless network of nodes randomly deployed on a rectangular S_d, according to the geometric model presented in Section 1.6. Border effects are taken into account even for a small S_d. In order to characterize the discrete probability distribution of node degree, the probability mass function (pmf) is computed and the exact average node degree is derived.

1.5 Related work on degree distribution of UDG

A uniform disk graph G_u models a network of N nodes uniformly randomly placed on a deployment surface S_d. The probability p_i that vertex v_i is connected to vertex v_j in G_u corresponds to the probability that, in the network, node v_j is inside the neighborhood surface of v_i. p_i can be regarded as the probability of success in a Bernoulli trial. Since each node has the same probability p_i of being a neighbor of v_i, the estimation of the number of neighbors that v_i has among a group of $N-1$ independent nodes consists in $N-1$ independent repetitions of the Bernoulli trial. Therefore, the probability that v_i has n_0 neighbors is given by:

$$P(k_i = n_0) = \binom{N-1}{n_0} p_i^{n_0} (1-p_i)^{N-1-n_0} \tag{1.1}$$

The function $P(k_i = n_0)$ for $n_0 = 0, 1, ..., N-1$ is the pmf of the degree of v_i and corresponds to a binomial distribution. The pmf of the degree of a generic node in G_u requires the evaluation of p_i, $\forall v_i \in G_u$. Several studies have been conducted to evaluate p_i and to give an expression of pmf [33, 34, 35]. Another characteristic of the degree distribution which has been analyzed is the average node degree [36, 37], defined as $\mu = \frac{1}{N}\sum_{i=1}^{N} k_i$. Table 1.1 summarizes previous related works.

In [33], random node placement is regarded as a finite homogeneous Poisson point process, with constant density $\rho = \frac{N}{A_d}$. Since the neighbors of node v_i are located within a circle of an area of πr^2, the average node degree is calculated as:

$$\mu = \frac{N\pi r^2}{A_d} \tag{1.2}$$

Table 1.1. Comparison of related works on degree distribution.

reference	μ	pmf	pmf type	border effects	assumptions
[33]	yes	yes	Poisson	no	$N > 1500\frac{A_d}{A_n}$, $A_d > 12.5A_n$
[34]	yes	yes	binomial	partial	$\mu \lesssim 18$
[35]	yes	yes	binomial	partial	low density, $r \leq \min(l, w)$
[36]	yes	no	—	yes	$r \leq \min(l, w)$
[37]	yes	no	—	yes	$r \leq \frac{1}{2}$, $l = w = 1$
this work	*yes*	*yes*	*integral of binomial*	*yes*	$r \leq \frac{1}{2}\min(l, w)$

By approximating (1.1) with a Poisson distribution, the pmf is calculated as:

$$P(k = n_0) = \frac{\left(\frac{N\pi r^2}{A_d}\right)^{n_0}}{n_0!} \cdot e^{-\frac{N\pi r^2}{A_d}} \tag{1.3}$$

Approximation of random node placement with a finite homogeneous Poisson point process requires $N > 1500\frac{A_d}{A_n}$ and $A_d > 12.5A_n$. Moreover, the use of Poisson distribution in (1.3) in order to approximate the binomial distribution in (1.1) is acceptable only if N is large and p is small. Finally, (1.2) is precise only in a toroidal model or with an infinite S_d. In these cases, the neighbors are located around the node, within a circle of an area of πr^2. By contrast, a real network is deployed on a finite surface and it is characterized by border effects: the nodes near the brim have neighbors only toward the middle of S_d. Thus, A_n is smaller than πr^2. Without taking into account border effects, the theoretical results in [33] differ from the experimental data. In order to compare them, only the nodes farther than r from the brim are considered for the statistics of the simulations, or, as an alternative, a toroidal distance metric is used.

The degree distribution is investigated through simulations in [34]. A rectangular S_d is dissected into m small squares of size ΔA_d. Each square is small enough to contain one node at the most: the suggested size is $\Delta A_d = \frac{r^2}{100}$. The authors conclude that, if border effects are negligible, the pmf of the node degree is approximated by a binomial distribution, with the following mean value:

$$\mu = \frac{2(N-1)}{m(m-1)} \sum_{i=1}^{m} \sum_{j=i+1}^{m} p(r_{ij}) \tag{1.4}$$

where $p(r_{ij})$ is the probability of having a link between two nodes v_i and v_j at distance r_{ij} from each other. However, the evaluation of (1.4) is $\Theta(m^2)$, while the expressions for μ provided in the other related works are faster to compute, being $\Theta(1)$. Furthermore, the probability of having a neighbor varies among nodes and is

lower for nodes close to the brim. The approximation of degree distribution with a binomial distribution is accurate only if border effects are negligible, as pointed out in [34]. The two conditions for limited border effects are $A_d \gg A_n$ and a low node density. Their combined effect is reflected in the average node degree: the threshold suggested in [34] for negligible border effects is $\mu \lesssim 18$.

A similar approach is followed in [35]. The main contribution of [35] is the closed-form expression of the binomial distribution that approximates the degree distribution, with the following mean value:

$$\mu = \frac{N-1}{l^2 w^2}\left(\frac{1}{2}r^4 - \frac{4}{3}lr^3 - \frac{4}{3}wr^3 + \pi r^2 lw\right) \tag{1.5}$$

where l and w are the length and the width of the rectangular deployment surface respectively. However, as noted in [34], the experiments conducted in [35] confirm that the binomial distribution is an accurate approximation only if the node density is small, thus reducing border effects.

Formula (1.5) is independently proved also in [36]. The analysis in [36] considers border effects and computes the probability that two arbitrary nodes are within the neighborhood surface of each other. Formula (1.5) is derived as a corollary. In section 1.7, (1.5) is obtained by the proposed analysis and a more accurate pmf that characterizes the degree distribution is provided.

A result similar to (1.5), although in a more specific context, is presented in [37]. In a unit Euclidean square ($l = 1$, $w = 1$), with $r \leq \frac{1}{2}\min(l, w)$, μ is estimated as:

$$\mu = (N-1)\left(\left(\frac{11}{3} - \pi\right)r^4 - \frac{8}{3}r^3 + \pi r^2\right) \tag{1.6}$$

1.6 Intersection between neighborhood and deployment surfaces

Let a rectangular deployment surface S_d and a circular neighborhood surface S_n be in a Cartesian coordinate plane. Let S_d be in the I quadrant, with one vertex in the origin of the axes and the others in a clockwise direction (as shown in Fig. 1.2). Let S_d have length l, width w and area $A_d = lw$. Let S_n have radius r, area $A_n = \pi r^2$ and center (x_c, y_c) such that $w \geq 2r, l \geq 2r, 0 \leq x_c \leq l$ and $0 \leq y_c \leq w$. The area A_I of the intersection $S_n \cap S_d$ depends on the position of (x_c, y_c), as $A_I = f_{A_I}(x_c, y_c, r, w, l)$.

S_d can be divided into 4 types of sub-surface, as shown in Fig. 1.2:

- a rectangular sub-surface S_{dA} $\{(r, r), (r, w-r), (l-r, w-r), (l-r, r)\}$, with length $l - 2r$, width $w - 2r$ and area $A_{dA} = lw - 2rw - 2rl + 4r^2$.

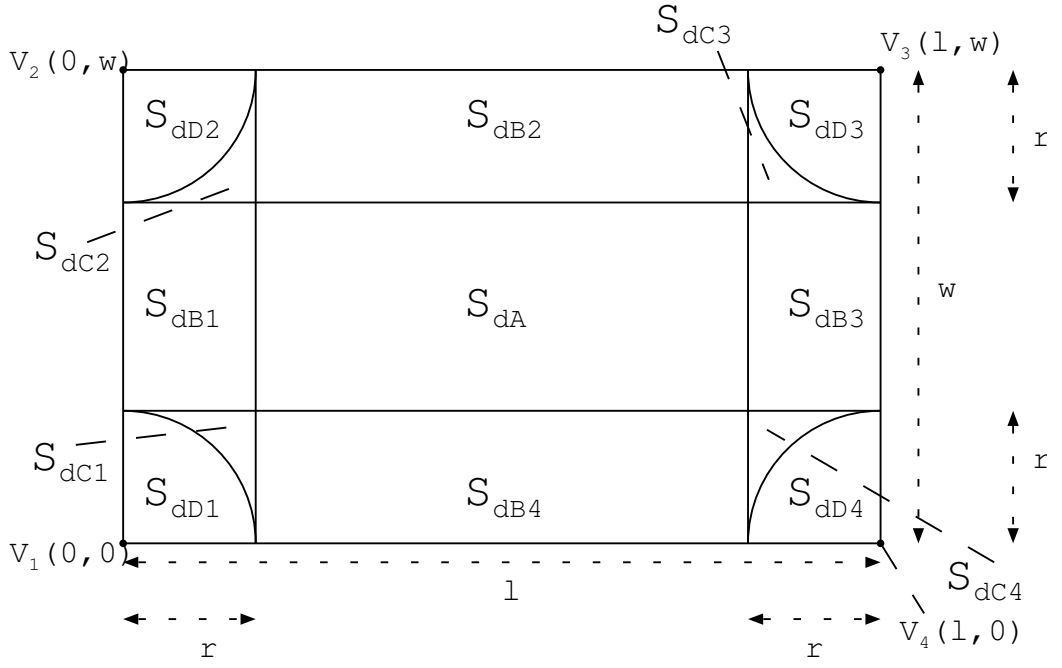

Figure 1.2. Deployment sub-surfaces

- a sub-surface S_{dB} composed by the union of 4 rectangular sub-surfaces, with total area $A_{dB} = 2rl + 2rw - 8r^2$.

- a sub-surface S_{dC} composed by the union of 4 sub-surfaces equal to the relative complement of a circle of radius r in a square of length r; the center of the circle is a vertex of the square. The total area of S_{dC} is $A_{dC} = (4 - \pi)r^2$.

- a sub-surface S_{dD} composed by the union of 4 circular sectors, with radius r, angle $\pi/2$, and total area $A_{dD} = \pi r^2$.

Given a point (x, y), let $f_d(x, y)$ be the function that calculates the distance d between the point and the nearest border of S_d, $f_{d1}(x)$ the function that calculates the distance d_1 between the point and the nearest vertical border of S_d, $f_{d2}(y)$ the function that calculates the distance d_2 between the point and the nearest horizontal border of S_d.

$$d = f_d(x, y) = \min(x, y, l - x, w - y) \tag{1.7}$$

$$d_1 = f_{d1}(x) = \min(x, l - x) \tag{1.8}$$

$$d_2 = f_{d2}(y) = \min(y, w - y) \tag{1.9}$$

Therefore, the area A_I of the intersection $S_n \cap S_d$ is:

$$f_{A_I}(x,y,r,l,w) = \begin{cases} \pi r^2 & \text{for } (x,y) \in S_{dA} \\ f_{A_{I1}}(d,r) & \text{for } (x,y) \in S_{dB} \\ f_{A_{I2}}(d_1,d_2,r) & \text{for } (x,y) \in S_{dC} \\ f_{A_{I3}}(d_1,d_2,r) & \text{for } (x,y) \in S_{dD} \end{cases}$$

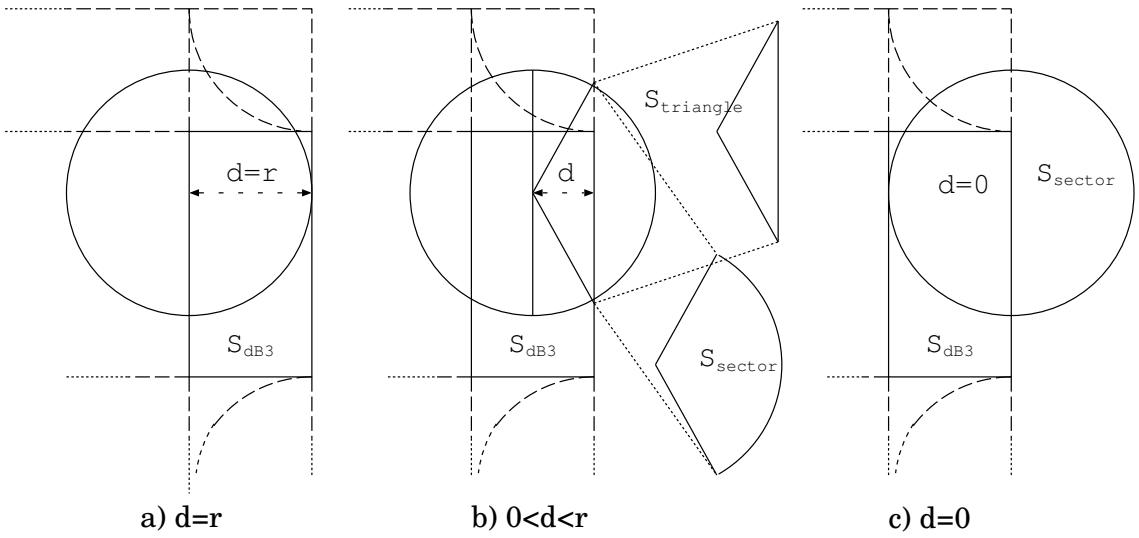

Figure 1.3. $A_n \cap A_d$ if $(x_c, y_c) \in S_{dB}$

If $(x_c, y_c) \in S_{dA}$, then $r \leq d$, so $S_n \subset S_d$ and $S_n \cap S_d = S_n$.

If $(x_c, y_c) \in S_{dB}$, then $d < r \leq \max(d_1, d_2)$, so a section of S_n, $\frac{\pi r^2}{2}$ at the most, does not overlap S_d, as shown in Fig. 1.3. $A_I = f_{A_{I1}}(d,r)$ is the area of $S_n \setminus (S_{sector} \setminus S_{triangle})$:

$$f_{A_{I1}}(d,r) = \pi r^2 - \frac{2\arccos\left(\frac{d}{r}\right)\pi r^2}{2\pi} + \sin\left(\arccos\left(\frac{d}{r}\right)\right) d \cdot r \tag{1.10}$$

If $(x_c, y_c) \in S_{dC}$, then $\max(d_1, d_2) < r \leq \sqrt{d_1^2 + d_2^2}$, so two separated sections of S_n do not overlap to S_d, as shown in Fig. 1.4, and $A_I = f_{A_{I2}}(d_1, d_2, r)$ is the area of $S_n \setminus (S_{sector1} \setminus S_{triangle1}) \setminus (S_{sector2} \setminus S_{triangle2})$:

$$f_{A_{I2}}(d_1,d_2,r) = \pi r^2 - \frac{2\arccos\left(\frac{d_1}{r}\right)\pi r^2}{2\pi} + \sin\left(\arccos\left(\frac{d_1}{r}\right)\right) d_1 \cdot r - \tag{1.11}$$
$$+ \frac{2\arccos\left(\frac{d_2}{r}\right)\pi r^2}{2\pi} + \sin\left(\arccos\left(\frac{d_2}{r}\right)\right) d_2 \cdot r$$

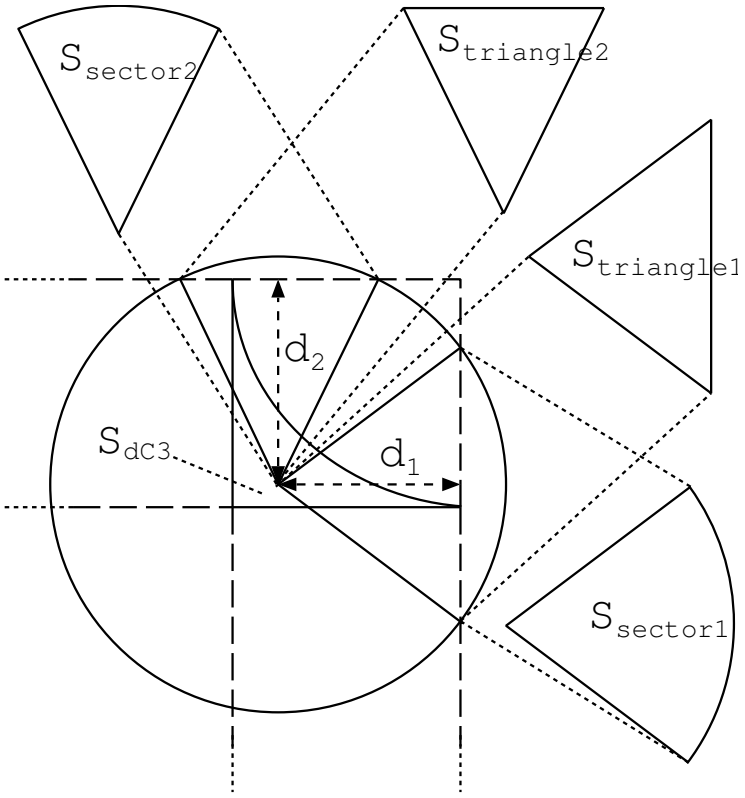

Figure 1.4. $A_n \cap A_d$ if $(x_c, y_c) \in S_{dC}$

If $(x_c, y_c) \in S_{dD}$, $r > \sqrt{d_1^2 + d_2^2}$, so S_n overlaps to a vertex of S_d, as shown in Fig. 1.5. $A_I = f_{A_{I3}}(d_1, d_2, r)$ is the area of $S_n \setminus (S_{1/2sector1} \setminus S_{1/2triangle1}) \setminus (S_{1/2sector2} \setminus S_{1/2triangle2}) \setminus (S_{\pi/2sector} \setminus S_{rectangle})$:

$$f_{A_{I3}}(d_1, d_2, r) = \pi r^2 - \frac{\arccos\left(\frac{d_1}{r}\right)\pi r^2}{2\pi} + \frac{1}{2}\sin\left(\arccos\left(\frac{d_1}{r}\right)\right) d_1 \cdot r - \tag{1.12}$$
$$+ \frac{\arccos\left(\frac{d_2}{r}\right)\pi r^2}{2\pi} + \frac{1}{2}\sin\left(\arccos\left(\frac{d_2}{r}\right)\right) d_2 \cdot r - \frac{\pi r^2}{4} + d_1 \cdot d_2$$

1.7 Proposed degree distribution

Let S_d and S_n be two surfaces as described in Section 1.6. Let N homogeneous nodes be uniformly randomly deployed on the deployment surface S_d. Let G be the UDG formed from the collection of the nodes, with threshold r. Degree distribution is the discrete probability distribution of the degrees over the graph. Given a node with neighborhood surface S_n, the event that another node is within S_n can be

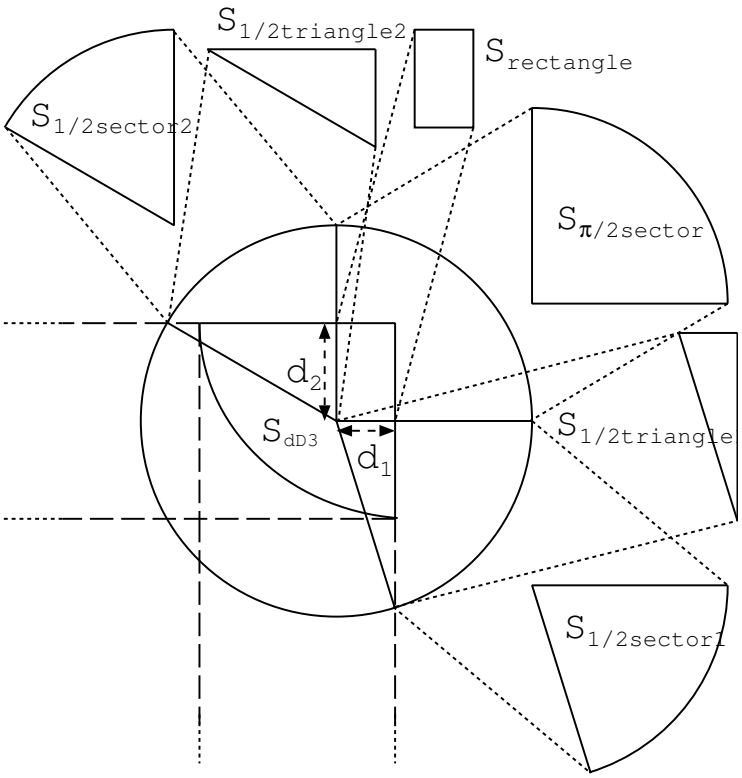

Figure 1.5. $A_n \cap A_d$ if $(x_c, y_c) \in S_{dD}$

considered as a Bernoulli trial, with success probability $\frac{f_{A_I}(x,y,r,l,w)}{A_d}$. Since each position of a node in S_d is equiprobable, the probability of being within S_n is equal to the ratio between $S_n \cap S_d$ and S_d. Therefore degree distribution is similar to binomial distribution.

1.7.1 Probability mass function

$k \sim D(N, r, w, l)$ denotes that the random discrete variable k follows the degree distribution with parameters N, r, w and l. In a network with N homogeneous nodes with neighborhood surface S_n, randomly deployed on a rectangular surface

S_d, the probability that a node has degree k is given by the pmf:

$$
\begin{aligned}
&P(k=n_0)=f(k;N,r,w,l)= \qquad (1.13)\\
&=\binom{N-1}{k}\frac{1}{A_d}\cdot\int_0^w\int_0^l\left(\frac{f_{A_I}(x,y,r,l,w)}{A_d}\right)^k\left(1-\frac{f_{A_I}(x,y,r,l,w)}{A_d}\right)^{N-k-1}\mathrm{d}y\,\mathrm{d}x=\\
&=\binom{N-1}{k}\frac{1}{A_d}\cdot\left(S_{dA}\left(\frac{\pi r^2}{A_d}\right)^k\left(1-\frac{\pi r^2}{A_d}\right)^{N-k-1}+\right.\\
&+\frac{S_{dB}}{r}\int_0^r\left(\frac{f_{A_{I1}}(d,r)}{A_d}\right)^k\left(1-\frac{f_{A_{I1}}(d,r)}{A_d}\right)^{N-k-1}\mathrm{d}d+\\
&\quad+4\int_0^r\int_{\sqrt{r^2-d_1^2}}^r\left(\frac{f_{A_{I2}}(d_1,d_2,r)}{A_d}\right)^k\cdot\left(1-\frac{f_{A_{I2}}(d_1,d_2,r)}{A_d}\right)^{N-k-1}\mathrm{d}d_2\,\mathrm{d}d_1+\\
&\quad\left.+4\int_0^r\int_0^{\sqrt{r^2-d_1^2}}\left(\frac{f_{A_{I3}}(d_1,d_2,r)}{A_d}\right)^k\cdot\left(1-\frac{f_{A_{I3}}(d_1,d_2,r)}{A_d}\right)^{N-k-1}\mathrm{d}d_2\,\mathrm{d}d_1\right)
\end{aligned}
$$

If S_d were toroidal, the pmf would correspond to the pmf of the binomial distribution with $p=\frac{A_n}{A_d}$. However, in a Euclidean surface the center of S_n can be close to the border of S_d, so $S_n\cap S_d\neq S_n$. Therefore, the pmf of the degree distribution corresponds to the integral of the pmf of the binomial distribution with a probability of success $\frac{f_{A_I}(x,y,r,l,w)}{A_d}$, where the coordinates of the center are the variables of integration, and S_d is the integration domain. The result of the integral is divided by the integration area. The integral is broken down in 4 parts, matched to the 4 types of deployment sub-surface. For S_{dA}, the symbolic integral is directly solved. For S_{dB}, the double integral is reduced to a single integral where the distance from the nearest border (d) is the variable of integration, and r is the integration domain. For S_{dC} and S_{dD}, the new variables of integration are the distances from the 2 nearest borders (d_1, d_2).

1.7.2 Mean

If $k\sim D(N,r,w,l)$, then the expected value of k is:

$$\mu=\sum_{k=0}^{N-1}\left(k\cdot f(k;N,r,w,l)\right)=\left(\pi wl-\frac{4}{3}r(w+l)+\frac{r^2}{2}\right)\left(\frac{r}{wl}\right)^2(N-1) \qquad (1.14)$$

Proof:

$$\mu=\mathrm{E}(k)=\sum_{k=0}^{N-1}\left(k\cdot f(k;N,r,w,l)\right).$$

According to the definition of the pmf:

$$\mu = \sum_{k=0}^{N-1} \left(k \cdot \frac{1}{A_d} \int_0^w \int_0^l \left(\frac{f_{A_I}(x,y,r,l,w)}{A_d} \right)^k \cdot \left(1 - \frac{f_{A_I}(x,y,r,l,w)}{A_d} \right)^{N-k-1} \right).$$

According to the linearity property, the integral of a linear combination is the linear combination of the integrals, so:

$$\mu = \frac{1}{A_d} \int_0^w \int_0^l \sum_{k=0}^{N-1} k \left(\frac{f_{A_I}(x,y,r,l,w)}{A_d} \right)^k \cdot \left(1 - \frac{f_{A_I}(x,y,r,l,w)}{A_d} \right)^{N-k-1} \mathrm{d}y\,\mathrm{d}x.$$

Therefore the function that must be integrated corresponds to the mean of the binomial distribution with a probability of success $\frac{f_{A_I}(x,y,r,l,w)}{A_d}$, so:

$$\mu = \frac{1}{A_d} \int_0^w \int_0^l (N-1) \frac{f_{A_I}(x,y,r,l,w)}{A_d} \mathrm{d}y\,\mathrm{d}x.$$

Then solving the integral:

$$\mu = \left(\frac{S_{dA} \cdot \pi + S_{dB}(\pi - \frac{2}{3}) + S_{dC} \frac{-3\pi 2 + 24\pi - 32}{24(4-\pi)} + \frac{S_{dD}(\frac{1}{6\pi} + \frac{\pi}{8})}{A_d} \right) \frac{r^2}{A_d} (N-1).$$

Finally simplifying:

$$\mu = \left(\pi w \cdot l - \frac{4}{3} r(w+l) + \frac{1}{2} r^2 \right) \left(\frac{r}{w \cdot l} \right)^2 (N-1)$$

□

1.8 Validation of the proposed results and comparison

The parameters that affect the degree distribution are N, r, w and l. In order to validate the proposed distribution, various simulations were performed and compared with the theoretical results. All the simulations were executed $5 \cdot 10^7$ times. The ratio between the area of the sub-surfaces close to the border (A_{dB}, A_{dC} and A_{dD}) and A_d affects the results of the state-of-the-art approaches, because they approximate border effects. For this reason, 100 nodes with $r = 1$ were deployed on squares of different size, with $2 \leq l = w \leq 2^{10}$.

1.8.1 Probability mass function

The proposed pmf does not present approximations, so it can provide the correct statistical result. However, the integrals required by (1.13) were numerically approximated, introducing a small error in the results.

Fig. 1.6 shows the pmf of the proposed distribution, compared to the simulation results and the pmf proposed in [33, 34, 35]. These results were obtained with $w = l = 4r$. Therefore, $S_{dA} = 4r^2, S_{dB} = 4r^2, S_{dC} = \pi r^2$ and $S_{dD} = (4 - \pi)r^2$. Therefore, $\frac{3}{4}A_d$ corresponds to the area of the borders. It is easy to observe that (1.13) is close to the simulation curve. The pmf proposed in [33] is very different, since it does not consider border effects, treating all the sub-surfaces as S_{dA}, and generating a higher mean. The pmf proposed in [34] corresponds to a binomial distribution with the approximated mean previously described. S_d is treated as a unique sub-surface with constant intersection $S_n \cap S_d$. The mean of the curve is slightly lower than the simulation, and its shape is clearly different. The pmf proposed in [35] corresponds to a binomial distribution where μ is equal to (1.14). Also this approach treats S_d as composed by a unique sub-surface with constant $S_n \cap S_d$. Its mean is close to the simulation, but with a different shape.

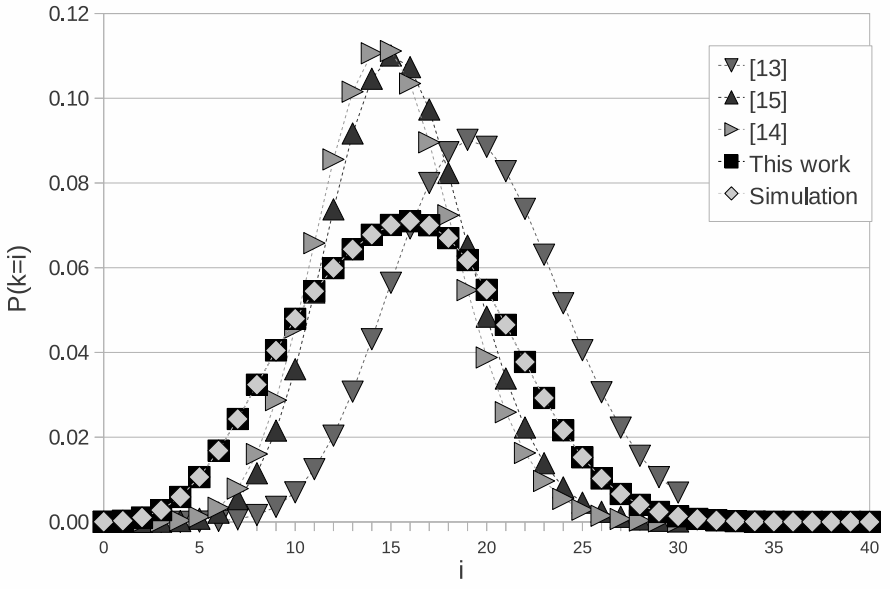

Figure 1.6. pmf with $N = 100$, $r = 1$ and $l = w = 4$

Fig. 1.7 shows the KullbackLeibler divergence (KLD) [38] between various means and the simulation results. KLD is a measure of the difference between two probability distributions: in this case it is used to quantify the difference between each

analyzed distribution and the simulative results. The KLD of two discrete probability distributions P and Q is defined as $D_{KL}(PL) = P(i) \log \frac{P(i)}{Q(i)}$. The quantity $0 \cdot \log 0$ is interpreted as 0. Since KLD is not symmetric, $P(i)$ corresponds to the simulations in all the comparisons.

For all the deployment surfaces showed in Fig. 1.7, the KLD between the proposed degree distribution and the simulation results is less than or similar to 10^{-8}, and is always the lowest. For the distribution proposed in [33], the KLD is always the highest. The distribution proposed in [34] provides an intermediate KLD. If $A_{dA} \ll A_d$, the distribution proposed in [33] provides a KLD close to [34], or otherwise close to the proposed distribution. That approach provides the best results among the state-of-the-art approaches, since its formula for the mean is exact.

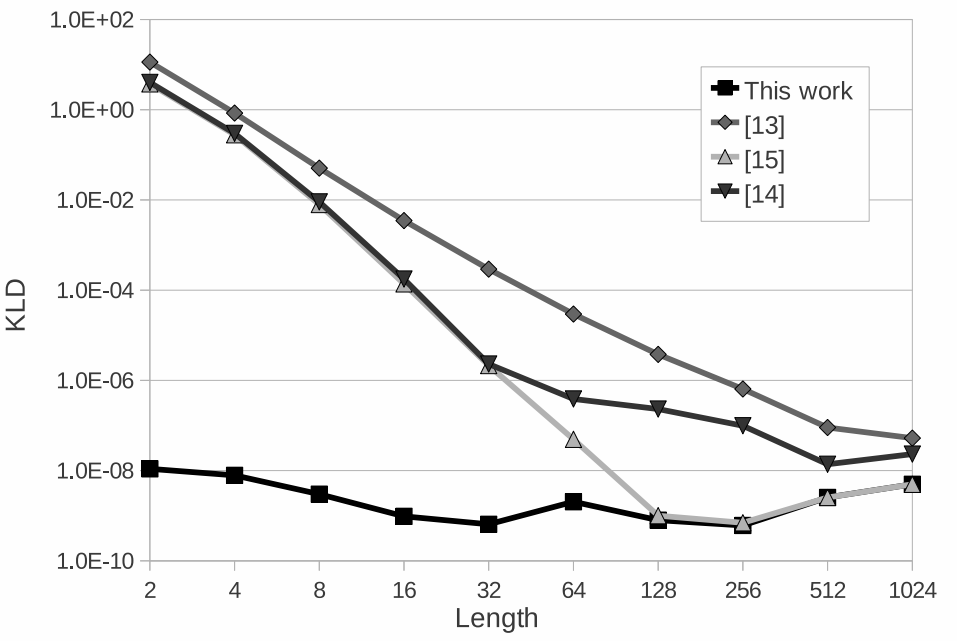

Figure 1.7. KullbackLeibler divergence

1.8.2 Mean

The mean of the proposed degree distribution is expressed by (1.14). This formula does not introduce any approximation, so it provides the exact result. However, the comparison between (1.14) and the result of the simulations shows a minimal difference due to statistical error.

Fig. 1.8 shows the relative difference between various means and simulation results ($\frac{\left|\mu_{symulation} - \mu_{theoretic}\right|}{\mu_{simulation}}$). When the size of A_d increases, the relative difference

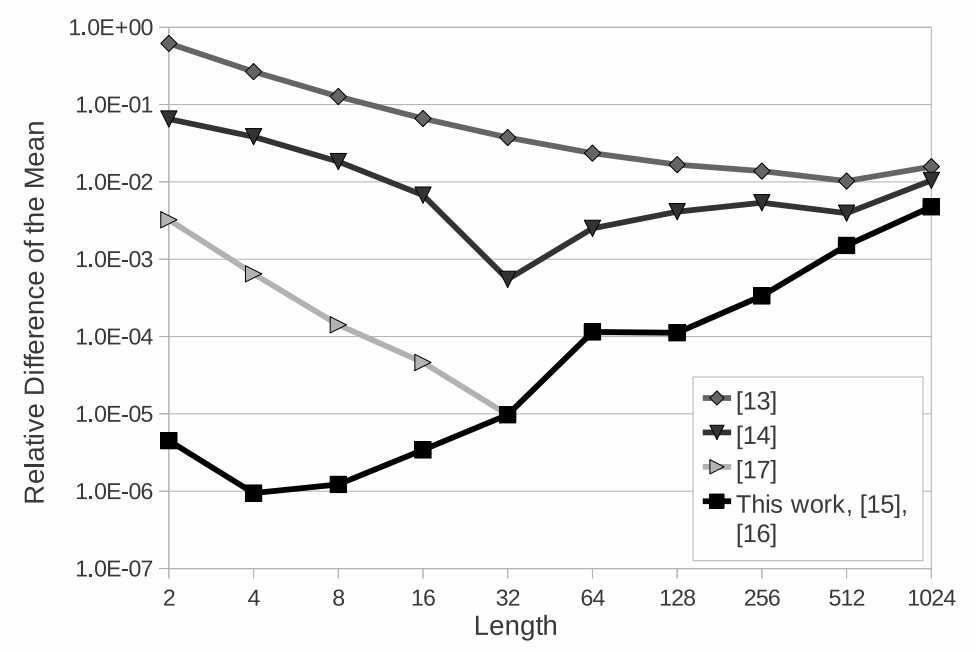

Figure 1.8. Relative difference of the mean

between (1.14) and the simulation results increases too, since μ decreases exponentially. The mean provided in [33] does not consider border effects, so it is characterized by a wide difference when $A_{dA} \ll A_d$. The mean provided in [34] is calculated by an algorithm ($\Theta(m^2)$) which approximates S_d, splitting it into m small squares. Border effects are correctly evaluated, but the result is affected by the approximation. Using $m = \frac{100wl}{r^2}$, as in [34], the difference is lower than [33], especially when $A_{dA} \ll A_d$. The mean provided in [37] derives the mean by analyzing the geometric characteristics of A_d. However, the sub-surfaces S_{dC} and S_{dD} are treated as a single sub-surface. The formula of the mean is similar to (1.14), with the exception of the contribution of S_{dC} and S_{dD}. Therefore, the mean is subject to a great deal of approximation when the ratio $\frac{A_{dC}+A_{dD}}{A_d}$ is high, but lower when $S_{dC} \cup S_{dD} \ll S_d$. The mean provided in [37] is equal to (1.14), even if it has been derived in a different way. Therefore, it does not introduce approximations.

The analyzed graph validates (1.14), showing that our mean is more accurate than the other state-of-the-art formulas [33, 34, 37].

Chapter 2

Interference analysis in RFID systems

An RFID system consists of small tags containing a microchip and an antenna, readers to acquire data stored in the tags by means of radio frequency signals, and a back-end server for data processing and storage. Due to low production cost, the majority of RFID systems exploits passive tags, i.e., tags without a battery. Their simple integrated circuit is fed by the electromagnetic field emitted by the readers: passive tags operate only in response to a reader interrogation.

RFID technology is a key component in the implementation of pervasive computing. By means of their automatic identification, physical objects can be easily mapped in an information system. In this way, pervasive applications – i.e. location-aware [39, 40], widespread [41] and transparent to users [42] – are implemented. Other advantages in RFID adoption include an increase in process efficiency, a complete item traceability and a better quality control [43, 44].

Interferences among readers and tags may prevent communication, as described in Section 2.2. Two types of collision can be generated: the *reader-to-tag collision*, where a tag in the intersection of the interrogation zones of two readers is simultaneously queried by both of them, and the *reader-to-reader collision*, where two readers disturb each other if they are located within a specific distance called *interference range*. Two types of reader collision can be generated: reader-to-tag and reader-to-reader collision. The reader-to-tag collision involves readers whose reading areas overlap. They could try to query the same tag at the same time. Although they use different frequency bands, none of them can identify the tag, since the tag has no filtering capabilities. The reader-to-reader collision prevents a reader from correctly identify tags due to the concomitant transmission of another reader. In this case, the weak response of the tags is distorted by the stronger signal of the other reader.

An evaluation of the reader-to-reader collisions is often based on simple models that consider only direct collisions among two readers, like for example the unit disk

graph model. Instead, more complex models capture the total signal power emitted by each reader and assume that the power of each signal decays as distance grows. The main models of the two families are described in Section 2.3. Section 2.4 presents the deployment scenarios that are used in Section 2.5 to compare the accuracy of the two families of models.

2.1 RFID systems

Radio Frequency IDentification (RFID) is a leading technology in Automatic Identification and Data Capture (AIDC). The architecture of an RFID system comprises several tags, one or more readers and a central server. At its simplest, a tag consists of a small microchip equipped with an antenna. A unique ID EPC (Electronic Product Code) is assigned to it. The tag is attached to or embedded in an object. Beside the identification code, the tag can store other information about the tied object. These data can be retrieved by a reader through radio frequency transmission. The range within a reader can communicate with tags is referred to as the *interrogation range* of that reader. This range is affected by the transmission power, the on-board antennas, and the environmental conditions [5]. Furthermore, the reader communicates with the back-end server via a proper communication network. The server receives, processes and stores the data sent by the reader.

RFID is emerging as the alternative to bar code for object identification, since it can automate hard-working activities. This technology is applied to several sectors, such as traceability [45, 46, 47, 48], emergency management [49], smart hospitals [50, 51] and supply chain management. Its use concerns all the areas of the supply chain [52]: transportation monitoring [53], inventory accuracy in warehouses [54], assembly assistance in manufacturing [55] and product availability in retail stores [56].

RFID systems are mainly characterized according to the operational frequency and to the energy supply of the tags. The frequency bands are:

- low frequency (LF), between 125 and 134 KHz;
- high frequency (HF), at 13.56 MHz;
- ultra high frequency (UHF), between 866 and 868 MHz in EU, between 902 and 928 MHz in USA;
- microwave at 2.45 GHz in EU, between 2.4 and 2.4835 GHz and between 5.725 and 5.85 GHz in USA.

The majority of RFID systems works at UHF frequency [57].

Tags are categorized into *passive*, *semi-passive* and *active*. UHF passive tags only respond to a reader's interrogation, since they use back scatter modulation to reflect the reader's signal right back. The microchip of the tag is powered by the electromagnetic field emitted by the reader. This energy requirement restricts the operating range of a passive tag to a maximum of 10 meters. UHF semi-passive tags include a battery to operate the microchip, but they exploit passive tag's backscatter mechanism for uplink communication. With self-sufficient power supply, the constraining factor in the operating range of semi-passive tags becomes the weakness of their generating signal and, thereby, the sensitivity of the reader's receiver. The theoretical operating range of a UHF semi-passive tag is more than 20 m. Active tags are supplied by a more powerful battery cell, so they can generate a radio frequency signal to reply to a reader interrogation and they can also initiate a communication. The interrogation range of active tags is considerably longer, up to some hundreds of meters. However, passive RFID applications are by far the most adopted for their best trade-off between cost and performance.

2.2 RFID interference

RFID systems are subject to various interference problems among readers and tags, which may prevent communication. Three types of collision can be generated:

- tag-to-tag collision: a reader communicates at the same time with multiple tags located inside its interrogation zone and is unable to distinguish their signals;
- reader-to-tag collision: two readers simultaneously query a tag inside the intersection of their interrogation zones;
- reader-to-reader collision: multiple readers using the same radio frequency can disturb each other if they are located within the intersection of their *interference ranges*.

Tag-to-tag collision is a well-known problem. The majority of the proposed solutions exploit Time Division Multiple Access (TDMA) [58], which splits the available channel among the tags. They are classified into the tag-driven and reader-driven categories, depending on the subject that controls the data transfer. In tag-driven protocols, the tags communicate only if they have information to send. A first solution was based on Aloha algorithm [59], in which successful communication is stopped by an acknowledge message. Subsequent implementations have divided time into timeslots, to reduce the occurrence of collisions [60, 61]. In reader-driven algorithms, the reader schedules the querying tags: the synchronization increases the

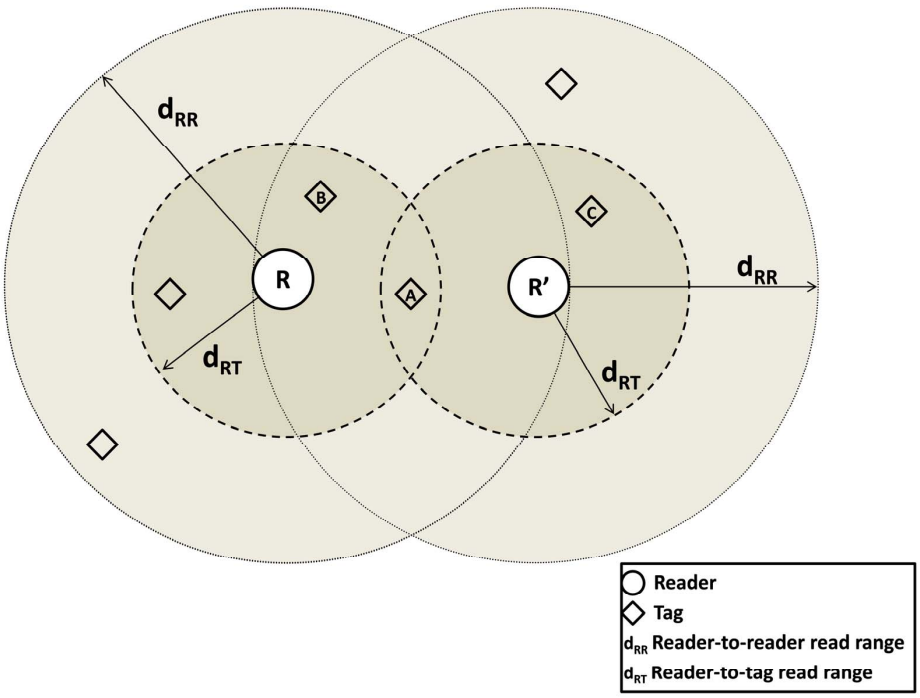

Figure 2.1. Reader interference

scalability and reduces the length of the communication. The most relevant protocols of this family are classified in polling [62] and tree-based approaches [63, 64]. With polling, the reader has a list of the serial numbers of all the tags in its interrogation zone, and queries them in turn [62]. Tree-based protocols recursively split the set of colliding tags, to identify subsets of tags that can consecutively transmit [63, 64].

Reader-to-tag collision occurs when two or more readers overlap their reader-to-tag read ranges and try to read the same tag simultaneously. In this case, the physical distance between these readers is lower than the double of the interrogation range. In Fig. 2.1, if R and $R^{'}$ try to identify tag A, A receives electromagnetic waves from both readers simultaneously. Reader-to-tag collision can be partially solved by managing reader-to-reader collisions [65, 66]. If simultaneous interrogations of nearby readers are avoided, tags are not queried by more than one reader at the same time. However, two readers can generate a reader-to-tag collision but not a reader-to-reader collision if they operate at different frequencies. Therefore, approaches based on Frequency Division Multiple Access (FDMA) are less effective than TDMA-based techniques for limiting the reader-to-tag collision.

Reader-to-reader collision happens when the signal generated by one reader interferes with the reception system of other readers. It only occurs when the physical

distance between two or more readers is lower than the interference range. Reader-to-reader collision hinders the tag identification process: a reader can receive strong signals from neighboring readers, interfering with the weak response signal from the tag. In Fig. 2.1, if R reads data from tag B and, at the same time, R' sends data to tag C, R' interferes with R. While tag-to-tag and reader-to-tag collisions are limited by the interrogation range, the range of the reader-to-reader interference amounts to a larger area [67]. Reader-to-reader collisions are particularly critical in *Dense Reader Environments* (DREs), where multiple readers are located in close proximity to each other. These scenarios are common when a single reader is not enough to cover a specific identification area, or simply when the final application requires the existence of multiple checking areas. DREs can also be implemented to improve read rate and reliability, as they ensure high probability of tag identification [68].

2.3 Reader-to-reader interference models

The models adopted for describing the reader-to-reader interference can be categorized into two groups. The first group assumes that each reader has a fixed interference range and it can collide only with other readers located within this distance. Under this hypothesis, several graph representations have been proposed, such as planar graphs and trees [69], but the most popular one is the unit disk graph model [2].

The second kind of interference models takes into account the power of all the exchanged signals. It is based on the following assumptions:

- the antenna gain of a reader is far better than the one of a tag;
- there is no shadowing and the signal power at the receiver is attenuated due to path loss;
- the total interference power from multiple interfering readers to the target reader is additive, i.e., the interference contributions are added non-coherently;
- the RFID medium access is using a single-channel operation mode, whereas the reader-to-tag query communication and tag-to-reader response communication are sharing a bidirectional channel.

Additive interference models can be categorized according to the estimation of the background noise power. The noise power can be included as a model parameter, or can be assumed as negligible with respect to the reader interferences.

2.3.1 Single interference model

The traditional model of the reader interference is specular to the model adopted for describing the tag interrogation [65]. Each reader is characterized by its interrogation range, which depends on the output power used to query the tags. Within this distance, the output power of the reader is enough to feed the circuitry of the tags and to receive a back scattered signal with adequate power. A reader can collect information from all the tags within its interrogation range, but can not query the tags that are located further. In a similar way, the output power of a reader determines its interference range, i.e. the distance within which the signal of the reader is strong enough to disturb the activity of the other readers, as shown in Fig. 2.2. When a reader transmits, it interferes with the readers that are located within its interference range and that are currently querying tags in the same channel. These readers are prevented from collecting any tag information at all. All the other readers, which are located outside the interference zone, are not disturbed. This model describes the reader collision in a boolean way: two readers may collide if and only if they are located within a certain distance. The collision happens if they transmit simultaneously on the same channel.

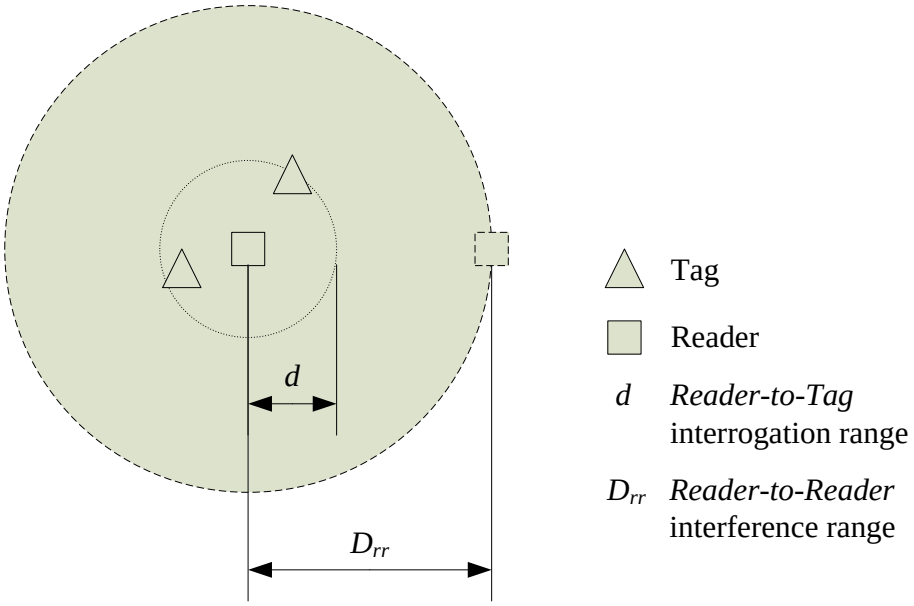

Figure 2.2. The single interference model

The relationship of potential collision among a set of readers can be described by a graph. Each reader is represented by a point. An edge exists between two nodes if and only if the Euclidean distance between the two nodes is below a fixed threshold. The graph obtained in this way is a unit disk graph. If two nodes are connected by

an edge in a unit disk graph, the corresponding readers may experience a collision.

2.3.2 Additive interference model without background noise power

In a passive RFID system, as tags do not incorporate a battery and are powered by the carrier signal from readers, the backscattered signal will arrive at the readers very weakly. In order to be recognized, the backscattered signal from the tag needs to satisfy two conditions: firstly, the strength of the signal must be above a lower bound, named *carrier receive level* (or receiver sensitivity), which guarantees that it can be correctly detected and decoded; on the other hand, the signal to interference ratio (SIR) must exceed a required threshold, which depends on the desired read rate and the bit error rate (BER). Let Θ and Γ respectively denote the carrier receive level and the required SIR, the following condition must be satisfied:

$$(P_{t,r} \geq \Theta) \wedge (\frac{P_{t,r}}{I_r} \geq \Gamma) \tag{2.1}$$

where $P_{t,r}$ represents the received signal power at the reader r from the tag t and I_r denotes the total interference that reader r receives.

Let d be the maximum interrogation range of reader r without any interference. In [6], the received signal power at tag t from reader r is expressed as

$$P_{r,t} = P_r \frac{G_r G_t}{K_0 d^\alpha} \tag{2.2}$$

where P_r is the transmit power of the reader, G_r and G_t represent the antenna gain of the reader and the tag, respectively, and α is the path loss exponent. K_0 is a coefficient integrating the channel path loss and the fractional power ratio in the bandwidth. As the distance between the reader and the tag is short and the transmission path is a simple line-of-sight, fading effects can be ignored. K_0 can be derived by measuring the power P_t received by a tag at a reference distance d_0 (usually 1 m). Therefore K_0 can be set such that $P_r \frac{G_r G_t}{K_0} = P_t {d_0}^\alpha$. When $d_0 = 1$, $K_0 = \frac{P_r}{P_t} G_t G_r$.

Let R_t be the effective power reflection coefficient of the tag antenna, i.e. the ratio of the power received by the tag that is reflected to the reader. Then, the power received by the reader from the tag is given by

$$P_{t,r} = R_t P_{r,t} \frac{G_t G_r}{K_0 d^\alpha}. \tag{2.3}$$

Based on equations (2.2) and (2.3), in order to satisfy the first condition in (2.1), the interrogation range d can be determined by the threshold Θ and the transmit

power P_r of the reader. Θ and P_r are tuned according to the integrated circuit design and the environmental condition of the antenna. When the transmit power P_r and the threshold Θ are specified, d can be calculated by let Equation (2.3) equal to Θ. Therefore, in order to satisfy the first condition in (2.1), P_r must be larger than the threshold power required for the tag operation.

The reader-to-reader collision occurs when the second condition in (2.1) is not satisfied, i.e., the backscattered signal from the tag to the reader is too weak with respect to the interfering signals of other readers. To prevent the reader-to-reader collision problem, the key point is to determine the potential interference range within which the reply signal from the tag is not interfered by signals from other readers. Once the potential interference range is determined, a FDMA or TDMA scheme prevent readers from concurrent tag interrogations.

Let D be the distance between two readers A and B. The interference power of reader B detected by reader A can be expressed as:

$$P_{r,r} = P_r \frac{G_r G_r}{K_0 D^\alpha}. \tag{2.4}$$

With only one interfering reader B, the total interference I_r received by reader A is given by Equation (2.4). The reader-to-reader interference range, i.e. the minimum distance D_{rr} beyond which two concurrent readers do not generate a collision, is obtained setting the SIR equal to the required threshold Γ, according to the second part of Equation (2.4). Substituting in this formula the power of the signal received by the tag, given by Equation (2.2), the reader-to-reader interference range follows:

$$D_{rr} = d^2 \cdot \sqrt[\alpha]{\frac{K_0 \Gamma}{R_t {G_t}^2}}. \tag{2.5}$$

In the presence of a group of n readers, the total interference that is generated towards one target reader A can be evaluated summing each individual contribution:

$$P_s = \sum_{i=1}^{n} P_r \frac{G_r G_r}{K_0 D_i^\alpha} \tag{2.6}$$

where D_i is the distance between reader A and reader i.

2.3.3 Additive interference models with background noise power

With the assumption that the background noise power N_0 is not negligible, the condition for a successfully tag identification is evaluated through the comparison

between the Signal to Interference plus Noise Ratio (SINR) and a required threshold Γ:

$$\frac{P_{t,r}}{I_r + N_0} \geq \Gamma \tag{2.7}$$

In [70] and [71], only the case of two interfering readers A and B is considered. The power of the signal back-scattered by the tag and received by reader A is given as:

$$P_{t,r} = R_t \alpha_{BW} P_r G_t G_r \cdot 10^{0.2 \cdot PL(x)} \tag{2.8}$$

where α_{BW} is the spectrum power of the channel normalized by the total power and PL is the free-space path loss between reader A and the tag (depending on their distance x). The interference power detected by reader A is given as:

$$I_r = h \cdot \beta_{mask}^{BA} P_r G_t G_r \cdot 10^{0.1 \cdot PL(D)} \tag{2.9}$$

where h is a fading coefficient in the channel between readers B and A, β_{mask}^{BA} is the spectrum mask level and D is the distance between the two readers.

A slightly different evaluation of Equations (2.8) and (2.9) is provided in [72]. The back-scattered power is given as:

$$P_{t,r} = R_t \alpha_{BW} P_r G_t G_r (P_0 x^{-\gamma})^2 \tag{2.10}$$

where P_0 is the reference path loss at the distance of 1 m. The interference power from reader B is:

$$I_r = h \cdot \beta_{mask}^{BA} P_r G_t G_r P_0 D^{-\gamma} \tag{2.11}$$

The analysis in [70] and [71] is extended in [7] and [73]. First, the free-path loss between reader A and the tag is evaluated as $\left(\frac{4\pi x}{\lambda_A}\right)^2$, where λ_A is the wavelength used by reader A. Since the forward and backward path-losses are the same, it is counted twice, and the power $P_{t,r}$ of the signal received by reader A becomes:

$$P_{t,r} = R_t \alpha_{BW} P_r G_t G_r \left(\frac{\lambda_A}{4\pi x}\right)^4 \tag{2.12}$$

In the presence of only one reader B that interferes with reader A, the interference power detected by A is given as:

$$P_{r,r} = h \beta_{mask}^{BA} P_r G_t G_r \left(\frac{\lambda_B}{4\pi D}\right)^2 \tag{2.13}$$

Furthermore, the analysis in [7] and [73] estimates the total interference generated by a group of n concurrent readers as follows:

$$\frac{\kappa_1 P_{t,r}}{x_i^4 \kappa_2 \sum_{i=1}^{n} (P_r \beta_{mask}^{iA} / D_i^2) + N_0} \geq \Gamma \tag{2.14}$$

where $\kappa_1 = \frac{R_t \alpha_{BW} G_t G_r \lambda_A^4}{(4\pi)^4}$ and $\kappa_2 = \frac{h G_t G_r \lambda_i^2}{(4\pi)^2}$.

2.4 Evaluation scenarios for the reader-to-reader interference models

In order to compare single and additive interference models, their accuracy is analyzed in two scenarios. The first one studies the interaction between a pair of interfering readers and a target reader. The second scenario inspects the relationship between the number of readers and the radius of the circular area within which the interference is detected. Furthermore, a particular hexagonal constellation deployment is considered.

2.4.1 Pair interaction

In this scenario, the interference produced by a pair of readers on a target reader is investigated. Adopting the unit disk graph model, if both the interfering readers are out of the reader-to-reader interference range there is no collision. Instead, in an additive model, a collision may occur even if both the readers are beyond the interference range.

Let D_x (D_y) be the distance between reader R_x (R_y) to a target reader R_s. According to the additive interference model described in Section 2.3.2, the overall interference caused by R_x and R_y and perceived by R_s is:

$$I_{xy} = P_r \frac{G_r G_r}{K_0 D_x^\alpha} + P_r \frac{G_r G_r}{K_0 D_y^\alpha}. \tag{2.15}$$

The relationship between the distances among the readers and the overall interference is obtained by setting the ratio between $P_{t,r}$, given by Equation (2.3), and the perceived interference I_{xy}, given by Equation (2.15), equal to Γ:

$$\frac{1}{D_x^\alpha} + \frac{1}{D_y^\alpha} = \frac{R_t G_t^2}{K_0 d^{2\alpha} \Gamma}. \tag{2.16}$$

In the above equation, D_y can be expressed as a function of D_x:

$$D_y = \sqrt[\alpha]{\frac{K_0 \Gamma d^{2\alpha} D_x^\alpha}{R_t G_t^2 D_x^\alpha - K_0 d^{2\alpha} \Gamma}}. \tag{2.17}$$

2.4.2 Ring deployment

In the additive interference models, the interference generated by each reader is directly summed, in order to obtain the overal interference. A reader may experience a reader-to-reader collision even if none of other n readers is located within the

interference range D_{rr}. We define the reader-to-n-readers interference range as the maximum distance D_{rn} within which a reader-to-reader collision between a target reader and a group of n readers occurs, as shown in Fig. 2.3.

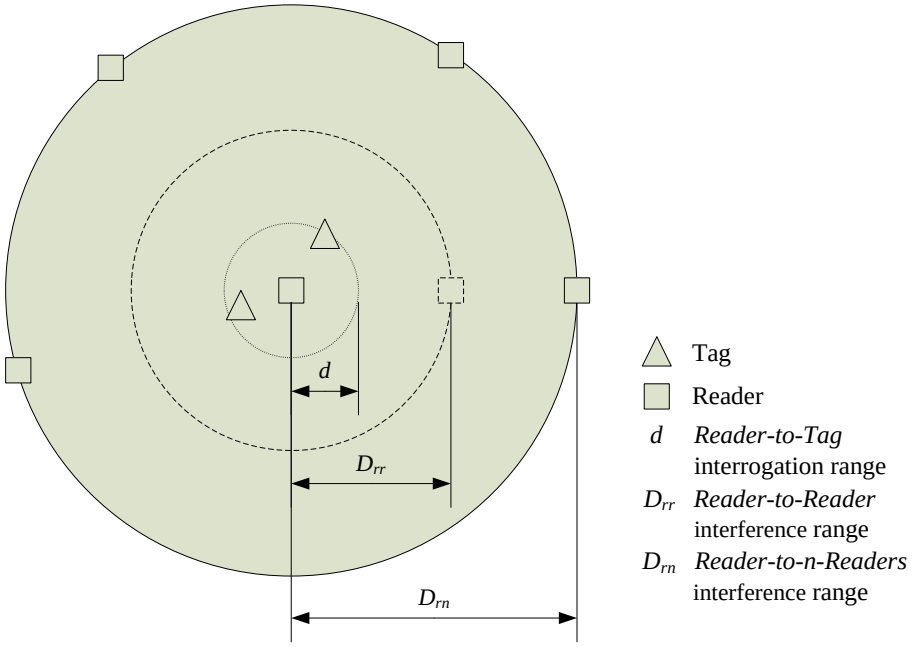

Figure 2.3. The additive interference model for the ring deployment scenario

The goal is to determine the minimum range D_{rn} from a target reader, at which n other readers can query tags without colliding with the target reader. The group of n readers is deployed along a ring, forming a circle with the target reader as the center. According to Equation (2.6), the overall interference perceived by the target reader is:

$$I_r = n \cdot P_r \frac{G_r G_r}{K_0 D_{rn}^{\alpha}}. \tag{2.18}$$

Substituting Equation (2.18) and Equation (2.3) into the second part of Condition (2.1), D_{rn} results as follows:

$$D_{rn} \geq \sqrt[\alpha]{\frac{n \cdot K_0 d^{2\alpha} \Gamma}{R_t G_t^2}}. \tag{2.19}$$

The minimum radius of the ring to avoid the interference of the group of n readers is determined only by the path loss exponent α and the threshold SIR Γ. However, D_{rn} is not related with the transmit power and the antenna gain of the reader when d is fixed.

2.4.3 Hexagonal constellation deployment

Given a target reader, all the other readers can be imagined as deployed on rings of different radius. We define the readers on the inner ring as the *tier-1* interfering readers. In this section, all the mutual interference generated by the target readers and the tier-1 readers are considered. No other readers are involved. As the interferences between the concurrent readers are mutual, every group of three readers should form an equilateral triangle (for example, reader S, A and B in Fig. 2.4. As a result, the maximum number of interfering readers on a ring is 6, independently of the radius D_{rn}. The readers are the vertices of a hexagonal constellation as in Fig. 2.4: this is also the optimal disposition to completely cover an area [6]. The distance between each pair of readers is given as:

$$D_{r6} \geq \sqrt[\alpha]{\frac{6 \cdot K_0 d^{2\alpha} \Gamma}{R_t G_t^2}}. \tag{2.20}$$

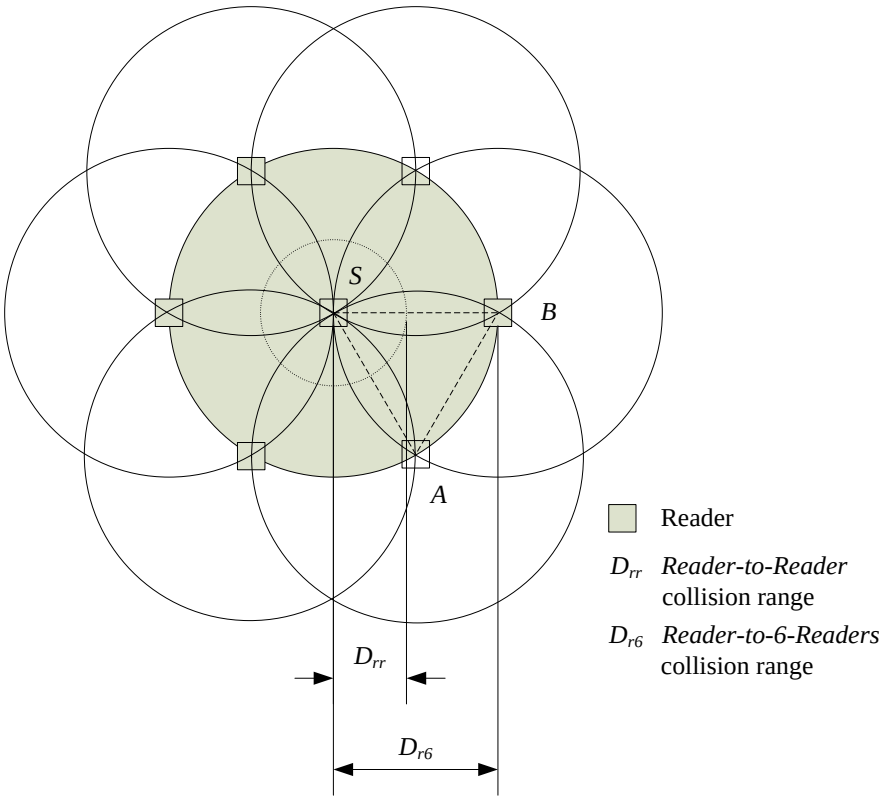

Figure 2.4. The hexagonal constellation deployment

2.5 Numerical evaluation of the reader-to-reader interference models

In this section, the previously described scenarios are used in order to compare how often a collision identified by an additive model is not considered by the unit disk graph model. The effect of the number of interfering readers and of their distance is evaluated according to the parameters listed in Table 2.1. The path loss exponent α varies from 2 to 3.5 and the SIR threshold Γ is tested from 1 to 15. The antenna gain of the reader and tag are set as 6 dBi and 1 dBi, respectively. The power reflection coefficient on a tag is 3/4. The transmit power of a reader, P_r is set to 10dBm. K_0 is set to be the lower bound, G_r^2, according to the received power P_0 measured at $d_0 = 1\ m$ [6]. The interrogation range d is set to 5 m when $\alpha = 2$. Given a fixed Θ in the first condition of (2.1), $d^{2\alpha}$ is fixed according to Equation (2.2) and (2.3). Therefore, d is set to $\sqrt[\alpha]{25}\ m$ with respect to different path losses.

Table 2.1. Evaluation Parameters

Parameters	Values
Path loss exponent (α)	2, 2.5, 3, 3.5
SIR Threshold (Γ)	1, 5, 10, 15
Reader antenna gain (G_r)	6 dBi
Tag antenna gain (G_t)	1 dBi
Tag's power reflection coefficient (R_t)	3/4
Reader's transmit power (P_r)	10 dBm
Constant coefficient (K_0)	G_r^2
Interrogation range (d)	$\sqrt[\alpha]{25}\ m$

Fig. 2.5 reports the results obtained by evaluating Equation (2.16) with respect to different SIR thresholds. In order to investigate the impact of SIR thresholds for the pair interaction scenario, α is set equal to 2, as in a free space model. As general rule, the results are symmetric since the interaction is mutual. For each line there are two asymptotes to D_{rr}, which indicates the minimum distance between readers to avoid collisions. When D_x (or D_y) is equal to D_{rr}, D_y (D_x) is infinite. As the SIR threshold decreases, the corresponding result approaches the asymptote more quickly: it means that the two readers interact with each other stronger. The minimum distance D_{rr} between two readers (i.e., the asymptote value) grows as the SIR threshold increases, as confirmed in Equation (2.5). When $D_x = D_y$, the scenario evolves into a ring deployment with two interfering readers X and Y; D_{r2} grows as SIR threshold raises. Fig. 2.6 shows the influence of α when SIR threshold Γ is set to 1, i.e. an ideal, perfect capture capability is assumed [74]. The lower the value of α is, the smaller the bound value of D_x (or D_y) is.

Fig. 2.5 and Fig. 2.6 also show the horizontal and vertical lines corresponding to the unit disk graph model. From the comparison between D_{rr} in the unit disk graph model and D_x (or D_y) in the model described in Section 2.3.2, it can be observed from Fig. 2.5 and Fig. 2.6 that with a lower α the unit disk graph model misses often to identify collisions, as in presence of a high SIR. For example, when $\alpha = 4$ and $SIR = 1$, D_x and D_y in the model in Section 2.3.2 are almost the same with D_{rr} as in the unit disk graph.

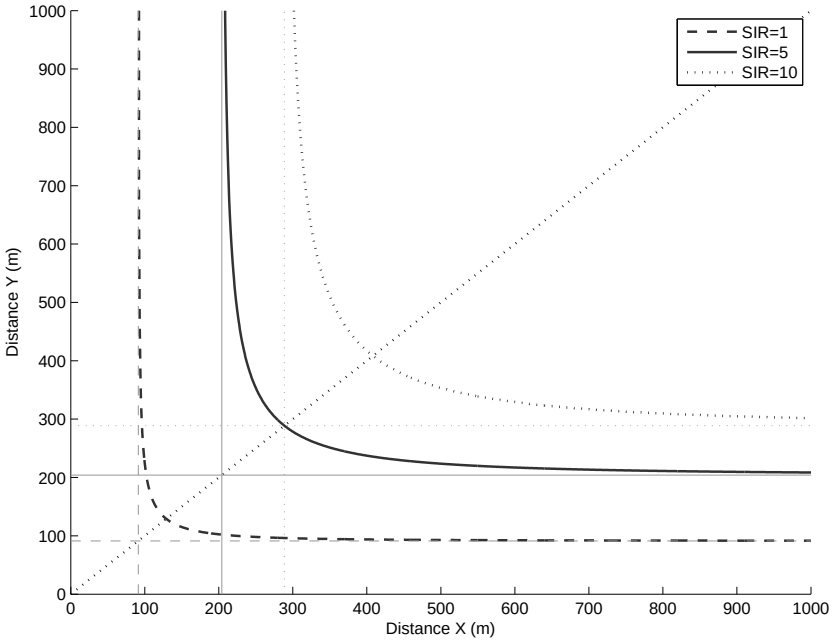

Figure 2.5. Reader pair interaction according to different SIR thresholds

In Fig. 2.7 and Fig. 2.8, the reader-to-n-readers interference range is shown as a function of the number of interfering readers n according to different SIR thresholds and α. As the number of interfering readers grows up, they need to be further from the target reader, in order to avoid a collision. When n is equal to 1, the distance is identical to D_{rr}. Considering the unit disk graph model, D_{rr} is always equal to D_{rn}. In Fig. 2.7, D_{rn} increases as α decreases. The reason is that a low value of α indicates a lower path loss. Besides, the larger the pass loss exponent α is, the faster the distance increases. For example, when $\alpha = 2$, the distance increases from 91.29 m to 288.70 m for 1 interfering reader and 10 interfering readers, respectively. The increase is much smaller when α is 4 (from 9.55 m for 1 reader to 16.99 m for 10 readers). On the other hand, D_{rr} rises up as SIR threshold increases as shown in Fig. 2.8. A larger SIR threshold implies that the object reader requires a less significant interference sum, consequently the radius needs to be larger in order to reduce the generated interference.

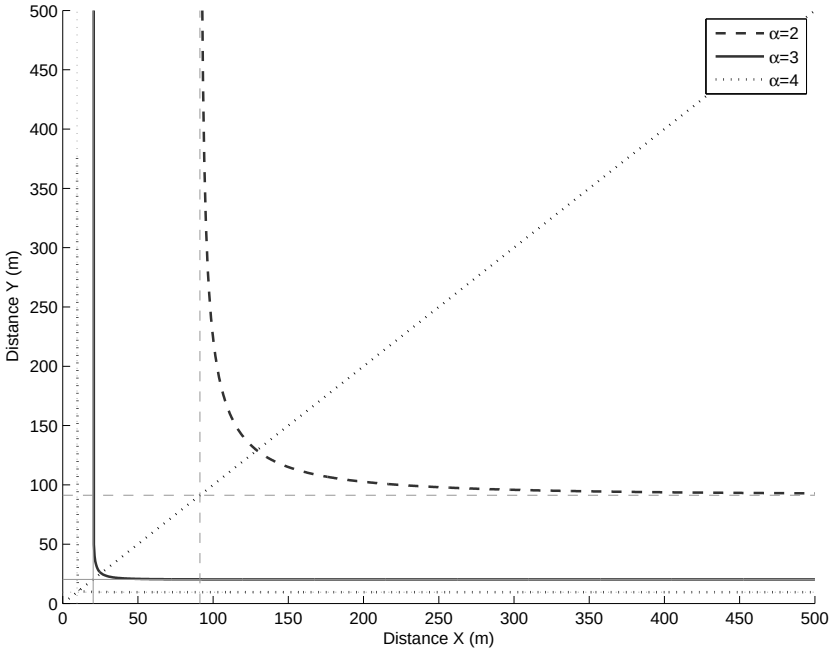

Figure 2.6. Reader pair interaction according to different path loss exponents

The difference between the unit disk graph model and the additive interference model increases as the number of interfering readers grows up. Besides, the results in the ring deployment reflect again that lower α and higher SIR increase the differences in the two models. For example, when the number of readers is 5 in Fig. 2.7, the gap grows from 4.74 m to 112.81 m when α falls from 4 to 2. On the other hand, in Fig. 2.8, the difference is equal to 112.81 m when $SIR = 1$, while it grows to 356.8 m when $SIR = 10$.

The results for different values of the side length of the hexagonal constellation with respect to various environments are shown in Fig. 2.9. Similarly to D_{rr}, the side length of the hexagonal constellation falls down as α grows, and it goes up as SIR threshold increases. The exact value of the path loss exponent in low power wireless links is between 4.3 and 5.1 in an outdoor environment, while it falls between 2.67 and 3.23 in an indoor environment [75].

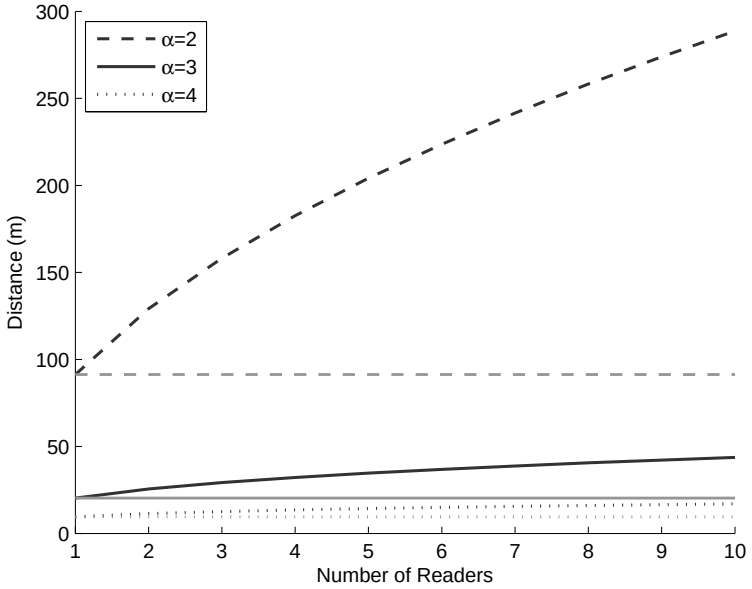

Figure 2.7. Ring deployment radius vs. Number of interfering readers according to the path loss exponent. D_{rr} is shown in light gray for the unit disk graph model and in dark gray for the additive interference model.

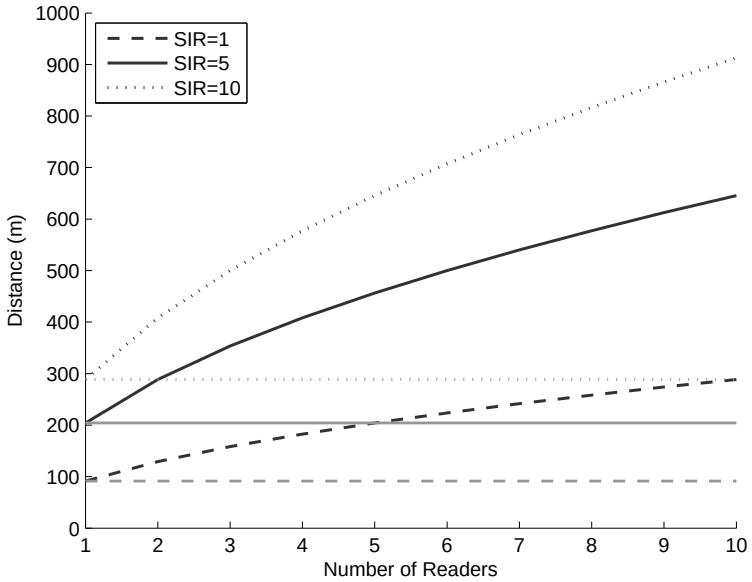

Figure 2.8. Ring deployment radius vs. Number of interfering readers according to the SIR threshold. D_{rr} is shown in light gray for the unit disk graph model and in dark gray for the additive interference model.

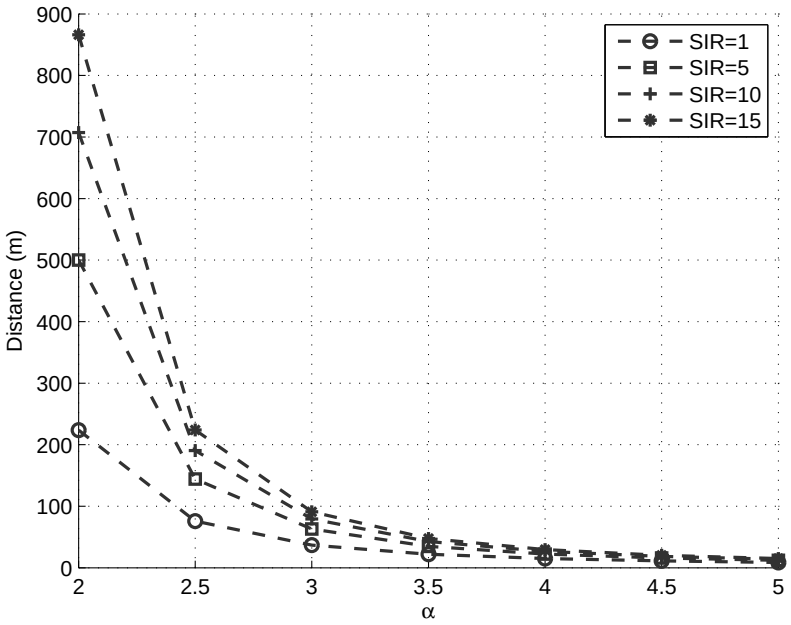

Figure 2.9. The side length of the hexagonal constellation according to different parameters

Chapter 3

Reader-to-reader anticollision protocols

Many protocols have been proposed to reduce reader-to-reader collisions in RFID systems. The majority of them exploits Carrier Sense Multiple Access (CSMA) or Time Division Multiple Access (TDMA) scheme. The main state-of-the-art approaches are detailed in Section 3.1. There is no existing accordance on the most effective criteria for performance evaluation of a general RFID reader-to-reader anticollision protocol. Section 3.2 describes the main evaluation approaches. Section 3.3 introduces a distinction among the protocols according to their requirements: beside the protocols that are characterized by limited requirements, there are other protocols that require an advanced communication system.

3.1 State-of-the-art protocols

Reader-to-reader collisions cause serious degradation in the performance and reliability of RFID systems, resulting in errors and in slowdown of the tag interrogation time. In order to resolve these problems, several multiple access schemes have been suggested [76].

Frequency Division Multiple Access (FDMA) utilizes separate frequency channels. However, some restrictions are innate to this technique. First of all, the available channels are a scarce resource, in contrast with the numbers of readers that can be very large, especially in DREs. ETSI standards specify the use of 4 channels [9]. Secondly, this method does not address reader-to-tag interference at all, since a passive tag lacks frequency selectivity and can not distinguish signals from different frequency channels.

Carrier Sense Multiple Access (CSMA) demands to verify if the channel is free before transmitting on it. The European Telecommunications Standard Institute

(ETSI) specifies the CSMA protocol Listen Before Talk [9], standardized as ETSI EN 302 208. Readers operate in the band between 865 MHz and 868 MHz. They listen the channel for 5 ms before transmitting, in order to reduce mutual collisions. However, the carrier sense mechanism is not effective by itself against reader collision problems, since it can not detect a concurrent transmission.

Code Division Multiple Access (CDMA) multiplexed several readers over the same channel. However, its implementation in passive RFID systems is difficult due to its heavy computational requirements and the extra circuitry necessary for tags.

Time Division Multiple Access (TDMA) allows several readers to share the same channel by allocating their transmissions into different timeslots. It is the easier solution to be taken for RFID systems, although a synchronization among the readers is required. However, this is a general requirements for effective collision detection in DREs or with passive tags.

3.1.1 CSMA protocols

Listen Before Talk (LBT)

According to the European standard ETSI EN 302 208 [9], RFID readers may optionally implement Listen Before Talk to detect interferences during transmission. If implemented, there are two requirements for the reader: the capability to detect radio signals emitted by other readers on the channel currently used, and the possibility of switching the channel. The European standard allows transmission within the frequency band of 865 to 868 MHz, dividing it in 15 channels. Before transmitting, a reader selects a channel and it stands in *listen mode* for at least 5 ms, measuring any signal on that channel. The channel is busy if a signal of at least -35 dBm is detected: in this case the reader monitors another channel. The reader switches to *talk mode* and starts the transmission if a free channel is found. The reader can transmit for no more than 4 seconds. After stopping communication, the reader must wait for at least 100 ms before listening again the same channel. However, in the meantime, it can switch to other channels and monitor them.

Pulse

Along with the data channel to read tags, in Pulse [77, 78] protocol readers use a control channel to manage their transmissions. The signals exchanged on the control channel are called *beacons*. When a reader communicates on the data channel, it sends beacons on the control channel with a frequency set to a period called *beacon interval*. In the initial *Waiting* state, each reader listens the control channel. If the reader does not detect any beacon for a period equal to 3 beacon intervals, it moves to the *Contend* state. It chooses a random backoff time, multiple of the beacon

interval, during which it monitors the control channel. If a beacon is received, the reader returns to the *Waiting* state, otherwise it moves to the *Reading* state and it communicates with tags. At the end, the reader returns to the *Waiting* state.

In order to improve the fairness of the protocol, if a reader in the *Contend* state receives a beacon, it stores the remaining backoff time. When it returns to the *Contend* state, it uses the residual time, instead of choosing a new random backoff time.

Pulse protocol has more requirements with respect to Listen Before Talk: a second channel to exchange control signals; a higher transmission power on the control channel in order to exchange signals among readers inside the interference range; the capability of working simultaneously with two channels.

3.1.2 TDMA protocols

Distributed Color Selection (DCS)

A network of readers can be modeled as an undirected colored graph, where readers are represented by nodes and are connected by an edge if they interfere in case of a simultaneous interrogation. Two connected readers are called *neighbors*. Communication is organized in *rounds*, formed by μ *timeslots*, where μ is the fixed number of colors. Each color is matched to a different timeslot. A collision occurs if two or more neighbors have the same color, i.e., use the same timeslot. DCS [10, 11] looks for an assignment of colors that minimizes the number of connected nodes with the same color.

Initially each reader selects a random color. In every round, a reader tries to communicate at the timeslot corresponding to its color. If no neighbor has the same color, it can query tags, otherwise a collision occurs. In this case, to avoid another collision with the same neighbor in the next round, the reader chooses a new color. Moreover, at the beginning of its new timeslot, it advises its neighbors to change their colors, by means of a signal called *kick*. If two or more readers send a kick mutually, they change color without querying tags.

The algorithm does not require a central control, since no synchronization of the round is needed among the readers. However, the beginning of the timeslots must be synchronized among all the readers (e.g. by on-board clocks).

Colorwave

A limit in DCS and PDCS is the fixed number of colors. The ideal value depends on the size of the neighborhood, the number of requests for querying tags, and the mobility of the network. A high value could lead to unused slots within a round, while a low value introduces more overhead, increasing collisions, kicks, and slot

re-selections. Colorwave [10, 11] solves this issue allowing the readers to change their number of colors. Every reader estimates the percentage of successful communications, dividing the number of collision-free interrogations by the total number of attempts. If this value is higher than an upper threshold, the reader decrements the number of currently used colors, in order to reduce empty slots. Otherwise, if the value is below a lower threshold, the reader had experienced too many collisions, so it increments the number of colors. After varying the number of available colors, the reader informs its neighbors about the new value sending a *kick*. All the readers receiving the kick will estimate their percentage of successful tag identifications and will compare it to two other thresholds (upper and lower) in order to evaluate the suitability of the induced variation.

Colorwave introduces more overhead with respect to DCS, requiring further signal exchange to set the color change. The performance of the algorithm is lower during the first stage of transmission, when the readers are tuning their color configuration, and in mobile networks, when the variable neighborhood may cause fluctuation in the optimal number of colors [79].

Anticollision for Mobile RFID (AC_MRFID)

AC_MRFID [80] is a protocol based on DCS. Similarly to Colorwave, each reader dynamically changes the number of timeslots in its own round.

After a collision, the colliding reader communicates with its neighbors in order to count the number of readers in its interrogation range. Then, it estimates the number of readers in its interference range, according to the ratio between the interrogation area and the interference area, and it sets the number of timeslots in the round equal to the number of readers in the interference range incremented by 1. This protocol is especially suitable for networks with a regular deployment, since the calculation is close to the real value. However, this protocol is not fair, since more resources are allocated to the readers with few neighbors in their interrogation range. Furthermore, it introduces additional communication overhead, in order to count the neighbors.

Neighbor Friendly Reader Anticollision (NFRA)

In NFRA [12], a polling server synchronizes the communication. It determines the beginning of a new round broadcasting an *arrangement command* (AC) to the readers. After receiving the signal, every reader selects a random number m, within a range specified in the AC (from 1 to M). Then, the server sends M consecutive *ordering commands* (OCs), that are univocally identified by an increasing number. When a reader receives the OC corresponding to the random number chosen at the beginning of the round, it sends a special signal, called *beacon*, to all its neighbors.

If two readers mutually exchange a beacon, they can't communicate in the current round. Otherwise, after sending the beacon, the reader sends an *overriding frame* (OF) and starts to query tags. The readers that receive an OF are disabled for the current round. In the meantime the other readers continue to receive the OCs for the remaining slots in the round. After sending the last OC, the server waits for the completion of the communication among readers and tags, before issuing the new AC.

The main drawback of NFRA arises from the random hierarchy among the readers established by the selection of m at the beginning of the round. Readers drawing the lowest value have the best opportunities to query tags: they experience a collision only if a neighbor has the same value. As m increases, the probability of receiving an OF from readers with lower numbers grows. However, this probability depends on the size of the neighborhood, too. The fewer the neighbors are, the lower the probability of receiving a beacon is. The uniform distribution probability used in NFRA gives to all the readers the same probability of selecting a low value, without correlating it with the size of the neighborhood.

The high requirements are another disadvantage of NFRA. The protocol exploits an additional channel at 433 MHz for the communication between the central server and the readers. This communication system requires that each reader owns an additional radio reception device for that frequency.

HiQ

HiQ [81] is a protocol based on reinforcement learning. It involves a hierarchical structure composed of three levels. The RFID readers, which represent the lowest level, require channel resources to the higher level (e.g., a computer in charge of multiple readers). The elements of the second level require resources to the highest level (e.g., a central server), and distribute them to the readers. This system requires a communication system for the resources management.

High Fairness Reader Anticollision Protocol (HF-RACP)

HF-RACP [82] protocol consists of a collision discovery algorithm and a scheduling algorithm, both carried out by a central unit. During the collision discovery phase, the central unit constructs a collision graph, where each node represents a reader and two nodes are connected by an edge if the relating readers could potentially collide. The central unit sends a signal, called *send beacon request*, to each reader in succession. The interval T_{beacon} between two requests is constant. When a reader receives this signal from the central unit, it sends a beacon over the control channel. Every reader that detects this beacons notifies the central unit of the possible

collision between them. In the scheduling phase, the central unit exploits the collision graph in order to dynamically schedule the readers in the data channel. The scheduling criteria are collision prevention and fairness improvement. Therefore, the new scheduled reader is the one with the highest access delay that is not connected with any other transmitting readers in the collision graph.

3.2 Evaluation criteria

A communication protocol is adopted in order to settle the interaction among readers. Collisions may occur, but the protocol must be able to manage them. Many state-of-the-art protocols has been proposed with the aim of guaranteeing a high number of tag identifications, regardless of concomitant collisions. In [11], the authors consider the requirements of real-time applications (such as inventory detection), so they suggest the goal of scheduling readers to communicate as often as possible. The total number of successful transmissions (NT) performed by a set of readers during the simulation time is used to evaluate DCS and Colorwave. However this measure lacks of generality, since it depends on the length of the simulation. In [10], also the total number of attempted transmission (AT) is considered. Different configurations of DCS are evaluated according to the successful transmission percentage ($\frac{NT}{AT}$). A drawback of this method is that it evaluates positively protocols where AT is close to NT, also if NT is low. Therefore, this kind of evaluation does not seem effective. In [77, 78], two parameters are used to evaluate the anticollision protocols. Beside the percentage of successful transmissions ($\frac{NT}{AT}$), which is called *efficiency*, another parameter is measured: the *throughput*, which corresponds to the total number of successful transmissions performed by all the readers per unit of time ($\frac{NT}{time}$). The throughput is adopted as an evaluation criterion also in [81], with the motivation that the goal of anticollision protocols is to maximize the number of readers that communicate simultaneously.

The throughput is a meaningful criterion, but it does not consider the different contribution of each reader and the distribution of the transmissions over the time. Therefore, it is not a suitable criterion for applications that require constant quality of service for the whole network. In these cases, the concept of *fairness* is important. A general purpose quantitative measure of fairness is Jain's fairness index [83]. It is defined as:

$$I_{Jain} = \frac{|\sum_{i=1}^{N} x_i|^2}{N \sum_{i=1}^{N} x_i^2} \tag{3.1}$$

where N is the number of readers and x_i is the throughput attained by reader i. This index ranges from 0 (unfair behavior) to 1 (fair behavior).

Another criterion to evaluate the performance of an anticollision protocol relies on the waiting time (WT) of the readers between their request of interrogation and

the identification of the tags. In [65], two goals for reader-to-reader anticollision protocols are identified: to schedule the activities of the readers so that they can communicate as often as possible (NT), and to minimize the time that is required in order to allow all the readers to communicate at least once. The second criterion corresponds to the maximum waiting time (MWT) among all the transmissions in the network. Other similar criteria are based on the average reader waiting time (ARWT), which corresponds to the average waiting time for all the interrogations of a specific reader. The overall average reader waiting time (OARWT) corresponds to the average ARWT of all the readers in the network. In a protocol with a low OARWT, the readers communicate as soon as possible. The variance of the average waiting time (VAWT) is the variance of the ARWT of all the readers in the RFID network. A high VAWT reveals the presence of readers with bad efficiency. Finally, the total waiting time variance (TWTV) corresponds to the variance of WT for all the transmissions in the network. A protocol with a low TWTV provides a steady performance.

3.3 Protocol requirements

The basic RFID reader-to-reader anticollision protocols [9, 10, 11, 80] use one or more data channels, according to the national regulations, no control channel, and no central server for the management of the RFID network. They involve RFID readers that can query RFID tags, listen the used channel, but which cannot receive and transmit simultaneously. However, many of the most effective anticollision protocols involve additional requirements (e.g., [12, 81, 82, 77, 78]), such as an additional channel for network control. Moreover, some protocols require high cost readers with advanced capabilities (e.g., readers able to transmit and receive simultaneously, or to work simultaneously on different frequencies). Among the state-of-the-art protocols that require high cost readers, the best throughput is provided by NFRA. However, it uses an additional channel to control transmission and requires readers able to transmit and receive simultaneously. Moreover, in NFRA readers are connected to a polling server by means of a wireless link at 433 MHz, but this frequency is defined for active RFID communications, instead of passive ones. At present, most of commercial readers in the market are composed of an Ethernet connection and WiFi module or slot to add it for different purposes, e.g. to receive configuration commands from a central server, or to send the tags identifications collected by the reader to a central server. Hence, a commercial reader working under the NFRA protocol should include an extra hardware for UHF RFID communications at 433 MHz.

Some anticollision protocols may require additional information about the network deployment in order to be properly configured and to provide the best performance. For instance, the parameter that mainly affects the performance of DCS is the number of colors (μ), which represent the sequence of timeslots that compose every round. Each reader is matched to a color and, at every round, it queries tags during the corresponding timeslot. With too low a μ there are many collisions, while with too high a μ many timeslots are not used. Therefore, in order to achieve good performance, μ must be configured according to the network density. Instead, in Colorwave and AC_MRFID the possibility for the readers to change their number of timeslots μ_i in the round makes the two protocols independent of the network characteristics. As a result, these protocols do not need a specific configuration. In NFRA, the quantity of OCs should be set according to network density. Nevertheless, the degradation of its performance with an improper configuration is very low. Therefore, NFRA can be considered independent of deployment knowledge.

Different anticollision protocols have been proposed, according to the parameter (throughput or fairness) which is optimized and to the requirements. The proposal are described in Chapters 4 and 5. For the sake of simplicity, a basic classification is adopted among protocols that use only one or more data channels and protocols that require an additional control channel.

Chapter 4

Proposed TDMA protocols with data channel only

Two popular state-of-the-art TDMA protocols that use only one data channel are DCS and Colorwave [10, 11]. A relevant quality of DCS is its fairness, due to the opportunity to reserve a timeslot for the nodes that experience a reader-to-reader collision. Colorwave represents an evolution of DCS, and its main novelty is the introduction of an adaptable parameter. Colorwave maximizes the network throughput, since the readers with few neighbors communicate more often than the ones in denser areas. Moreover, Colorwave is suitable for networks with mobile readers, because it can manage deployment changes, avoiding performance loss.

In this chapter, three different protocols are proposed, adopting the basic mechanisms common to DCS and Colorwave, and without introducing any additional requirements. Table 4.1 summarizes their characteristics.

Table 4.1. Main characteristics of the proposed TDMA anticollision protocols that exploits only one or more data channels

protocol	throughput	fairness	network requirements	density knowledge
PDCS	high	very high	low	high dependence
DCNS	very high	low	low	no dependence
PCW	configuration dependent	configuration dependent	low	no dependence

Probabilistic Distributed Color Selection (PDCS), described in Section 4.1, introduces in the collision resolution of DCS an additional parameter p, representing the probability of adopting a different behavior after the detection of a collision. Consequently, the number of collisions decreases. Moreover, this protocol allows a multichannel transmission, according to the international RFID regulations.

Distributed Color Natural Selection (DCNS) (Section 4.2) is specifically developed in order to exploit a new configuration, called the Killer configuration. The goal of the proposed configuration is to generate a selfish behavior similar to the natural selection. As a result, the throughput of the network improves and the largest benefit can be get by the RFID readers chosen according to the application specification.

Probabilistic Colorwave (PCW), described in Section 4.3, introduces a probabilistic parameter in the collision resolution routine of Colorwave. The effects of this factor are analyzed for two different configurations: the one proposed in [10, 11] and the killer configuration adopted by DCNS.

4.1 Probabilistic Distributed Color Selection

Probabilistic Distributed Color Selection (PDCS) is a multichannel protocol, which can manage an arbitrary number of channels, according to the various regulations regarding RFID. After a collision in PDCS, readers choose both a new color and a new channel. Moreover, a new parameter p is introduced in order to decrease the number of collisions generated by the change of color due to a previous collision. p represents the probability of changing color after a collision. In DCS, after sensing a collision, all the involved readers choose a new color and reserve it. However, if a high number of the timeslots is used, a change of color probably generates a second change without timeslot reservation, so a collision between two readers is more likely to occur. Furthermore, the kicked reader will not transmit during the reserved round, and during the subsequent collision round, so it have to wait two rounds before transmitting. After a collision between two readers, both of them reserve a new color: this double color change could generate two consecutive collisions.

The variables of PDCS are the following:

- $color_i$, the index of the timeslot used by reader$_i$ for transmitting;
- $channel_i$, the index of the frequency channel used by reader$_i$ for transmitting;
- $prev\_channel_i$, the index of the previous channel used by reader$_i$;
- μ, the number of timeslots in a round;
- μc, the number of channels in a round;
- $kickflag_i$, a boolean flag that is true when reader$_i$ requires a kick;
- $transflag_i$, a boolean flag that is true when reader$_i$ requires a transmission.

As in DCS, in PDCS the transmissions are organized in rounds divided in timeslots. The total number of slots available at each round is equal to $\mu \cdot \mu c$. Each slot is composed of the following phases and subroutines:

- *Timeslot initialization*, the readers update the value of their variables;
  - **New timeslot**:
    $\forall i : color_i = (color_i + 1) \bmod \mu$;
    `if (reader`$_i$ `has to read tags)`
    `then` $transflag_i =$ `true;`
- *Kick phase*, the readers send the kicks in order to manage the slot reservation, and choose a new color if they receive a kick.
  - **Kick sending**:
    `if (`$kickflag_i =$ `true AND` $color_i = 0$`)`
    `then reader`$_i$ `sends the kick;`
    $kickflag_i =$ `false;`
  - **Kick resolution**:
    `if (reader`$_i$ `receives a kick on` $channel_i$ `AND` $color_i = 0$`)`
    `then` $prev\_channel_i = channel_i$`;`
    `while` $(color_i = 0$ `AND` $channel_i = prev\_channel_i)$
    $color_i = random(\mu)$;
    $channel_i = random(\mu c)$;
- *Transmission phase*, the readers try to communicate with the tags, and eventually choose a new color if they collide.
  - **Transmission**:
    `if (`$transflag_i =$ `true AND` $color_i = 0$`)`
    `then reader`$_i$ `transmits`
    $transflag_i =$ `false;`
  - **Collision resolution**:
    `if (reader`$_i$ `collides AND` $random(1.0) < p$`)`
    then $color_i = random(\mu)$;
    $channel_i = random(\mu c)$;
    $kickflag_i =$ true;
    $transflag_i =$ true;

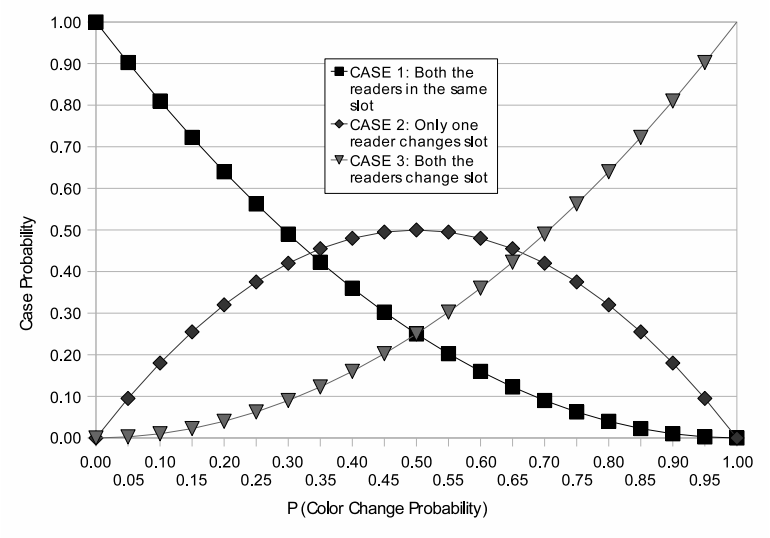

Figure 4.1. Color change after a collision between 2 Readers

4.1.1 Theoretical analysis

The difference between PDCS and DCS relies in the collision resolution, whose behavior is characterized by the probability p. If $p = 1$, the behavior of PDCS corresponds to DCS. The first step of this theoretical analysis is focused on the behavior of PDCS after a collision between two readers. A reader involved in a collision changes its color with probability p, so after a collision between two readers three cases are possible:

1. No reader changes its color, so at the subsequent round the involved readers will receive a kick and they will change color without reservation;

2. Only one reader changes its color, so at the subsequent round a reader will transmit with the previous color, and the other one will reserve a new color;

3. Both readers change color, this case corresponds to the DCS collision resolution.

Case 1 is worse than DCS, since the involved readers will lose a second round. Case 2 is better than DCS, since one reader probably will not produce second generation collisions. Case 3 corresponds to DCS. Figure 4.1 shows the probability of each case (c_i), according to p. Roughly analyzing the effects of p on the performance of the RFID reader network, it is possible to consider that Case 1 is negative, Case 2 is positive, and that Case 3 is intermediate. Starting from $p = 1$, a short decrease of p corresponds to:

- a rise of Case 1 (*negative case*);
- a increase of Case 2 (*positive case*);
- a fall of Case 3 (*intermediate case*).

Therefore, since Case 2 improves the performance of the protocol, and Case 1 decreases it, the values of $0.5 < p < 1$ should bring positive results, as shown in Figure 4.1.

The effects of the different cases on the performance of the protocol are analyzed observing the number of *second generation collisions (γ)*, which represents the average number of readers involved in collisions produced by the *first generation collisions (ϕ)*.

Second Generation Collisions

The collisions affect the performance of RFID networks, since the involved readers have to wait before transmitting. Both in DCS and PDCS, each collision can generate new collisions. This behavior can produce a relevant number of collisions at each round. This section carefully analyzes the effects of a collision between two readers. γ can be partitioned in three γ_i related to each case described in the previous section:

$$\gamma = c_1 * \gamma_1 + c_2 * \gamma_2 + c_3 * \gamma_3 \ . \tag{4.1}$$

where c_i represents the probability of Case i, as reported in Fig. 4.1, and γ_i represents the average number of readers involved in second generation collision due to Case i. The formulas to calculate each γ_i are presented in the following, where γ_i is function of μ and of the number of engaged colors (ϵ).

Case 1. The probability of Case 1 is:

$$c_1 = (1-p)^2. \tag{4.2}$$

This case involves a couple of concurrent kicks. After the kick each reader changes color without reservation, so the number of second generation collisions is related to the state of the new colors. If:

- both colors are free, then no second generation collision is produced and the contribution to γ_1 is null;
- one color is free and one color is engaged, then one second generation collision between two readers is produced; the contribution to γ_1 is $\gamma_{1a} \cdot c_{1a}$:

$$\gamma_{1a} = 2;\ c_{1a} = 2 \cdot \frac{\epsilon}{\mu - 1} \cdot \left(1 - \frac{\epsilon}{\mu - 1}\right); \tag{4.3}$$

- both colors are engaged, then two second generation collisions between two couples of readers are produced; the contribution to γ_1 is $\gamma_{1b} \cdot c_{1b}$:

$$\gamma_{1b} = 4;\ c_{1b} = \frac{\epsilon}{\mu - 1} \cdot \frac{\epsilon - 1}{\mu - 1}; \tag{4.4}$$

- the same free color is selected, then one second generation collision between two readers is produced; the contribution to γ_1 is $\gamma_{1c} \cdot c_{1c}$:

$$\gamma_{1c} = 2;\ c_{1c} = \left(1 - \frac{\epsilon}{\mu - 1}\right) \cdot \frac{1}{\mu - 1}; \tag{4.5}$$

- the same engaged color is selected, then one second generation collision between three readers is produced; the contribution to γ_1 is $\gamma_{1d} \cdot c_{1d}$:

$$\gamma_{1d} = 3;\ c_{1d} = \frac{\epsilon}{\mu - 1} \cdot \frac{1}{\mu - 1}; \tag{4.6}$$

The contribution of Case 1 is:

$$\gamma_1 = \gamma_{1a} \cdot c_{1a} + \gamma_{1b} \cdot c_{1b} + \gamma_{1c} \cdot c_{1c} + \gamma_{1d} \cdot c_{1d}. \tag{4.7}$$

Case 2. The probability of Case 2 is:

$$c_2 = 2 \cdot p \cdot (1 - p). \tag{4.8}$$

In this case the reader that has not changed color will not produce second generation collisions, but it can collide with the second reader, since it could choose the same color again. The second reader changes color, so the number of second generation collisions is related to the state of the new color. If:

- the color is free, then no second generation collision is produced; the contribution to γ_2 is null;

- the color is engaged, then one reader changes color without reservation, so a collision between 2 readers has probability equal to the percentage of engaged colors; the contribution to γ_2 is $\gamma_{2a} \cdot c_{2a}$:

$$\gamma_{2a} = 2;\ c_{2a} = \frac{\epsilon}{\mu} \cdot \frac{\epsilon}{\mu - 1} \tag{4.9}$$

- the color is the same as the previous collision, then there is a couple of concurrent kicks between the two readers of the first collision; the contribution to γ_2 is $\gamma_{2b} \cdot c_{2b}$:

$$\gamma_{2b} = \frac{4 \cdot \epsilon}{\mu - 1} \cdot \left(1 - \frac{\epsilon}{\mu - 1}\right) + \frac{4 \cdot \epsilon}{\mu - 1} \cdot \frac{\epsilon - 1}{\mu - 1} + \frac{2}{\mu - 1} \cdot \left(1 - \frac{\epsilon}{\mu - 1}\right) + \frac{3}{\mu - 1} \cdot \frac{\epsilon}{\mu - 1}$$

$$c_{2b} = \frac{1}{\mu} \tag{4.10}$$

The contribution of Case 2 is:

$$\gamma_2 = \gamma_{2a} \cdot c_{2a} + \gamma_{2b} \cdot c_{2b}. \tag{4.11}$$

Case 3. The probability of Case 3 is:

$$c_3 = p^2. \tag{4.12}$$

In this case both readers change color. The number of second generation collisions is related to the state of the new colors. If:

- both colors are free, then no second generation collision is produced; the contribution to γ_3 is null;
- one color is free and one color is engaged, then one reader changes color without reservation, so a collision between 2 readers has probability equal to the percentage of engaged colors; the contribution to γ_3 is $\gamma_{3a} \cdot c_{3a}$:

$$\gamma_{3a} = 2;\ c_{3a} = 2 \cdot \frac{\epsilon}{\mu} \cdot \frac{1 - \epsilon}{\mu} \cdot \frac{\epsilon}{\mu - 1}; \tag{4.13}$$

- both colors are engaged, then two readers change color without reservation, so they could produce:
  - one collision between two readers,

$$\gamma_{3b1} = 2;\ c_{3b1} = 2 \cdot \frac{\epsilon - 1}{\mu - 1} \cdot \left(1 - \frac{\epsilon - 1}{\mu - 1}\right) + \left(1 - \frac{\epsilon - 1}{\mu - 1}\right) \cdot \frac{1}{\mu - 1} \tag{4.14}$$

  - two collisions between two couples of readers,

$$\gamma_{3b2} = 4;\ c_{3b2} = \frac{\epsilon - 2}{\mu - 1} \cdot \frac{\epsilon - 2}{\mu - 1} + \frac{1}{\mu - 1} \cdot \frac{\epsilon - 1}{\mu - 1}, \tag{4.15}$$

– one collision between three readers,

$$\gamma_{3b3} = 3;\ c_{3b3} = \frac{\epsilon - 2}{\mu - 1} \cdot \frac{1}{\mu - 1}, \tag{4.16}$$

– or no collision;

the contribution to γ_3 is $\gamma_{3b} \cdot c_{3b}$:

$$\gamma_{3b} = (\gamma_{3b1} \cdot c_{3b1} + \gamma_{3b2} \cdot c_{3b2} + \gamma_{3b3} \cdot c_{3b3});\ c_{3b} = \frac{\epsilon}{\mu} \cdot \frac{\epsilon - 1}{\mu}; \tag{4.17}$$

- the same free color is selected, then there is a couple of concurrent kicks between the two readers of the first collision; the contribution to γ_3 is $\gamma_{3c} \cdot c_{3c}$:

$$\gamma_{2b} = \frac{4 \cdot \epsilon}{\mu - 1} \cdot \left(1 - \frac{\epsilon}{\mu - 1}\right) + \frac{4 \cdot \epsilon}{\mu - 1} \cdot \frac{\epsilon - 1}{\mu - 1} + \frac{2}{\mu - 1} \cdot \left(1 - \frac{\epsilon}{\mu - 1}\right) + \frac{3}{\mu - 1} \cdot \frac{\epsilon}{\mu - 1}$$

$$c_{3c} = \left(1 - \frac{\epsilon}{\mu}\right) \cdot \frac{1}{\mu} \tag{4.18}$$

- the same engaged color is selected, then three readers change color without reservation, so they could produce:

– one collision between two readers,

$$\gamma_{3d1} = 2; \tag{4.19}$$

$$c_{3d1} = 3\frac{\epsilon - 1}{\mu - 1}\left(1 - \frac{\epsilon - 1}{\mu - 1}\right)\left(1 - \frac{\epsilon}{\mu - 1}\right) + \left(1 - \frac{\epsilon - 1}{\mu - 1}\right)\left(1 - \frac{\epsilon}{\mu - 1}\right)\frac{2}{\mu - 1}$$

– two collisions between two couples of readers,

$$\gamma_{3d2} = 4; \tag{4.20}$$

$$c_{3d2} = 3\frac{\epsilon - 1}{\mu - 1}\left(1 - \frac{\epsilon - 1}{\mu - 1}\right)\frac{\epsilon - 2}{\mu - 1} + \frac{\epsilon - 1}{\mu - 1}\left(1 - \frac{\epsilon - 1}{\mu - 1}\right)\frac{3}{\mu - 1}$$

– three collisions between three couples of readers,

$$\gamma_{3d3} = 6;\ c_{3d3} = \frac{\epsilon - 1}{\mu - 1} \cdot \frac{\epsilon - 2}{\mu - 1} \cdot \frac{\epsilon - 3}{\mu - 1} \tag{4.21}$$

– one collision between three readers,

$$\gamma_{3d4} = 3; \tag{4.22}$$

$$c_{3d4} = \left(1 - \frac{\epsilon - 1}{\mu - 1}\right) \cdot \left(\frac{1}{\mu - 1}\right)^2 + 3 \cdot \frac{\epsilon - 1}{\mu - 1} \cdot \left(1 - \frac{\epsilon - 1}{\mu - 1}\right) \cdot \frac{1}{\mu - 1}$$

– one collision between three readers and one collision between two readers,

$$\gamma_{3d5} = 5;\ c_{3d5} = \frac{\epsilon - 1}{\mu - 1} \cdot \frac{\epsilon - 2}{\mu - 1} \cdot \frac{2}{\mu - 1} \tag{4.23}$$

– one collision between four readers,

$$\gamma_{3d6} = 4;\ c_{3d6} = \frac{\epsilon - 1}{\mu - 1} \cdot \left(\frac{1}{\mu - 1}\right)^2 \tag{4.24}$$

– or no collision.

The contribution to γ_3 is $\gamma_{3d} \cdot c_{3d}$:

$$\gamma_{3d} = \sum_{i=1}^{6} \gamma_{3di}\ ;\quad c_{3d} = \frac{\epsilon}{\mu} \cdot \frac{1}{\mu}. \tag{4.25}$$

According to previous formulas, the contribution of Case 3 is:

$$\gamma_3 = \gamma_{3a} \cdot c_{3a} + \gamma_{3b} \cdot c_{3b} + \gamma_{3c} \cdot c_{3c} + \gamma_{3d} \cdot c_{3d}. \tag{4.26}$$

Results. Figure 4.2 shows the values of γ_1, γ_2, and γ_3, and of their components, with $\mu = 20$. The component that mainly affects the value of γ_1 is $\gamma_{1b} \cdot c_{1b}$, which represents the number of second generation collisions due to the choice of two engaged new colors. γ_1 rises constantly, according to the increase of ϵ. The component that mainly affects the value of γ_2 is $\gamma_{2a} \cdot c_{2a}$, which represents the number of second generation collisions due to a kick on an engaged color, and to the subsequent change to a new engaged color. The component that mainly affects the value of γ_3 is $\gamma_{3b} \cdot c_{3b}$, which represents the number of second generation collisions due to two kicks on an engaged color, and to the subsequent change to two new colors.

Figure 4.3 compares the γ_i values according to $\mu = 20$, and shows that γ_1 represents the largest number of second generation collisions, and γ_2 the smallest.

Figure 4.4 shows γ according to various values of p, with $\mu = 20$. The graph roughly highlights the effects of p on γ, with $p = 0$ and $p = 1$, $\gamma = \gamma_1$ and $\gamma = \gamma_3$, respectively. Since γ_1 is always larger than γ_3, the value of γ reached by $p' < 0.50$ is larger than γ reached by $p'' = 1 - p'$, so the minimization of γ requires $p >= 0.50$. When $0 \leq \epsilon \leq 3$, the smallest γ is reached by $p = 1$, when $4 \leq \epsilon \leq 12$, the smallest γ is reached by $p = 0.75$, and when $15 \leq \epsilon \leq 19$, the smallest γ is reached by $p = 0.50$. Therefore, in order to minimize γ, at the rise of ϵ there should be a corresponding decrease of p from 1 to 0.50.

When a collision among readers produces new collisions among a larger number of readers, the number of collisions increases, but the engaged colors decrease. The

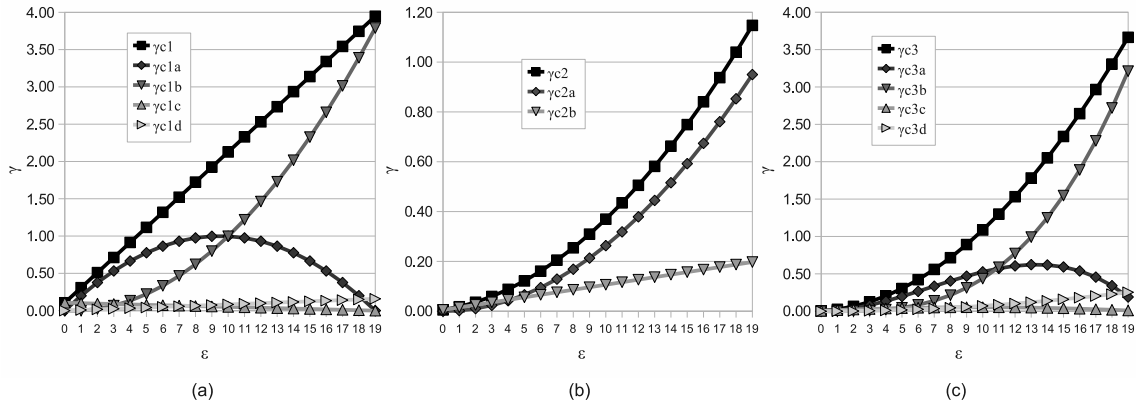

Figure 4.2. (a) γ_1 (b) γ_2 (c) γ_3 with $\mu = 20$

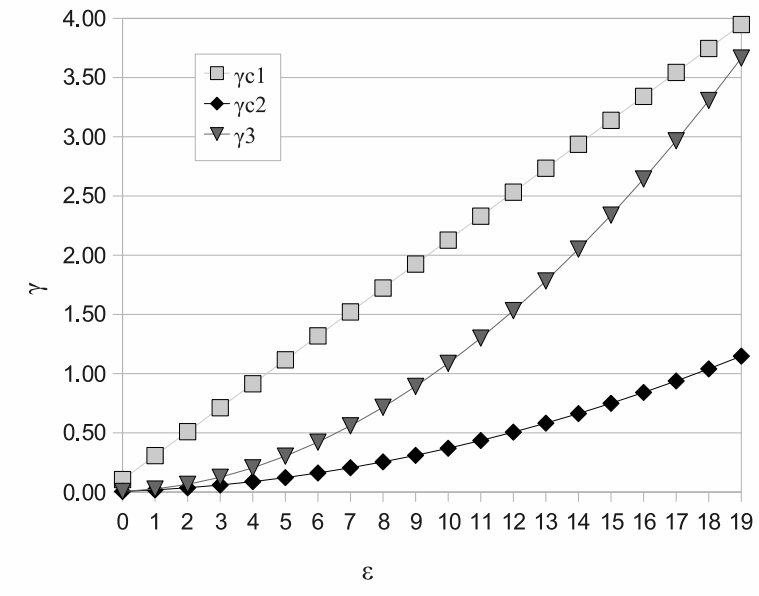

Figure 4.3. γ_i with $\mu = 20$

decrease of engaged colors produces a decline in γ, until the number of colliding readers is stable. Since γ is the average number of second generation collisions produced by the collision of two readers, if $\gamma > 2$, the number of collision rises, while $\gamma < 2$, the number of collision decreases.

In order to find the optimal values of p that minimizes γ, the first derivative of (4.1) is set to 0 and it is solved for p:

$$\gamma(p) = (1-p)^2 \cdot \gamma_1 + 2 \cdot p \cdot (1-p) \cdot \gamma_2 + p^2 \cdot \gamma_3 \; ; \tag{4.27}$$

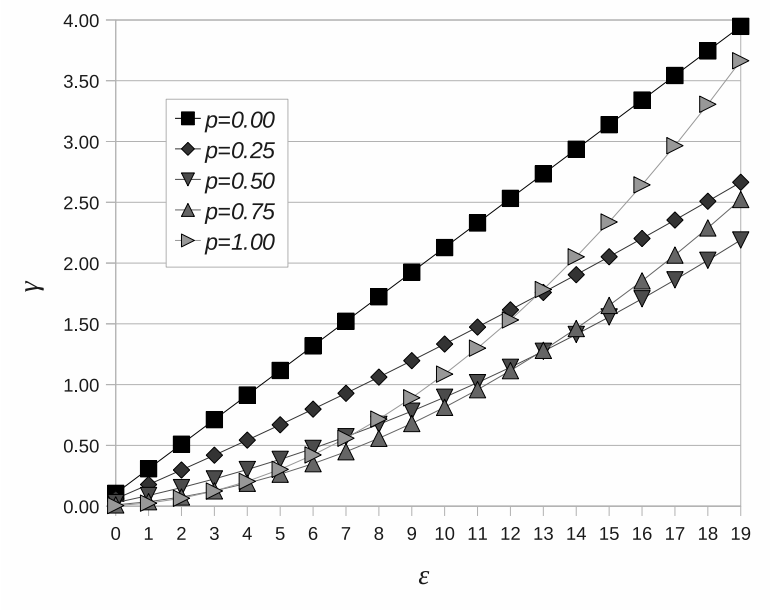

Figure 4.4. γ with $\mu = 20$, according to p.

$$\frac{d\gamma}{dp} = (2p - 2) \cdot \gamma_1 + 2 \cdot (1 - 2p) \cdot \gamma_2 + 2p \cdot \gamma_3 = 0 \; ; \tag{4.28}$$

$$p = \frac{2\gamma_1 - 2\gamma_2}{2\gamma_1 - 4\gamma_2 + 2\gamma_3}. \tag{4.29}$$

Figure 4.5 shows the values on p that minimize γ with $\mu = 20$. Figure 4.6 shows the comparison among the γ values reached by PDCS and DCS. The comparison is performed for values of ϵ between $\frac{\mu}{2}$ and $\mu - 1$, since an efficient protocol should work with a value of ϵ close to μ. Setting p to a value consistent with the value of ϵ, PDCS reaches over 30% of reduction of γ, with respect to DCS.

Collisions with More Readers. The effects of a collision are different when more than two readers collide in the same timeslot. Figure 4.7 shows the color change probability after a collision among 3 readers:

1. no reader changes its color, so at the subsequent round the involved readers will receive a kick and they will change color without reservation;

2. one reader changes its color, so at the subsequent round two reader will receive a kick and they will change color without reservation, and the second reader will reserve a new color, maybe requiring another reader to change;

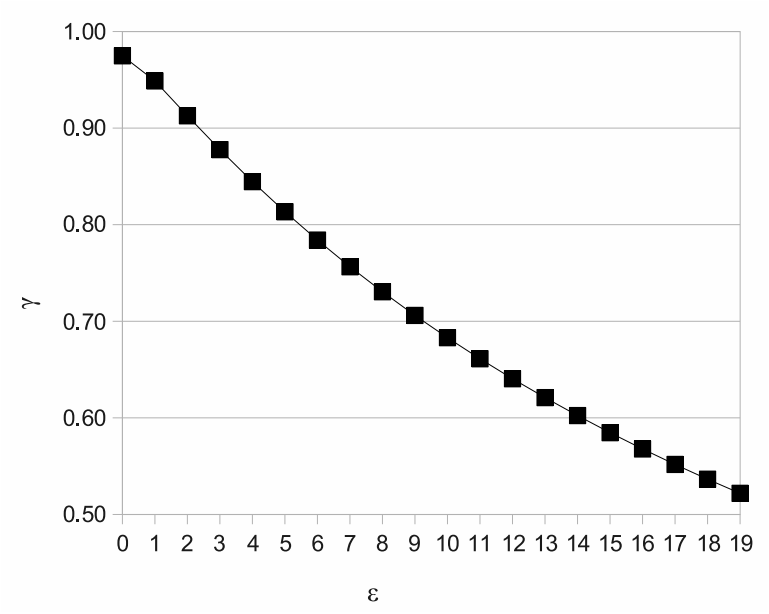

Figure 4.5. Values of p that minimize γ with $\mu = 20$.

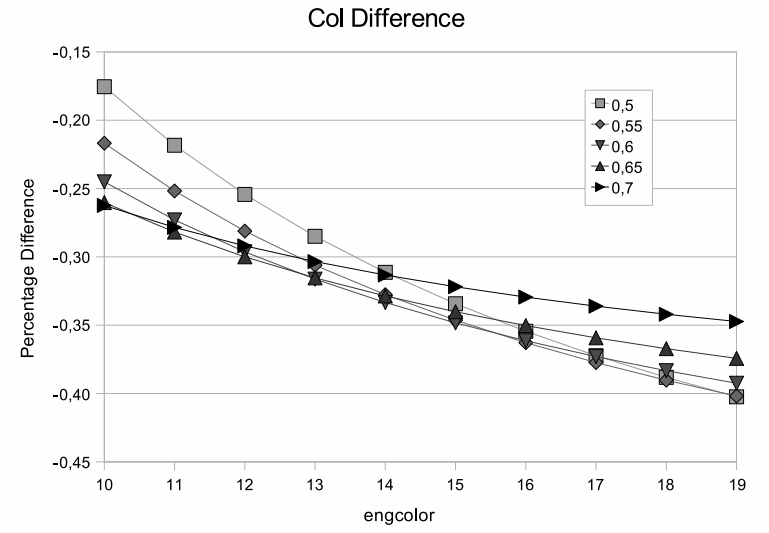

Figure 4.6. Gain of γ between PDCS with various p and DCS.

3. two reader changes its color, so at the subsequent round one reader will transmit with the previous color, and the other readers will reserve a new color, maybe requiring to other readers to change;

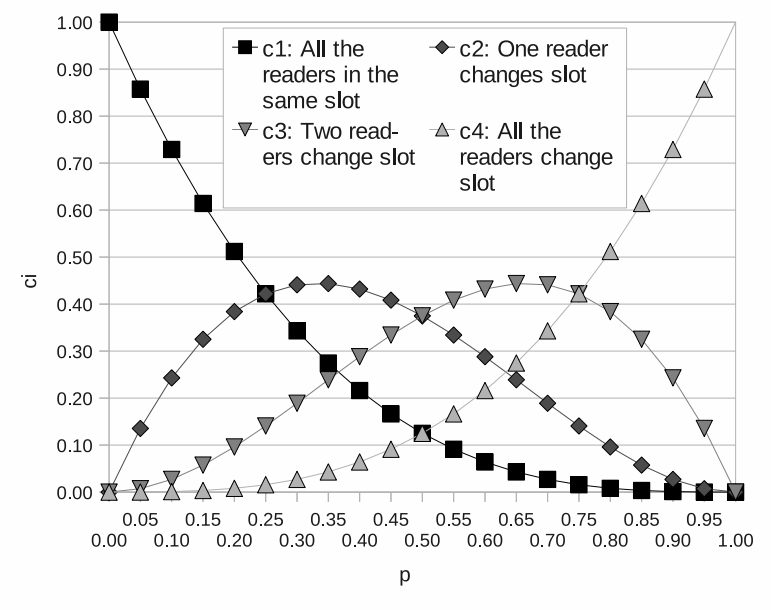

Figure 4.7. Color change after a collision between three Readers

4. all the readers change color, this case corresponds to the DCS collision resolution.

Case 3 is the best, since one reader does not change color, with high probability to transmit. However, Case 1 and Case 2 are worse than Case 4, which corresponds to DCS, since they involve a larger number of kicks.

The highest value of c_3 is reached for $p = 0.66$, so the lowest γ can be reached when $0.66 < p \leq 1$, while after a collisions between 2 readers, the lowest γ can be reached when $0.50 < p \leq 1$. Also for collision among more readers, the best case requires always that only one reader doesn't change color. When the number of colliding readers is N, the probability of the best case is maximized by $p = \frac{N-1}{N}$. Therefore, collisions among a large quantity of readers require a larger value a p.

DCS-Like Protocol Behavior

ϕ and γ are evaluated in order to analyze the behavior of DCS. If:

- $\frac{\gamma}{\phi} > 1$, ϵ decreases due to the larger number of colliding slots, so $\frac{\gamma}{\phi}$ decreases;
- $\frac{\gamma}{\phi} = 1$, the network is steady;
- $\frac{\gamma}{\phi} < 1$, ϵ increases, so $\frac{\gamma}{\phi}$ also increases;

The network should aim at a steady condition, where $\frac{\gamma}{\phi} \cong 1$. Moreover, the behavior of the protocols changes according to three classes of configuration:

1. $\mu \ll number\ of\ neighbors$, in this class the number of colors is too low, so the network is characterized by several collisions, the network tends towards high γ and ϕ, and their values are greater when μ is lower. Thus, the resulting WT could be poor, as the readers often have often to wait for many rounds;

2. $\mu \gg number\ of\ neighbors$, this class is characterized by some starting random collisions, and $\frac{\gamma}{\phi} \gg 1$, so the network tends towards a steady condition, without collisions; however, WT converges to $\mu - 1$, because each reader must wait for $\mu - 1$ slots between two transmissions;

3. $\mu \cong number\ of\ neighbors$, the best configurations can be found in this class, since it contains the configuration with the lowest μ so that the network tends towards a steady condition without collision. Apparently the best configuration should be $\mu = number\ of\ neighbors + 1$, but according to the previous analysis, if $\frac{\gamma}{\phi} > 1$ then ϕ increases, so the effects of the starting random collisions and the collisions due to a change of slot generated by a neighbor with a different neighborhood together with the high ϵ can cause a steady condition with collisions; therefore the best configuration shall require a larger μ.

The main effect of a proper $p < 1$ is the reduction of γ. This configuration also decreases the value of $\frac{\gamma}{\phi}$, so when $\mu \cong number\ of\ neighbors$, it shall tend towards a steady condition if there are also no collision with a lower μ.

4.1.2 Evaluation

Simulations of DCS, Colorwave, AC_MRFID, and PDCS were performed on several kinds of RFID networks, with 250 readers, randomly and regularly deployed, considering a variable number of neighbors described by the average number of neighbors (AN) and its variance (NV).

Each protocol configuration was simulated 50 times for $2 \cdot 10^5$ timeslots. The simulator was written in Java language, and the simulations were run on a DELL Workstation Precision T7500, under Linux Operating System.

Colorwave has been simulated with different configurations changing the values of the 4 thresholds with a step of 5%, in order to find the best configuration. The configuration which provides the best OARWT has been selected and used for the comparison. The selected thresholds are 85% (hard up), 75% (soft up), 55% (soft down), 25% (hard down). The provided performance is OARWT 7.54 s; TAWT 7.17 s; MWT 88.49 s; TWTV 64.80 s^2; VAWT 3.46 s^2; throughput 32.70 NT/s.

In Colorwave μ is dynamic, so in the following graphs that compare the performance of the described protocols according to μ, Colorwave is represented by a horizontal line.

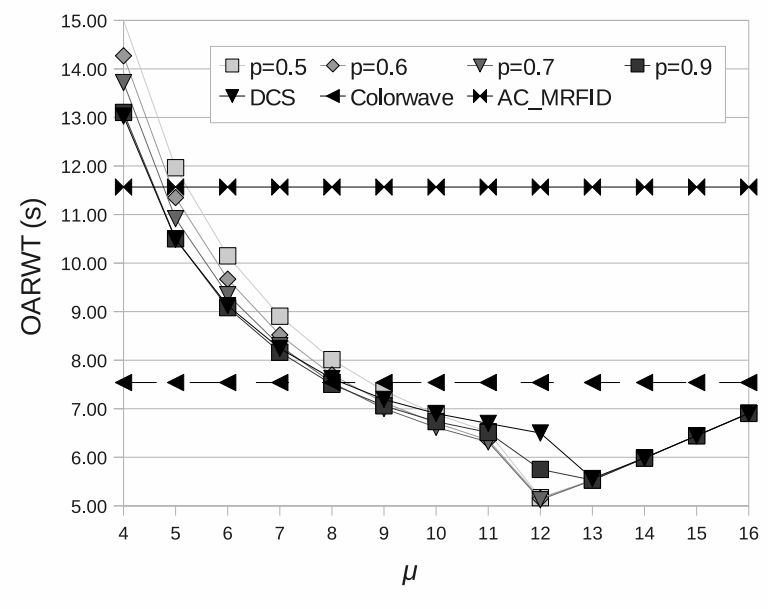

Figure 4.8. OARWT provided by DCS, PDCS, Colorwave, and AC_MRFID with $AN = 9.94$, $NV = 9.41$, and random deployment

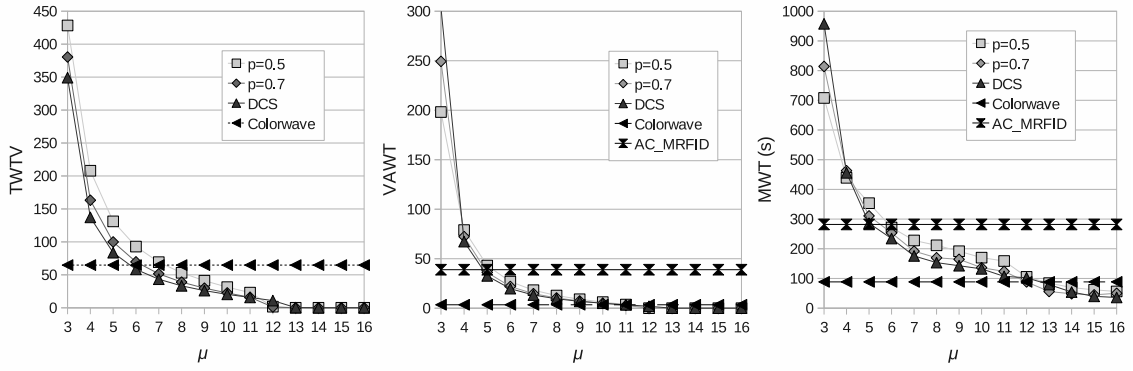

Figure 4.9. TWTV (a), VAWT (b), and MWT provided by DCS, PDCS, Colorwave, and AC_MRFID with $AN = 9.94$, $NV = 9.41$, and random deployment

Table 4.2. Performance of DCS and PDCS with $\mu = 12$, $AN = 9.94$, $NV = 9.41$, and random deployment

	PDCS				DCS
p	0.5	0.6	0.7	0.9	1.0
NT/s	44.31	44.46	44.85	41.11	37.13
MWT	105.41	99.42	88.29	85.52	102.28
TAWT	5.09	5.10	5.10	5.16	6.28
TWTV	1.68	0.78	1.15	6.72	10.92
VAWT	0.03	0.03	0.00	0.79	1.93
OARWT	2.37	2.36	2.36	2.65	2.99

Table 4.3. Time reduction provided by PDCS with respect to standard DCS, with $\mu = 12$, $AN = 9.94$, $NV = 9.41$, and random deployment

	$p = 0.5$	$p = 0.6$	$p = 0.7$	$p = 0.9$
NT/s	+19.34%	+19.75%	+20.79%	+10.73%
MWT	+3.06%	-2.79%	-13.68%	-16.38%
TAWT	-18.98%	-18.75%	-18.82%	-17.82%
TWTV	+243.27%	-66.33%	+135.67%	+371.97%
VAWT	-98.35%	-98.70%	-99.85%	-59.27%
OARWT	-20.78%	-20.97%	-20.99%	-11.44%

PDCS Behavior According to μ

The value of μ must be carefully selected, in order to reach good performance. When μ is too low, the percentage of colliding transmissions is high, so WT is high and it is not steady. When μ is too high, WT is close to $\mu - 1$ timeslots. According to the theoretical analysis, the best value of μ is the lowest one that allows a steady WT. Furthermore, the theoretical analysis states that the introduction of $p < 1$ decreases the best μ improving WT.

Fig. 4.8 shows the OARWT provided by DCS and PDCS according to several μ and p, on a network with $AN = 9.94$, $NV = 9.41$, and random deployment. This graph is a good indicator of the time performance of the network. Fig. 4.9 shows the TWTV, VAWT, MWT, in the same conditions. The graphs support the results of the theoretical analysis presented in Section 4.1.1:

1. $\mu \ll number\ of\ neighbors$ ($\mu \ll 10$), the provided WT is not good, since the readers collide many times; DCS provides better performance, and PDCS provides the best OARWT with p as close as possible to 1;

2. $\mu \gg number\ of\ neighbors$ ($\mu \gg 10$), the network is steady, since there are no collisions; however, WT converges to $\mu - 1$ timeslots, because each reader must wait $\mu - 1$ slots between two transmissions; DCS and PDCS provide the same performance, independently from p;

3. $\mu \cong number\ of\ neighbors$ ($\mu \cong 10$), the best configurations are in this class, where the network tends towards a steady condition without collisions at the lowest μ; the best configurations require $\mu > 10$. In DCS and PDCS with a high probability ($p \geq 0.9$), the best OARWT is provided with $\mu = 13$. In PDCS with a probability $p < 0.9$, the best OARWT is provided with $\mu = 12$. The best OARWT is provided by PDCS with $p = 0.72$ and $\mu = 12$, where OARWT= 5.08 s, 21.87% better than DCS with the same μ, and 8.69% better than the best configuration provided by DCS. The provided TWTV rapidly falls, according to the lower number of colliding transmissions. Tab. 4.2 shows the performance provided by PDCS and DCS with $\mu = 12$, and Tab. 4.3 shows the difference between PDCS and DCS in percentage. All the indicators show that a low p provides good performance.

Furthermore, Fig. 4.8 and Fig. 4.9 compare PDCS and DCS with Colorwave and AC_MRFID. Fig. 4.8 shows the OARWT provided by Colorwave and by AC_MRFID. AC_MRFID does not provide a good OARWT, since this algorithm gives more resources to the readers with less neighbors, decreasing the fairness among readers and OARWT. Colorwave provides a good OARWT, but it can not reach the one provided by the best configurations of DCS and PDCS.

Observing Fig. 4.8, Fig. 4.9, Table 4.2, and Table 4.3, we can state that:

- with a low p and $\mu \cong number\ of\ neighbors$, PDCS provides shorter OARWT;
- with a very low μ, a minor p in PDCS provides worse performance;
- with a very high μ, all the protocols provide the same efficiency;
- with a high μ, when all the configurations reach a steady network, all the protocols provide the same fairness, since VAWT is 0;
- when $\mu \cong number\ of\ neighbors$, PDCS with low p is the fairest, since more readers are reaching a steady behavior;
- with a very low μ, DCS is the fairest;
- the introduction of p reduces γ, decreasing WT, but it increases the possibility of a single reader to collide several consecutive times, according to Case 1 described in Section 4.1.1. The best MWT is normally provided by PDCS with a high p, since it decreases WT, with a low occurrence of Case 1.

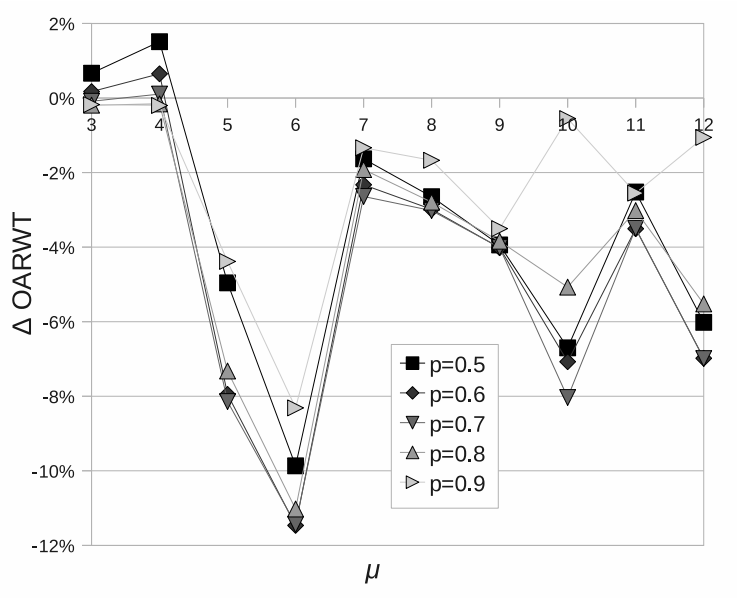

Figure 4.10. Difference between the OARWT provided by DCS and PDCS with various p, with $AN = 9.94$, $NV = 9.41$, and random deployment

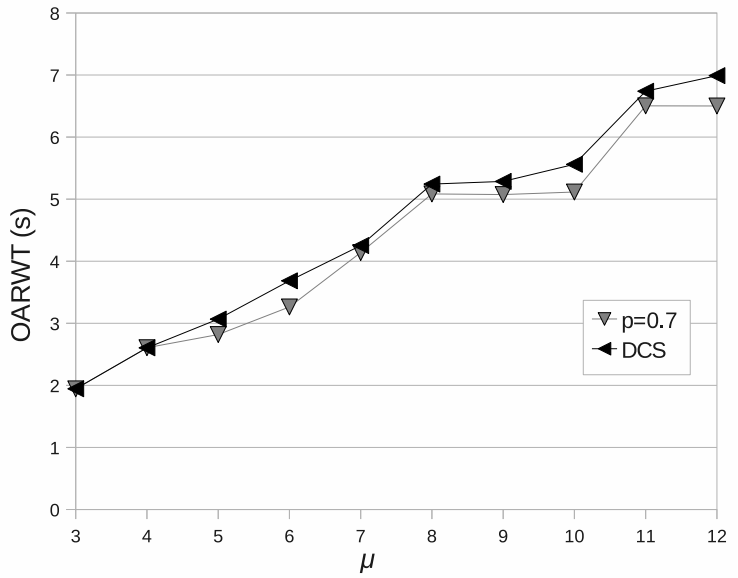

Figure 4.11. OARWT provided by DCS and PDCS ($p = 0.7$) with $AN = 9.94$, $NV = 9.41$, and random deployment

PDCS Behavior According to AN

In order to analyze the behavior of PDCS according to networks with different size, PDCS and DCS have been simulated with networks with $3 \leq \mu \leq 12$.

Fig. 4.10 shows the difference between the OARWT provided by DCS and PDCS with various p. With a sparse network (AN$\leq$ 4) low values of p (0.5 and 0.6) provide results worse than DCS, instead with denser networks PDCS is always better than DCS. The best p is 0.7, which provides an optimal OARWT. Fig. 4.11 shows the OARWT provided by PDCS with $p = 0.7$ compared to DCS.

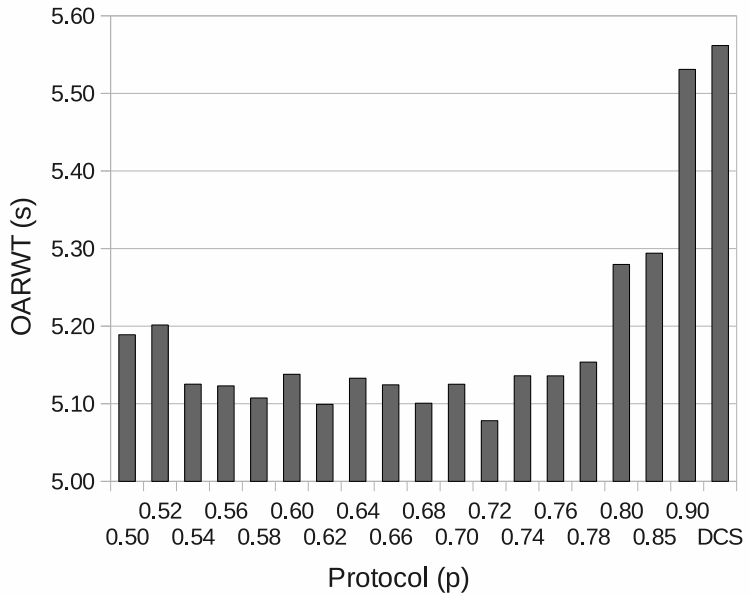

Figure 4.12. OARWT provided by DCS and PDCS with $AN = 9.94$, $NV = 9.41$, and random deployment

Best PDCS Configurations

In order to find the best PDCS configuration, it is possible to observe which value of p provides the best OARWT. Fig. 4.12 shows the performance provided by DCS and PDCS in a network with $AN = 9.94$, $NV = 9.41$, and a random deployment. The best results are provided from $p = 0.5$ to $p = 0.78$. In this range OARWT fluctuates between 5.08 and 5.19.

Since several values of p provide good results with a proper μ, also their performance with a worse μ must be analyzed. When μ is too high, p does not affect the performance, and always PDCS provides the same result. However, when μ is too low p strongly affects the performance. Fig. 4.13 shows PDCS with $0.5 \leq p \leq 0.7$, $5 \leq \mu \leq 7$. Although the values of p are similar, OARWT does not fluctuate, and the higher p always provides a lower OARWT.

Therefore, $p = 0.7$ is an optimal configuration, since it provides good OARWT with a proper μ, and an OARWT better than the one provided with a lower p and

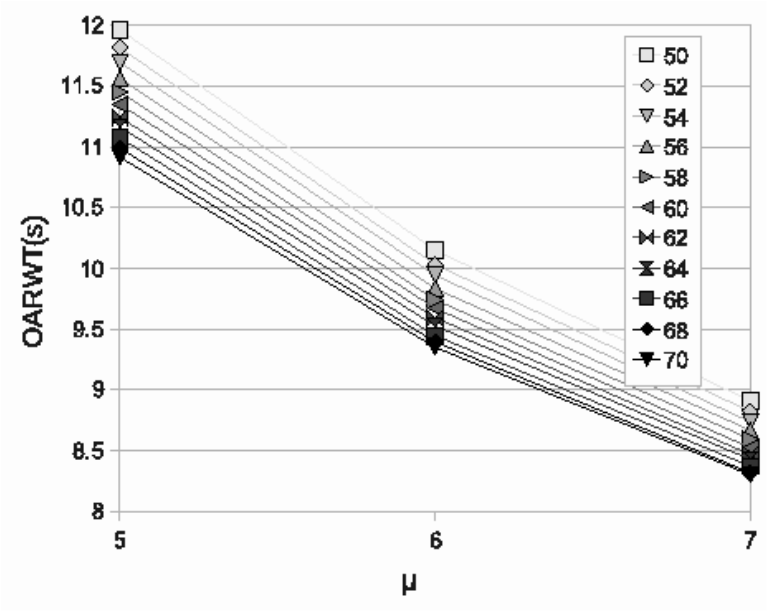

Figure 4.13. OARWT provided by PDCS, with $AN = 9.94$, $NV = 9.41$, and random deployment

a low μ.

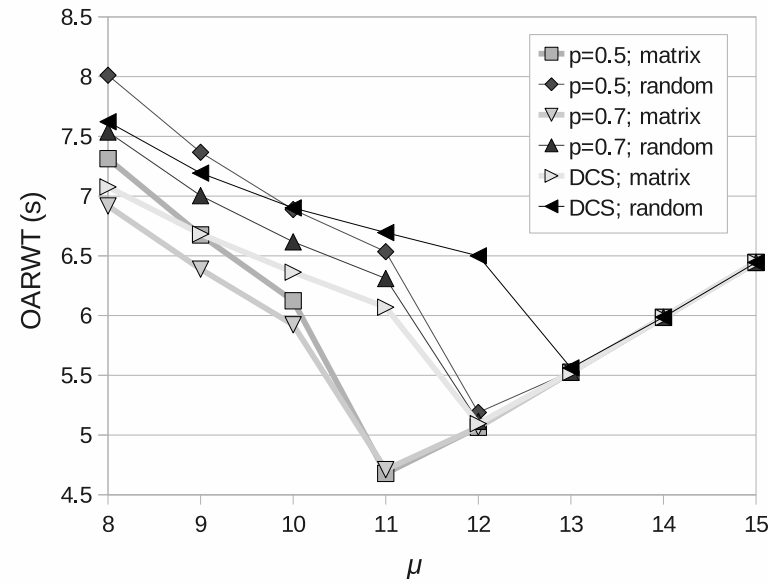

Figure 4.14. OARWT provided by DCS and PDCS with $AN = 9.94$, $NV = 9.41$, random deployment and $AN = 9.94$, $NV = 3.90$, and matrix deployment

Matrix Vs Random Deployment

In order to reach a selected number of neighbors, several random deployments have been considered, with the same number of readers but on areas with different sizes. However, in order to check how different deployments with similar AN affect performance, we have simulated also a network with matrix deployment, where the locations of the readers create a regular shape representing a matrix. The performance of PDCS and DCS on a network with random deployment, $AN = 9.94$, and $NV = 9.41$, and on a network with matrix deployment, $AN = 9.94$, and $NV = 3.90$ have been analyzed. Fig. 4.14 shows the provided OARWT. All the protocols provide better performance on the matrix deployment. The best OARWT is provided by PDCS with $p = 0.5$ and $\mu = 11$, where OARWT= 4.68 s, 22.92% better than OARWT provided with the same μ, and 8.17% better than the best DCS configuration.

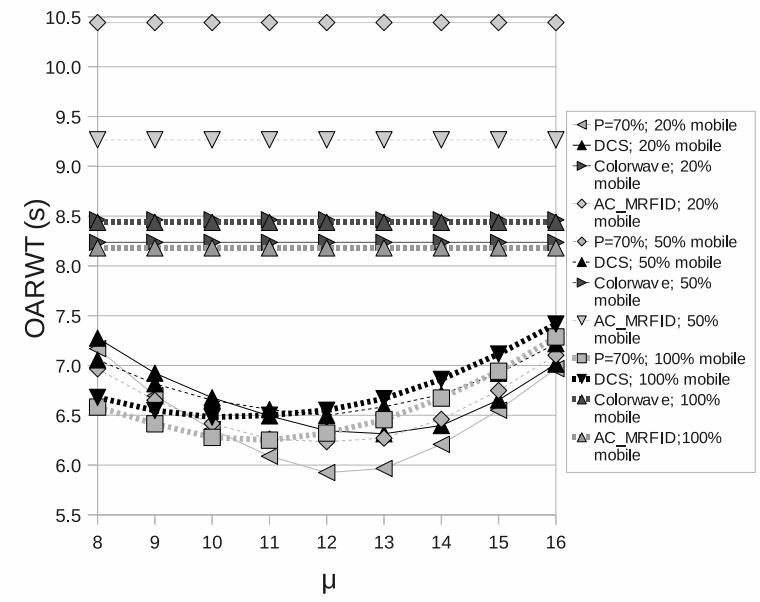

Figure 4.15. OARWT provided by DCS, PDCS, Colorwave, and AC_MRFID with starting $AN = 9.94$, $NV = 9.41$, random deployment, and 20%, 50%, and 100% of mobile readers

Mobile RFID Networks

Real RFID applications can require networks composed of mobile readers mixed to static readers. The presence of mobile readers affects the performance of anticollision protocols, because when a reader changes location it finds new neighbors with new colors.

Fig. 4.15 shows the OARWT provided by PDCS, DCS, Colorwave and AC_MRFID in a network with $AN = 9.94$, $NV = 9.41$, random deployment, and 20%, 50%, and 100% of mobile readers. Similarly to static networks, the best results, at $\mu = 12$, are provided by PDCS with $p = 0.7$. However, the curves of DCS and PDCS change more slowly than in previous graphs, and they are shifted up, since mobile readers can not reach a steady color, and shifted left, since the quantity of neighbors is more regular. The OARWT provided by Colorwave is only slightly worse with several mobile readers, since the negative effects due to the impossibility to reach a steady color configuration are reduced by the adaptable parameter μ. Differently from other protocols, the OARWT provided by AC_MRFID improves with mobile readers, since this protocol adjusts rapidly its configuration to the new position of readers, and the adopted method is suitable to regular quantity of neighbors per reader.

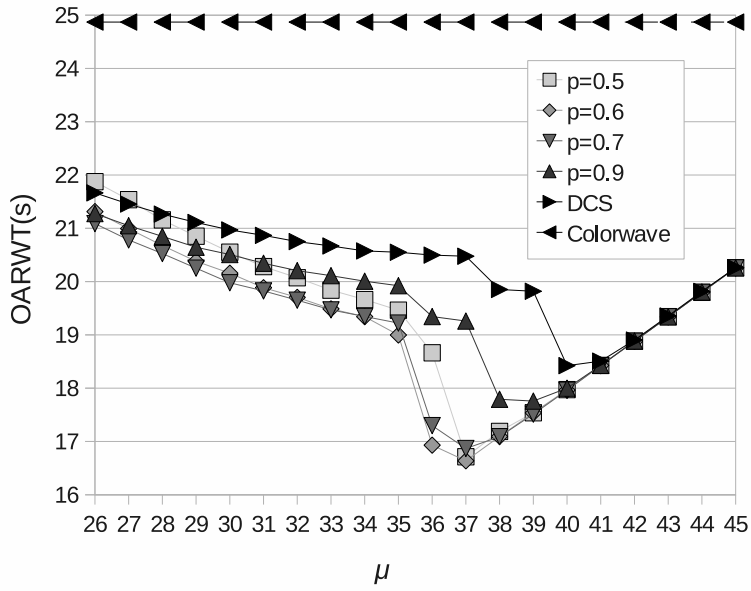

Figure 4.16. Effects of p on OARWT with $AN = 29.92$, $NV = 70.19$, and random deployment

Dense RFID Networks

The results of the simulation of PDCS with dense RFID networks are similar to the results for networks with less neighbors, but the gap between PDCS and DCS time performance is wider. The simulations have been performed considering $0.5 \leq p \leq 1$, with a step of 0.1.

Figure 4.16 shows the OARWT provided by PDCS and DCS for a network with $AN = 29.92$, $NV = 70.19$, and random deployment. The best OARWT, with $p = 0.6$ and $\mu = 37$ reaches 18.75% time reduction with respect to the OARWT of DCS with the same μ, and 9.69% with respect to the best OARWT provided by DCS with $\mu = 40$.

4.2 Distributed Color Natural Selection (DCNS)

In Colorwave, the opportunity to change the value of μ is evaluated comparing the percentage of collisions to four thresholds. The thresholds strongly affect the behavior of the network: very high or very low percentages of collisions may lead to dramatically low performance. If the percentage is very high, the reader usually collides, without querying tags. On the contrary, if the percentage is too low, the channel could often be unused, wasting resources. In [10] and [11], the authors proposed to set the two highest thresholds close to 1, and the two lowest thresholds close to 0. With such thresholds, the readers only change μ when the percentage of collisions is very high or very low. Therefore, if the performance is not significantly low, the network does not evolve.

In contrast to the configurations proposed in [10, 11], the Killer configuration is presented. Its main effect is that each reader always tries to get more resources, in a dynamic way. In order to reach this selfish behavior, the values of all the thresholds are set to an intermediate value (e.g., 0.5). A reader does not change μ only when it has a percentage of collisions between UpTrigger and DownTrigger. Therefore, with a reduced distance between the UpTrigger and DownTrigger, the majority of readers change μ repeatedly. In this way, the readers that are less subject to reader-to-reader collisions can frequently query tags. Their neighbors will find many timeslots occupied, so they will increase their μ reducing the opportunities to query tags. This extremely competitive behavior reduces the quantity of unused timeslots, increasing throughput. However, this kind of configuration exposes the weakest readers to the risk of starvation. Therefore, its adoption requires specific countermeasures.

In order to fully exploit the characteristics of the Killer configuration, a new protocol named Distributed color natural selection (DCNS) is proposed. Communication is organized in rounds composed of timeslots, as in DCS. As in Colorwave, each reader has an adaptable number of colors. However, with the aim of decreasing the channel control overhead, the changes of μ are not notified in DCNS. Therefore, the readers only change the number of colors according to two thresholds (UpSafe and DownSafe). Moreover, they do not exchange any information about the number of used colors. In this way, the readers with a percentage of collisions higher than UpSafe or lower than DownSafe act as in Colorwave. The readers with a percentage

of collisions between UpSafe and DownSafe do not change μ.

In order to improve how the readers scale the rate at which they query tags, the parameter μ is replaced by the couple μ^I and μ^{II}. μ^I represents the total number of colors, and $0.5 <= \mu^{II} <= 1$ represents the probability of querying tags. Normally a reader tries to query tags every μ^I timeslot, as in Colorwave. When $\mu^I = 2$ and the percentage of collisions is still lower than DownSafe, the reader starts to randomly choose whether to query tags according to the probability μ^{II}. Therefore, when the percentage of collisions exceeds UpSafe, if $\mu_i^{II} > 0.5$, then reader$_i$ decreases μ_i^{II}, otherwise it increases μ_i^I. When the percentage of collisions is less than DownSafe, if $\mu_i^I \geq 2$, then reader$_i$ decreases μ_i^I, otherwise it increases μ_i^{II}.

In order to avoid the starvation problem, a new kick sending routine has been introduced in the protocol. The new routine acts according to the reader state and the reader priority. Each reader sets its state comparing μ^I with a lower threshold equal to 2, and a higher threshold called KilledThreshold. The available states are the following:

- killer, for the readers with $\mu^I = 2$; since they have the opportunity to frequently query tags, they do not send kicks, in order to give the other readers more opportunities to interrogate tags;
- normal, for the readers with $2 < \mu^I <$ KilledThreshold; they reserve a slot by means of a kick only after a collision, as in DCS and Colorwave;
- killed, for the readers with $\mu^I \geq$ KilledThreshold; since they can seldom try querying tags, they always send kicks, in order to increase the probability of successfully querying tags, avoiding too long a delay.

A further novelty of DCNS, with respect to DCS and Colorwave, is represented by the dynamic priority management. When a reader is in the killer or killed state, it works according to its state; by contrast, when a reader is in the normal state, it works according to its priority. The priority levels are:

- high priority, which allows readers to reserve a slot each round; this reservation does not ensure a successful tag interrogation, since even other readers could reserve the same slot; however, the reservation avoids collisions with readers which are not reserving the slot, and increases the percentage of successful tag interrogations, facilitating the reduction of μ;
- medium priority, which allows readers to reserve a slot only after a collision, as in DCS and Colorwave;
- low priority, which does not allow readers to reserve slots; when low priority readers are close to readers with higher priority, they have longer waiting time;

low priority readers increase the performance of their neighbors with higher priority.

Table 4.4. Use of the kick before querying tags, according to the state and the priority of the reader

Priority	**State**		
	Killer	**Normal**	**Killed**
High	No	Yes	Yes
Medium	No	After a Collision	Yes
Low	No	No	Yes

The priority of a reader can be dynamically modified according to the application behavior. Therefore, the dynamic priority management cannot be considered only a starvation countermeasure, since it allows higher throughput to be obtained if it is required. The overall kick sending strategy is summarized in Table 4.4.

Finally, DCNS is a multi-channel protocol, according to the majority of the international regulations for UHF RFID. In order to manage multiple channels, a proper method for the selection of the color and the channel has been designed, taking into account the state of the readers. The main rules to select the channel are that: the killers do not change channel, in order to avoid collisions with other killers; the other readers select a random channel after a collision or a kick, avoiding both the same channel and color being maintained after a kick.

In order to present a detailed description of the proposed protocol, some definitions are required. The list of the variables used in DCNS and the procedures are shown in Table 4.5. Although most of the variables have been introduced in the previous section, there are some new elements. CTrans_i is a first-in-first-out (FIFO) buffer that contains the sequence of CTransFlags (true for collisions and false for successful interrogations) for the tag interrogations of reader_i among the attempted tag interrogations with the current couple μ_i^I and μ_i^{II}; the flags are true for successful interrogations and false for colliding ones. KickFlag_i and TransFlag_i are two boolean flags that are set to true when reader_i has to send a kick or to query tags, respectively. ColorIncrement^I and $\text{ColorIncrement}^{II}$ represent the steps used to increase and decrease μ_i^I and μ_i^{II}, respectively.

In the proposed algorithm, the types of transmission performed by the readers are the following:

- interrogation, when a reader queries tags,
- kick, when a reader sends the reservation message.

Table 4.5. List of the variables and procedures used in DCNS

Variable	**Description**
UpSafe	high threshold
DownSafe	low threshold
μ_i^I	number of available colors for reader$_i$
μ_i^{II}	probability for reader$_i$ to query tags when $\mu_i^I = 2$
μCh	number of channels used in the network
MinTimeInColor	minimum number of slots between two changes of μ_i^I and μ_i^{II}
TimeInColor$_i$	number of timeslots spent with the current couple μ_i^I and μ_i^{II}
CTransFlag	flag true for a collision and false for a successful interrogation
CTrans$_i$	buffer containing the sequence of CTransFlags for the tag interrogations of reader$_i$
Color$_i$	index of the timeslot used by reader$_i$ to query tags
Channel$_i$	index of the channel used by reader$_i$ to query tags
OldChannel$_i$	index of the previous channel used by reader$_i$
KilledThreshold	value of μ_i^I beyond which the reader is killed
KickFlag$_i$	boolean, true when reader$_i$ has to send a kick
TransFlag$_i$	boolean, true when reader$_i$ has to query tags
Priority$_i$	priority level of reader$_i$
ColorIncrement^I	increment step of μ^I
ColorIncrement^{II}	increment step of μ^{II}
Procedure	**Description**
CTrans$_i$.add()	adds a new CTransFlag
CTrans$_i$.clear()	deletes all the CTransFlags
CTrans$_i$.getCollisions()	returns the percentage of true CTransFlags

At each timeslot, DCNS executes the following three consecutive phases:

- initialization,

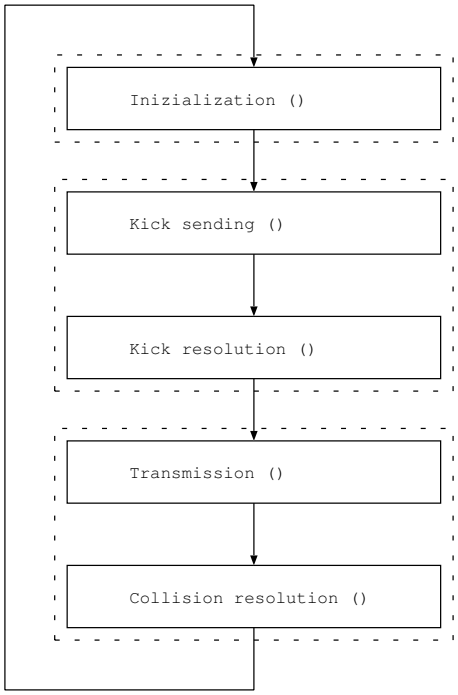

Figure 4.17. DCNS subroutines

- kick,
- transmission.

These phases are composed by five subroutines, as shown in Fig. 4.17.

During the *initialization* phase, which is shown in Fig. 4.18, the readers update their variables and flags. According to the application behavior, the priority of some readers is updated (Fig. 4.18, step 6), and new queries are required (Fig. 4.18, step 3). The reading request and the priority modification requests of the user are forwarded to the readers. They check UpSafe and DownSafe and eventually change μ_i^I or μ_i^{II}, according to their status and priority. KickFlag is true for readers that have to send a kick. It is modified by each reader according to its priority and status (e.g., killer readers always set it to false, while killed ones set it to true).

The *kick* phase contains the Kick Sending subroutine (Fig. 4.19) and the Kick Resolution subroutine (Fig. 4.20). It is used to reserve the current timeslot. The readers that have to reserve the slot (i.e., with KickFlag=true) send a kick. All the readers that receive a kick randomly choose a new couple, composed of a color and a channel. Normally readers must select a couple different from the previous one, apart from the killers, which maintain their previous channel in order to avoid sharing the same channel with another killer.

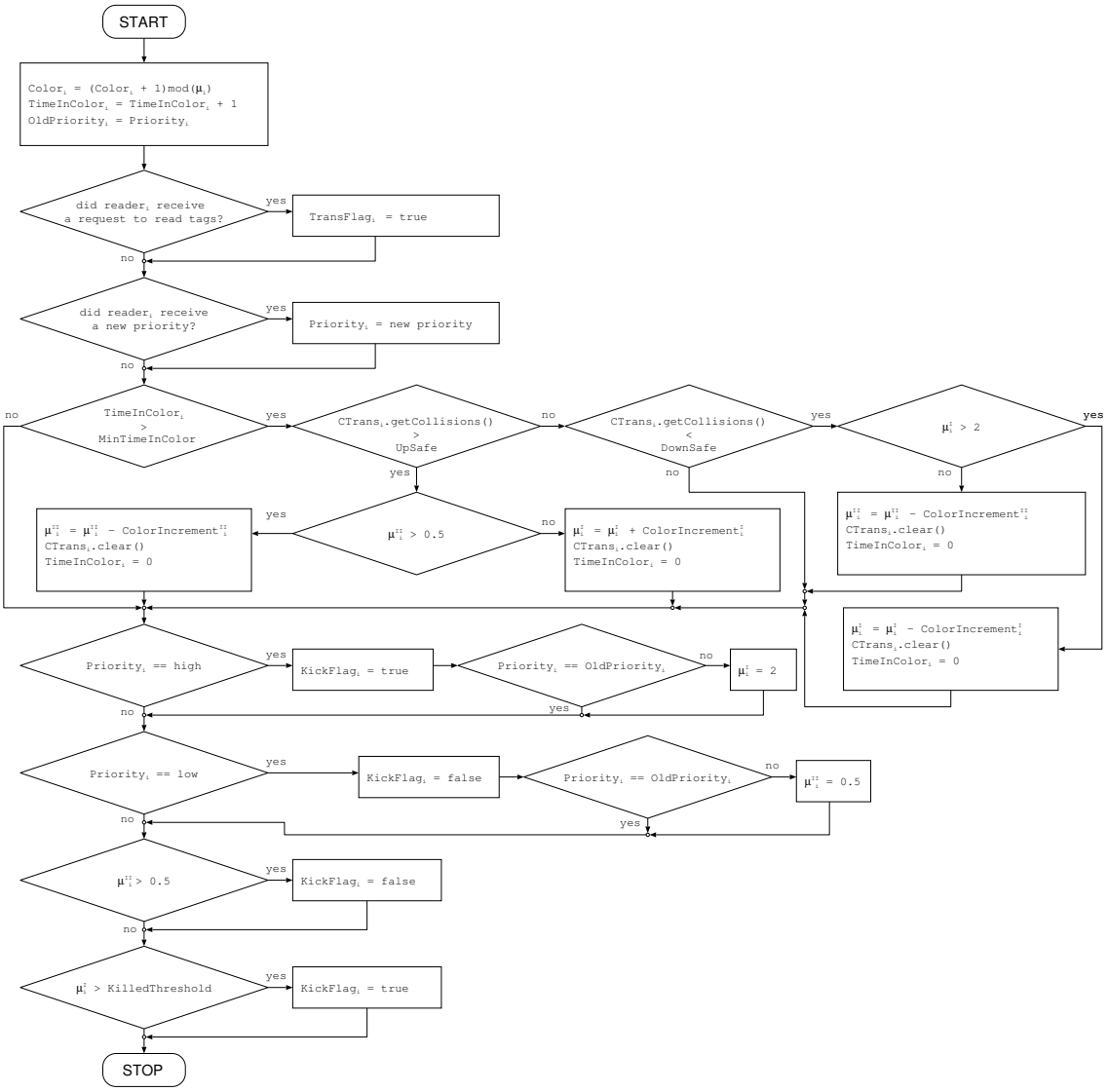

Figure 4.18. Initialization subroutine

The *transmission* phase is used to query the tags. Each reader assigned to the current color can query tags. The colliding readers set KickFlag to true, in order to send a kick during the subsequent round. Then, they randomly choose a new couple composed of a color and a channel. Killer readers follow a different strategy, since they hold their previous channel, as in the Kick Resolution subroutine. Fig. 4.21 and 4.22 show the Transmission and Collision Resolution subroutines, respectively.

The protocol can be implemented both with readers able to transmit and receive simultaneously or not. If the readers can transmit a kick and simultaneously listen

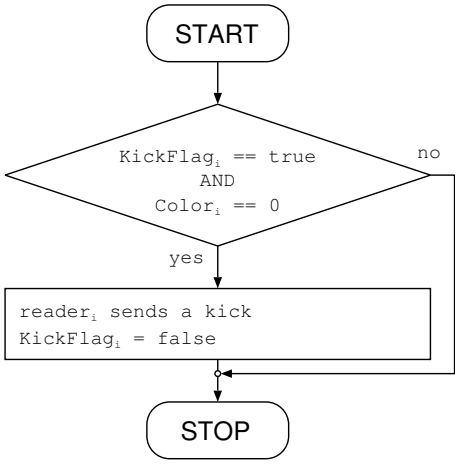

Figure 4.19. Kick sending subroutine

for other kick signals, the Kick Resolution subroutine can be applied. If the readers cannot listen when they are transmitting a kick, even if there is a kick collision, they will try to query tags during the transmission phase. In this case, they collide in the transmission phase. Therefore, they will apply the Collision Resolution subroutine, instead of the Kick Resolution one.

4.2.1 Evaluation

In this section, the Killer configuration is analyzed and the best configuration parameters of DCNS are studied. Finally, the performance of DCNS is evaluated and compared with previous protocols.

The analysis has been performed simulating the protocols with a network of 250 readers, randomly deployed on a rectangular area. The deployments have been characterized according to the average number of neighbors per reader (AN). In order to reach a fair comparison, all the protocols have been simulated with the time parameters proposed in [12]. In particular, the kick phase has been set to 1 ms, and the transmission phase to 460 ms. For all the protocols, the same transmission time has been used. According to [12] and [60], it can be assumed that this time allows 100 tags to be identified. However, the number of tags that can be identified in this time varies according to the type of readers and tags employed.

μ_i update

In Colorwave the readers communicate the changes of μ_i. Theoretically, in this way the μ_i of each reader is more likely to be similar to the ones of its neighbors, reducing the collisions due to color desynchronization; nevertheless, this transmission

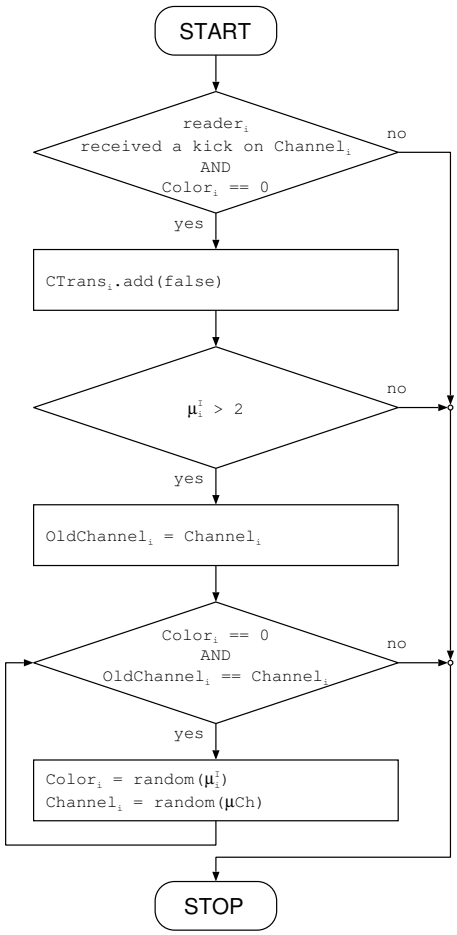

Figure 4.20. Kick resolution subroutine

increases occupation of the channel, increasing the probability of collisions in the kick phase. Moreover, each reader may have a different amount of neighbors, so a different best value of μ_i.

In order to evaluate the effects of these messages, Colorwave has been simulated with and without exchanging them. Fig. 4.23 shows the throughput provided by Colorwave according to the values of the 4 thresholds (reported on the Y axis) with and without the messages about the new μ_i. The first set of thresholds (i.e., 40-40-30-30) represent values compliant with the proposed Killer configuration. The subsequent sets correspond to the configurations proposed in [10]. The simulations have been performed over 20 random deployments with AN=10. It can be observed that, for the thresholds proposed in [10], the effects of the messages about the new μ_i are negligible; whereas, for the proposed thresholds, the throughput is higher without them. The difference between the effects of these messages is due to the

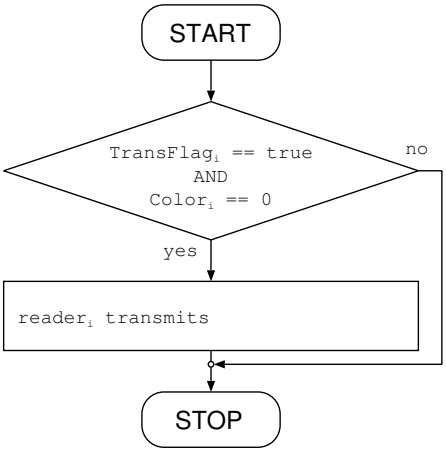

Figure 4.21. Transmission subroutine

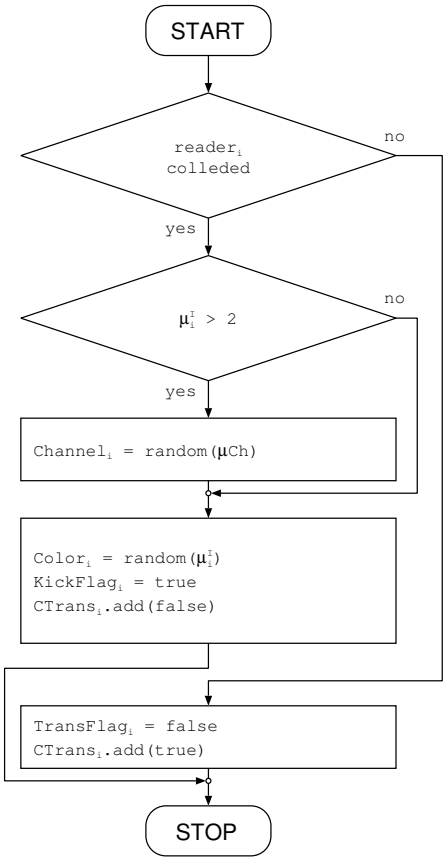

Figure 4.22. Collision resolution subroutine

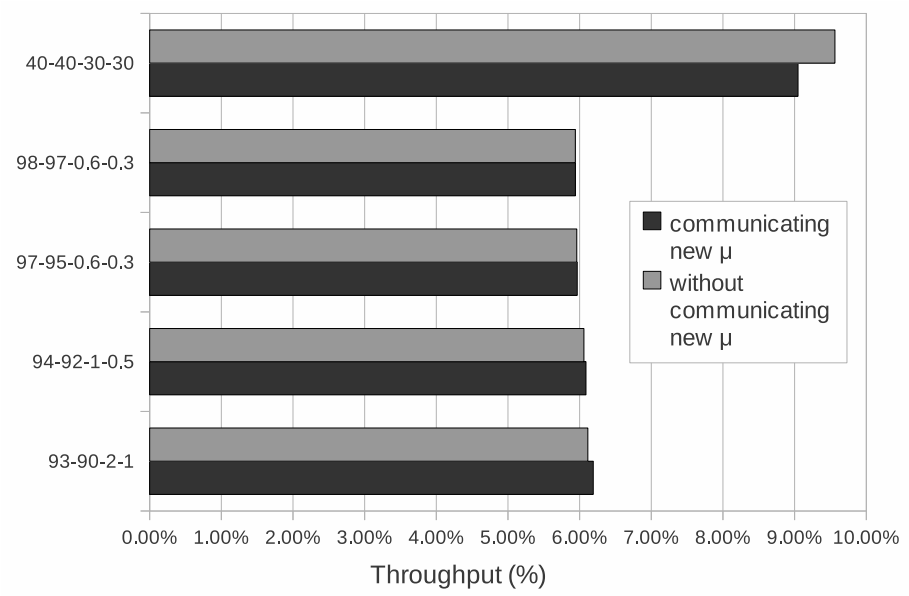

Figure 4.23. Throughput of Colorwave with and without messages about the new μ_i.

fact that in [10] the gap between DownTrigger and UpTrigger is smaller than the one between DownSafe and UpSafe. By contrast, in the Killer configuration, the gap is the same. Therefore, with the thresholds proposed in [10] the reduction of the gap increases the quantity of readers that change μ_i, compensating control overhead, while with the killer thresholds this effect is null.

These results indicate that the messages that specify changes of μ_i do not provide relevant benefits, especially with the proposed configuration. Therefore, these messages have not been implemented in DCNS, and the two thresholds UpTrigger and DownTrigger have been suppressed.

Killer configuration and selection of the parameters

The scope of the Killer configuration is to increase throughput, using thresholds close to an intermediate value. DCNS has only two thresholds, DownSafe and UpSafe. In order to find the best thresholds, DCNS has been simulated with all the possible couple of values of these thresholds. Fig. 4.24 plots the average throughput provided by DCNS with networks composed of 250 readers randomly deployed and AN=10. The best throughput is provided when UpSafe is between 15% and 50%, and DownSafe is between UpSafe and UpSafe less 15. These values are consistent with the analysis provided in Section 4.2. When the gap between UpSafe and UpSafe is larger, throughput decreases fast. Independently from the gap, if the two thresholds are too high or too low, the throughput is still low, since all the readers

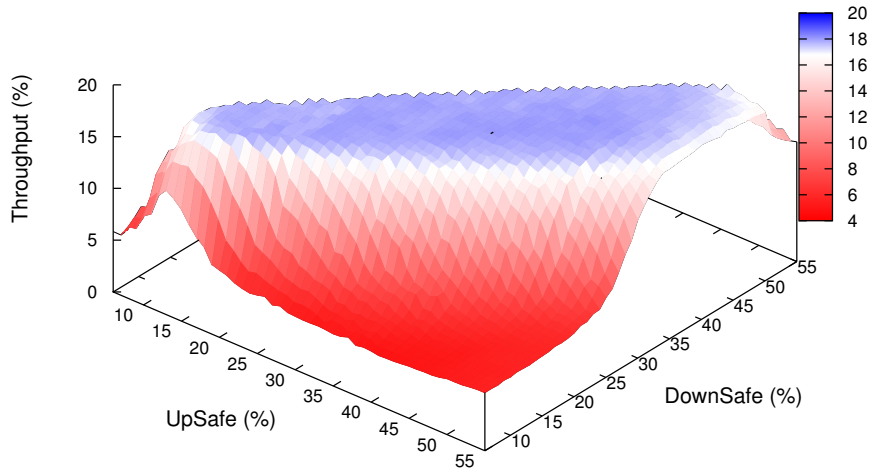

Figure 4.24. Throughput of DCNS according to UpSafe and DownSafe.

are not able to increase or to decrease μ. According to these results, we have selected UpSafe=0.40 and DownSafe=0.30 for the Killer configuration of DCNS.

According to the differences between DCNS and Colorwave, the Killer configuration must be properly suited to the specific protocol. Fig. 4.25 displays the average throughput provided by Colorwave with the previous deployments. Colorwave has four thresholds, so the results have been calculated selecting for each couple of UpSafe and DownSafe the best results provided with different selected values of the other two thresholds (UpTrigger and DownTrigger). The configurations used are the following:

- UpTrigger = DownTrigger = DownSafe;
- UpTrigger = (UpSafe+DownSafe)/2, DownTrigger = DownSafe;
- UpTrigger = DownTrigger = (UpSafe+DownSafe)/2;
- UpTrigger = UpSafe, DownTrigger = DownSafe;
- UpTrigger = UpSafe, DownTrigger = (UpSafe+DownSafe)/2;
- UpTrigger = DownTrigger = UpSafe.

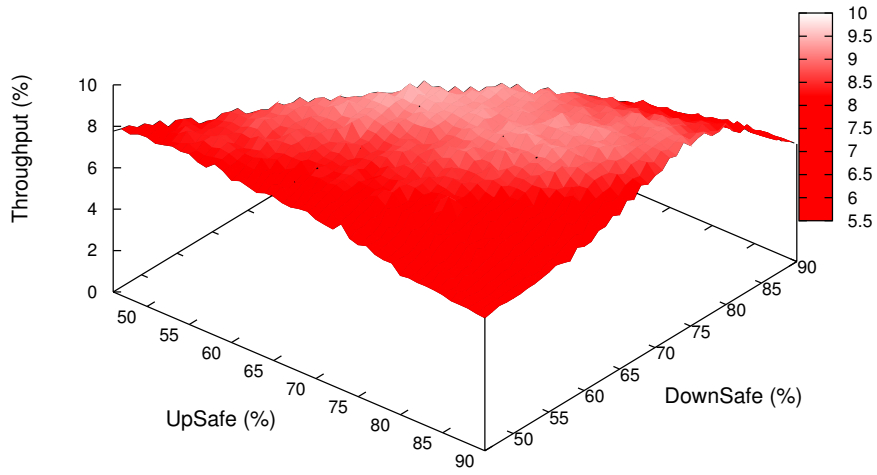

Figure 4.25. Throughput of Colorwave according to UpSafe and DownSafe.

According to the results reported in Fig. 4.25, the selected values of the Killer configuration applied to Colorwave are: UpSafe = 66%, UpTrigger = 66%, DownTrigger = 64%, DownSafe = 64% (UpTrigger = UpSafe, DownTrigger = DownSafe). The differences between these values and the ones used in DCNS are mainly due to the presence of the messages about new values of μ_i, which strongly affect the changes of μ.

Table 4.6. Selected parameters of DCNS

Parameter	**Value**	**Parameter**	**Value**
UpSafe	40%	DownSafe	30%
ColorIncrement^I	2	ColorIncrement^{II}	5%
MinTimeInColor	200 slots	Starting μ	6
KilledThreshold	200		

The other parameters of DCNS have been analyzed simulating the protocol over 40 random deployments with AN=10 and AN=20, as reported in Fig. 4.26. ColorIncrement^I, ColorIncrement^{II}, MinTimeInColor and the starting μ must be careful set, since they can guarantee fast adaptation. KilledThreshold must be set to a value that provides good network throughput and guarantees fair behavior

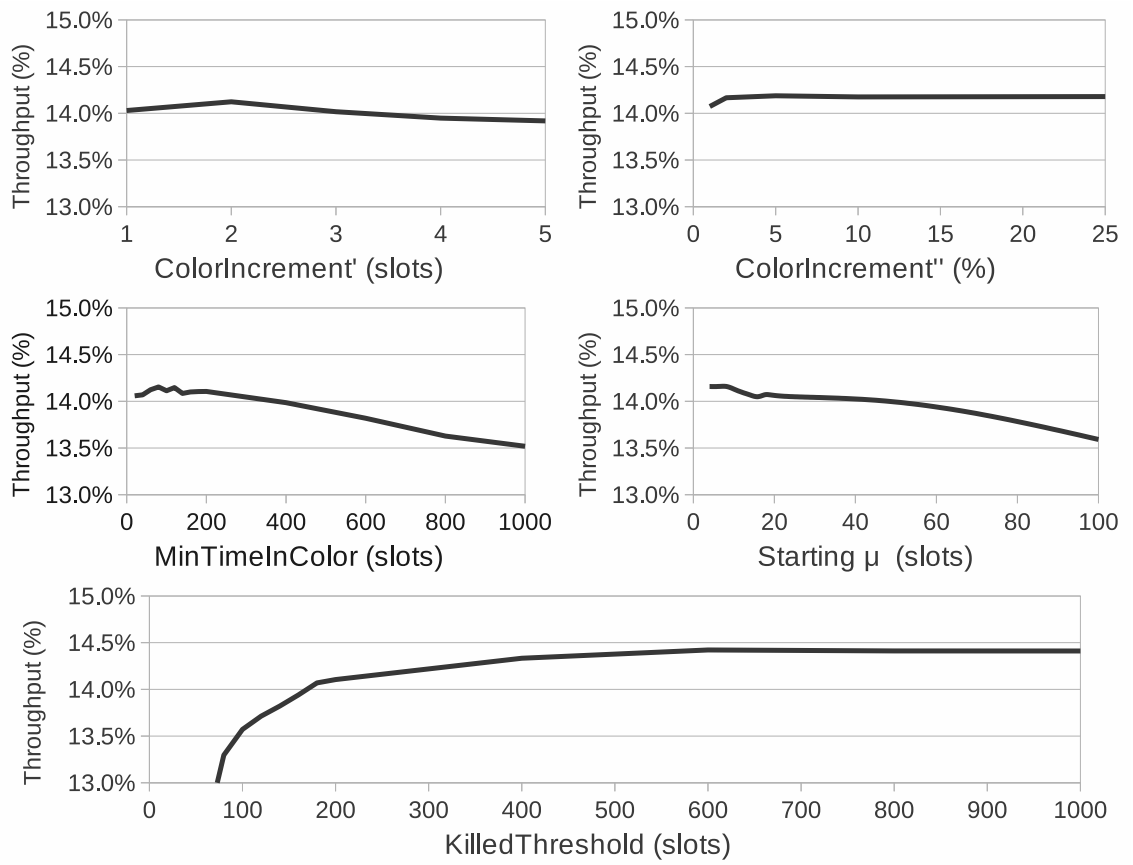

Figure 4.26. Average throughput of DCNS, according to the configuration parameter.

with minimum throughput to each reader. The selected parameters, summarized in Table 4.6, have been chosen according to the results of the simulations.

Priority analysis

In DCNS, network control is distributed and communication among readers is limited as much as possible. The priority management does not require additional messages among readers, but simply modify the Kick Sending subroutine. In order to verify the validity of the priority management mechanism, its effects on performance have been analyzed. Figure 4.27 shows the average throughput provided in deployments with AN=10. 5 readers (2% of the readers) have high priority and 25 readers (10% of the readers) have low priority. The throughput provided by the readers with high priority is strongly affected by the priority of their neighbors: without high priority neighbors, the average throughput is higher than the one with a high priority reader in the neighborhood. As evident from the curves, the average

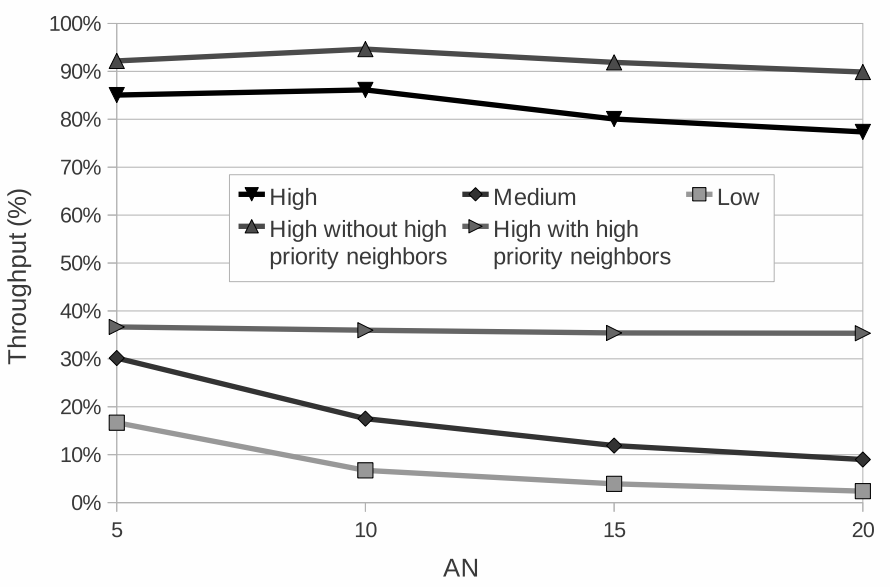

Figure 4.27. Effects of the priority on throughput

throughput provided by the readers is proportional to the priority level. Therefore, the priority management works properly, but the quantity of high priority readers must be limited.

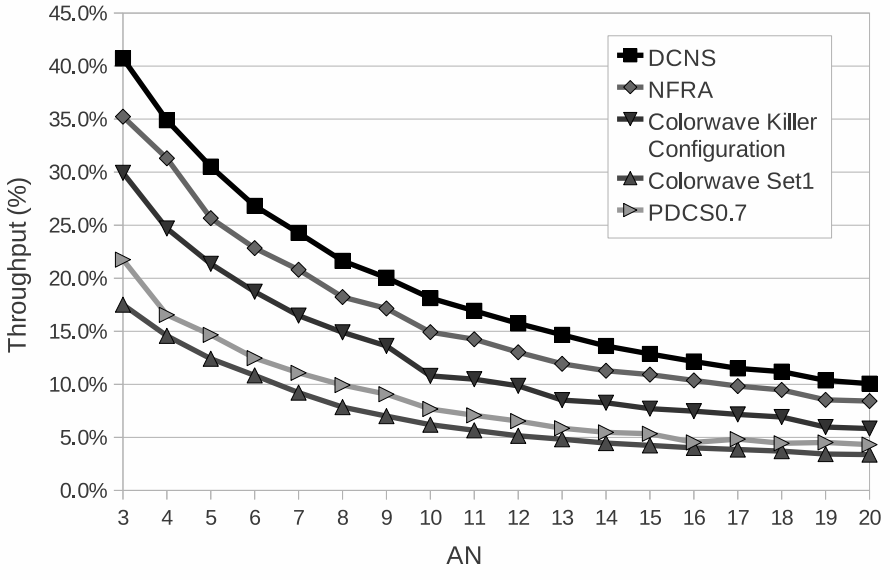

Figure 4.28. Throughput of DCNS and of the single-channel state-of-the-art approaches.

Table 4.7. Normalized throughput

Protocol	AN=3	AN=10	AN=20
	Throughput (%)		
DCNS	1.15	1.21	1.19
NFRA	1.00	1.00	1.00
Colorwave Killer conf.	0.84	0.72	0.69
Colorwave Set1 conf.	0.49	0.41	0.40
PDCS	0.61	0.51	0.51

Comparison

In order to compare DCNS to state-of-the-art approaches, 360 deployments with AN between 3 and 20 have been generated. All the protocols have been simulated with these deployments, and the average throughput is presented in Fig. 4.28. The throughput provided by the compared protocols is also shown normalized to NFRA one, in Table 4.7. Increasing AN, the throughput provided by all the protocols decreases. However, DCNS always provides the best throughput: on average 18% better than NFRA, the best state-of-the-art protocol. Fig. 4.28 shows the throughput provided by Colorwave both with the Killer configuration and with the first configuration (i.e., 93%, 90%, 2%, 1%) presented in [10] (the other configurations proposed in [10] are not shown, since their throughput is similar). The application of the Killer configuration allows the performance of Colorwave to be increased on average by 80%. Finally, Fig. 4.28 shows the throughput provided by PDCS with the best configuration proposed in Section 4.1 (i.e., $p = 0.7$). DCS is not shown, since its throughput is always lower than or similar to PDCS. The throughput of PDCS is higher than Colorwave without the Killer configuration, but it requires the density of the deployment to be known.

As for the single channel comparison, 360 deployments with AN between 3 and 20 have been generated. All the multi-channel protocols have been simulated with these deployments on 4 channels. The average throughput is shown in Fig. 4.29. DCNS always provides the best throughput, and it is at least 10% better than LBT.

4.3 Probabilistic Colorwave (PCW)

In Colorwave, after colliding, the readers select another color. As the authors point out in [11], this greedy algorithm for the collision resolution may produce the unique worst possible solution: both the readers select the same color and therefore they

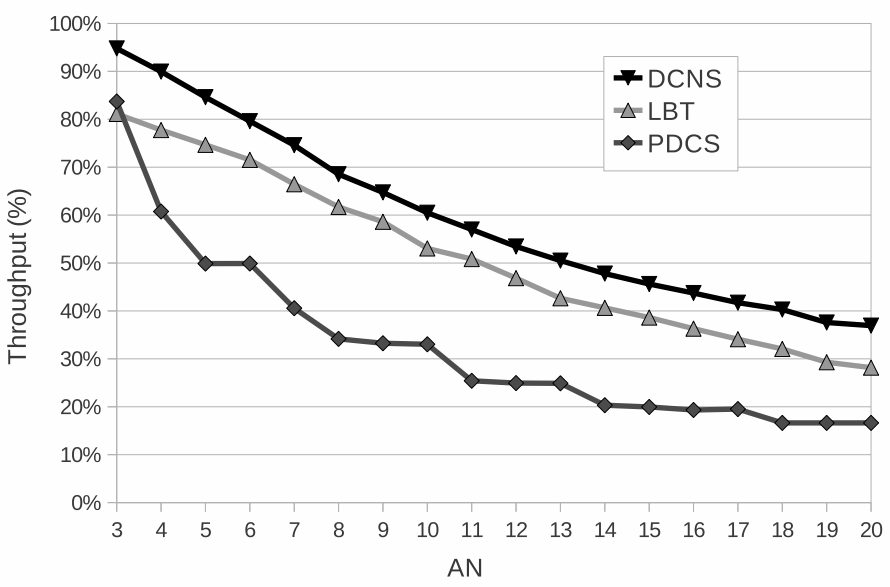

Figure 4.29. Throughput of DCNS and of the multi-channel state-of-the-art approaches.

exchange a kick in the following round. In order to minimize this drawback, a probabilistic version of Colorwave, henceforth called Probabilistic Colorwave (PCW), is proposed. In PCW each reader is not forced to change color after a collision: instead, it chooses whether doing it according to a probability p. If only a reader changes color, a further collision between the two readers is avoided. p needs to be enough high to minimize the possibility that neither reader chooses a different color.

Data architecture

Table 4.5 lists the variables used in PCW. The inputs to the PCW algorithm are the probabilistic factor p, the four thresholds and the stabilization period *minTimeInColor*. These parameters are fixed, whereas all the others can vary during the execution of the algorithm.

The specifications of Colorwave require that each reader counts the number of rounds concluded with a successful tag identification and the overall number of attempts. The comparison of their ratio with the thresholds determines if the reader should vary the number of used colors. However, a simple counter of the successful tag identifications is not able to provide an optimal performance of the algorithm. In a static scenario, when the optimal setting is found, it is kept indefinitely. The amount of all the successful operations executed with the current parameter setting avoids a quick response to any variation in the neighborhood, such as the deployment

Table 4.8. Variables in PCW

Variable	Description
p	probability of changing color after a collision
$buffer_i$	a circular buffer storing the activity of reader$_i$, since the last variation of μ_i
$UpSafe$	highest threshold
$UpTrigger$	second highest threshold
$DownTrigger$	second lowest threshold
$DownSafe$	lowest threshold
$color_i$	index of the timeslot used by reader$_i$ to transmit
μ_i	number of colors used by reader$_i$
$minTimeInColor$	minimum number of timeslots between two subsequent changes of μ_i
$timeInColor_i$	number of timeslots spent with the current μ_i
$kick_i$	an index with value ≥ 0 if reader$_i$ will send a kick in the next transmission
$queryFlag_i$	boolean flag, true if reader$_i$ will query tags in the next transmission

of a new reader inside the interference range, or the removal of a neighbor. Even if the performance of the reader starts to drop dramatically, the average performance can remain adequate for a long period, so the reader does not vary the number of color. As a counter-measure, only the most recent activity of the reader is considered. Therefore, the information on the successful tag interrogations and on the collision is stored in a circular buffer, instead of a counter. In this way, when the buffer is full, a new transmission is recorded discarding the oldest one. It is implemented as a circular First In First Out (FIFO) boolean buffer (the true value is inserted in case of a successful tag interrogation). In order to manage the circular buffer, the following operations are defined:

- $buffer_i$.add(boolean): adds a new boolean value to the buffer. The true value means a successful interrogation of the tags, the false one represents a failed attempt;

- $buffer_i$.clear(): deletes all the values. It is executed when reader$_i$ changes μ_i, in order to compute the statistics with the new value;

- $buffer_i$.getTransmissions(): returns the ratio of values equal to true out of the total values, corresponding to the percentage of successful transmissions.

The maximum number μ_i of colors used by reader$_i$ can be changed in two occasions:

- at the beginning of a timeslot, as soon as the percentage of successful transmissions is higher than the *UpSafe* threshold or lower than the *DownSafe* one;
- at the receiving of a kick, if the value stated in the kick is higher than *UpTrigger* or lower than *DownTrigger*.

μ_i can be changed only if the time spent by reader$_i$ since the last variation of its maximum number of colors is higher than *minTimeInColor*. In order to compute this time, which is incremented at the beginning of every timeslot, the counter $timeInColor_i$ is used.

In the algorithm, a kick is sent by a reader to notify the new value of its μ or to reserve the use of a timeslot after a collision. The information about the triggering event is immediately stored into the variable $kick_i$, and then sent with the kick at the beginning of the next timeslot used by reader$_i$.

Finally, $queryFlag_i$ is a boolean flag that reader$_i$ sets to true at the beginning of a timeslot, as soon as the identification of tags in its interrogation zone is demanded. The flags stay true until the tags identification is not completed.

Algorithm 1 Initialization

$color_i = (color_i + 1) \bmod (\mu_i)$;
$timeInColor_i = timeInColor_i + 1$;
if reader$_i$ received a request to read tags **then**
  $queryFlag_i$ = true;
end if
if $buffer_i$.getTransmissions() > *UpSafe*
and $timeInColor_i > minTimeInColor$ **then**
  $\mu_i = \mu_i + 1$;
  $buffer_i$.clear();
  $timeInColor_i = 0$;
  $kick_i = \mu_i$;
else if $buffer_i$.getTransmissions() < *DownSafe*
and $timeInColor_i > minTimeInColor$ **then**
  $\mu_i = \mu_i$ - 1;
  $buffer_i$.clear();
  $timeInColor_i = 0$;
  $kick_i = \mu_i$;
end if

Description of the algorithm

In PCW, the transmission performed by a reader can be of two types:

- interrogation, in order to query the tags inside the interrogation range,
- kick, which acts as a timeslot reservation or as a notification of a μ change.

The algorithm is iterated at each timeslot, and it is organized in three consecutive phases:

- Initialization,
- Kick,
- Transmission.

During the Initialization phase, which is shown in Algorithm 1, the readers update their variables and flags. Depending on the position of the tags to identify, the network administrator identifies the readers that have to perform an interrogation and forward the request to them. The readers in charge of the tags identification set their flag *queryFlag* to true. Moreover, every reader checks *UpSafe* and *DownSafe* and eventually changes its μ.

The Kick phase, which contains the Kick Sending subroutine (Algorithm 2) and the Kick Resolution subroutine (Algorithm 3), is used to reserve the current timeslot and to communicate a new μ_i. If a reader experiences a collision at the end of a timeslot, it sends a kick with value 0 during the Kick Sending procedure in order to reserve the next timeslot. In the Kick Resolution procedure, all the readers that receive a kick with value 0 randomly choose a new color, different from their previous one. Similarly, in the Kick Sending subroutine, the readers that have changed their μ indicate the new value in the kick. In the Kick Resolution procedure, after receiving a kick with a value higher than 0, the reader decides whether updating its μ comparing the percentage of successful transmissions to *UpTrigger* or *DownTrigger* thresholds.

Algorithm 2 Kick_sending

```
if color_i = 0 and kick_i ≥ 0 then
    reader_i sends a kick with value kick_i;
    kick_i = -1;
end if
```

The Transmission phase contains the Transmission subroutine (Algorithm 4) and the Collision Resolution subroutine(Algorithm 5). In the Transmission procedure, each reader in charge of the tags identification attempts to use the timeslot

Algorithm 3 Kick_resolution

```
if reader_i receives a kick with value kickValue then
  if kickValue = 0 and color_i = 0 then
    buffer_i.add(false);
    color_i = (int) random(0, μ_i -1) +1;
  else if kickValue > μ_i
  and buffer_i.getTransmissions() > UpTrigger
  and timeInColor_i > minTimeInColor then
    μ_i = kickValue;
    buffer_i.clear();
    timeInColor_i = 0;
    kick_i = μ_i;
  else if kickValue < μ_i
  and buffer_i.getTransmissions() < DownTrigger
  and timeInColor_i > minTimeInColor then
    μ_i = kickValue;
    buffer_i.clear();
    timeInColor_i = 0;
    kick_i = μ_i;
  end if
end if
```

Algorithm 4 Transmission

```
if queryFlag_i = true and color_i = 0 then
  reader_i transmits;
end if
```

Algorithm 5 Collision_resolution

```
if reader_i collides then
  if random(0, 1) < p then
    color_i = (int) random(0, μ_i);
  end if
  kick_i = 0;
  buffer_i.add(false);
else
  buffer_i.add(true);
  queryFlag_i = false;
end if
```

corresponding to its current color in order to query tags. In the Collision Resolution subroutine, the colliding readers randomly choose a new color with probability p. Instead, readers which successfully completed the tags interrogation reset their *queryFlag*.

4.3.1 Evaluation

The effects of the probabilistic factor in Colorwave have been studied with two different sets of thresholds. The first set is 93%, 90%, 2%, 1%, which corresponds to Set 1 in [10]. The second one is 66%, 66%, 64%, 64%, which is compliant with the analysis of the killer configuration proposed in Section 4.2.1. *minTimeInColor* has been set to 100 timeslots, and for each reader μ is initialized to 6. In order to evaluate the proposed technique, the two configurations have been simulated with networks of 100 readers characterized by different density. All the results are calculated as the average of 4 simulations executed on 100 different deployments with the same density. PCW has been simulated with values of p ranging from 50% to 90%.

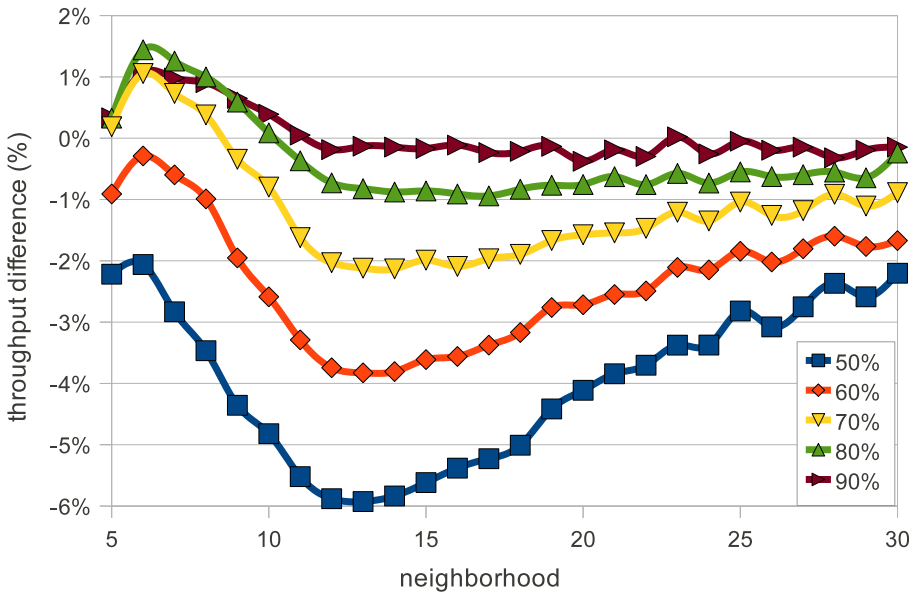

Figure 4.30. Throughput difference (in percentage) of PCW with respect to Colorwave using the configuration proposed in [10]

The gain in throughput and fairness of PCW with respect to Colorwave is shown in Fig. 4.30 and 4.31, when the configuration proposed in [10] is used. Adopting this configuration, any throughput improvement provided by PCW impacts on the fairness, and vice versa. Moreover, the behavior of PCW changes as the network becomes denser. In case the average number of neighbors is up to 10, PCW can

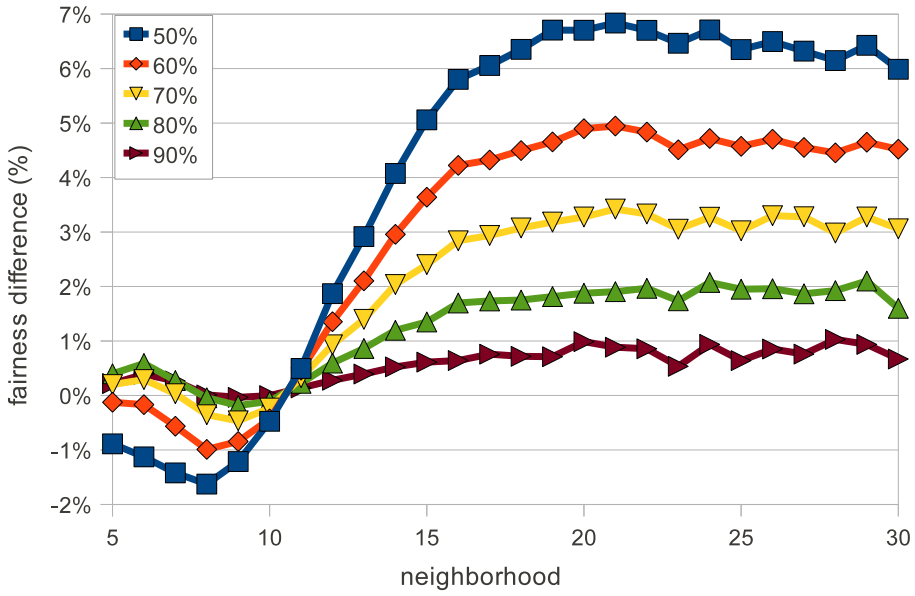

Figure 4.31. Fairness difference (in percentage) of PCW with respect to Colorwave using the configuration proposed in [10]

provide a higher throughput than Colorwave, if the value of p is set up in the range between 70% and 90%. However, no improvement on fairness can be achieved. On the other hand, if the average size of the neighborhood is higher than 10, PCW is fairer than Colorwave, indipendently of the value of p. The throughput becomes more similar among the readers, but the overall throughput of the network decreases. With the configuration proposed in [10], there is a direct relationship between the fairness improvement and the throughput reduction. The lower the value of p is, the higher the fairness is, and the higher the throughput loss is. On the contrary, with values of p close to 90%, the throughput loss is negligible, but the fairness gain is moderate.

Fig. 4.32 shows the comparison of PCW with respect to Colorwave when the killer configuration is adopted. The probabilistic approach should generally be preferred, since both the throughput and the fairness increase. In particular, a throughput gain is guaranteed, independently of the value of p, for networks with an average size of the neighborhood equal to 10 or higher. The fairness always rises, and the improvement is in inverse proportion to the value of p. Therefore, the optimal value of p to be applied to PCW in conjunction with the killer configuration is 50%, because it guarantees the highest fairness improvement a throughput gain close to the maximum. Higher values of p can be used only for sparser networks, with less than 10 neighbors on the average, if the application requirements privilege throughput rather than fairness.

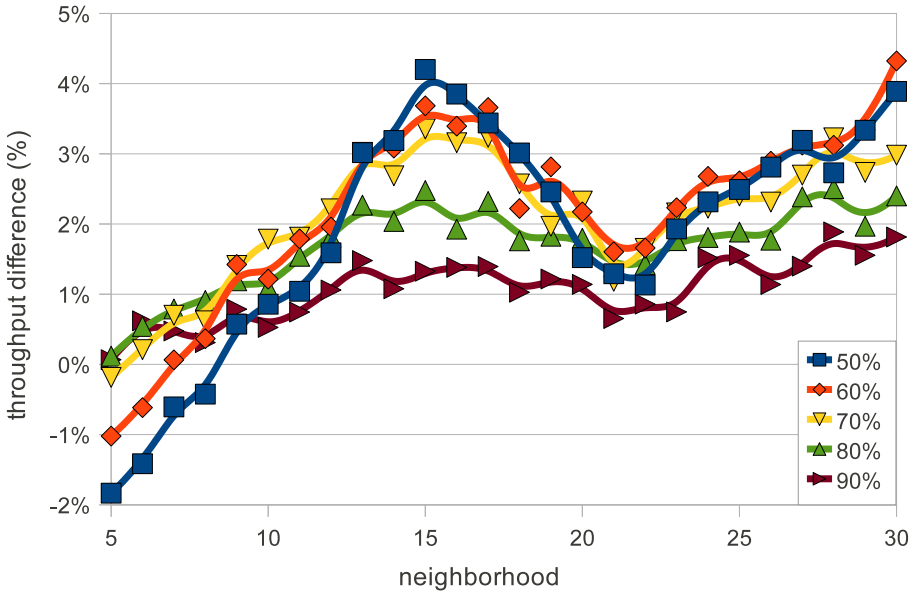

Figure 4.32. Throughput difference (in percentage) of PCW with respect to Colorwave using the killer configuration

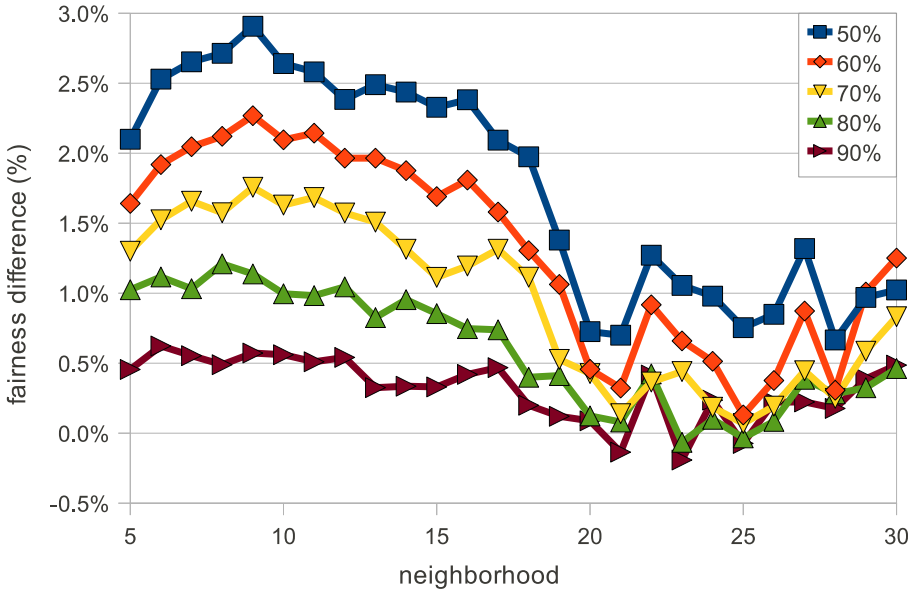

Figure 4.33. Fairness difference (in percentage) of PCW with respect to Colorwave using the killer configuration

4.3.2 Applicability of the proposed approach

According to the results presented in Section 4.3.1, when the configuration proposed in [10] is applied, the probabilitic approach should be applied to Colorwave in relation to the desidered performance. If the application requires a high throughput,

the introduction of the probability p in the collision resolution routine gives benefit in case of networks with an average neighborhood equal to or lower than 10. Vice versa, if the fairness among the readers is privileged, PCW can guarantee higher performance than Colorwave for networks where the readers have more than 10 neighbors on the average. As a consequence, the adoption of the proposed approach in conjunction to the configuration proposed in [10] requires a careful network analysis. As proved in Section 1.7, if N readers are randomly deployed on a rectangular surface of length l and width w, then the average size of the neighborhood is given by:

$$k = \left(\pi wl - \frac{4}{3}r(w+l) + \frac{r^2}{2}\right)\left(\frac{r}{wl}\right)^2 (N-1) \tag{4.30}$$

The interference range r can be evaluated through the Signal to Interference plus Noise Ratio (SINR) thresholding for the correct signal identification, which is described in Section 2.3.2. This model sets the condition in order that the signal backscattered by tag k can be recognized by reader i, despite the interferencing activity of reader j. The tag is identified if the SINR exceeds a required threshold Γ, which depends on the bit error rate (BER):

$$\frac{G_{k,i}P_k}{G_{j,i}P_j + N} \geq \Gamma \tag{4.31}$$

where P_k is the power of the signal backscattered by tag k, P_j is the transmit power used by reader j, $G_{k,i}$ is the propagation gain including the antenna gains from tag k to reader i, $G_{j,i}$ is the propagation gain from reader j to reader i and N is the background noise power. An isotropic path loss is generally considered:

$$G_{x,y} = \left(\frac{\mid x - y \mid}{d_0}\right)^{-\eta} \tag{4.32}$$

where $\mid x - y \mid$ is the Euclidean distance between x and y, d_0 is a constant and η is the path loss exponent. Under this assumption, the interference range, i.e. the maximum distance within which reader j interferes with reader i if both are concurrently active, is:

$$r = \left(\frac{1}{\Gamma \mid k - i \mid^{\eta}} - \frac{N}{P_j d_0^{\eta}}\right)^{-\frac{1}{\eta}} \tag{4.33}$$

If the killer configuration is used, PCW generally shows a higher performance than Colorwave. The fairness achieved by PCW is always higher than the one of Colorwave. The throughput improvement is guarantees when the average number of neighbors is equal to or higher than 10: if the primary goal of the application is the throughput, the suitability of PCW should be evaluated according to equation 4.30.

Chapter 5

Proposed TDMA protocols with a control channel

With respect to the TDMA protocols that exploits one additional control channel, NFRA [12] provides an optimal management of the readers inside the interference range (*neighborhood*). Howewer, two drawbacks can be identified in this algorithm. First of all, the algorithm maximizes the throughput, privileging readers with a limited neighborhood, since they have lower probability to be overridden by close transmission. As a consequence, their frequent queries could prevent readers with a larger neighborhood from communicating. To schedule the readers for transmitting, the algorithm assigns to disabled readers the same priority of transmitting ones, so during long executions there may be significant differences among the transmissions performed by each reader. Secondly, some hardware assumptions make the implementation of NFRA in passive RFID systems hard.

Two different approaches are described in order to mitigate the main drawbacks of NFRA. Their characteristics are summarized in Table 5.1. NFRA++ (Section 5.1) includes two techniques to improve both the fairness and the throughput of NFRA. Geometric Distribution Reader Anticollision (GDRA) (Section 5.2) is a second approach based on NFRA. It exploits the *Sift* geometric probability distribution function to minimize reader collision problems. GDRA shows better performance than NFRA, it can be implemented in a real DRE without extra hardware and it is compliant with EPC-ETSI requirements.

Table 5.1. Main characteristics of the proposed TDMA anticollision protocols that exploits one additional control channel

protocol	throughput	fairness	network requirements	density knowledge
NFRA++	very high	high	high	low dependence
GDRA	very high	low	medium	low dependence

5.1 NFRA++

Two improvements are proposed in the NFRA protocol. The first one, denoted as NFRA+, ensures fair performance among the readers. The second one increase the throughput for each readers. The new algorithm with the two improvements is called NFRA++.

5.1.1 Introducing fairness in NFRA

The key idea to improve fairness in NFRA is to reserve low values of m to readers that have not queried tags for the longest time. This constraint prevents readers with few neighbors, and therefore communicating frequently, from selecting low values with the same frequency of readers that have more neighbors.

In order to consider the recent history of the readers, the set of available numbers, varying from 1 to M, is partitioned into n levels of priority, with $n < M$. At the beginning of the round, each reader randomly chooses a value included in the range corresponding to its level of priority. The assignment of the priority to a reader r_i is based on its *waiting time* w_i. This parameter is evaluated as the number of rounds elapsed from the first attempt to the tag identification. A reader increases its priority every u rounds spent without any identification. After receiving an AC, each reader estimates its priority l_i according to the following formula:

$$l_i = \begin{cases} n - \lfloor \frac{w_i}{u} \rfloor & \text{if } w_i < n \cdot u \\ 1 & \text{if } w_i \geq n \cdot u \end{cases} \tag{5.1}$$

Adopting n priority levels and a granularity of u rounds, a reader has the lowest priority (n) if it queried tags in the last u rounds; the highest priority (1) is assigned to readers waiting from more than $(n-1)u$ rounds. The set of M values is partitioned into n subsets. Each priority level is matched to a subset, ranging from $\lfloor \frac{M}{n} * (l_i - 1) \rfloor + 1$ to $\lceil \frac{M}{n} * l_i \rceil$ (the highest value of level l_i may coincide with the lowest value of level l_{i+1}). Every sequence contains $\lceil \frac{M}{n} \rceil$ distinct values, large enough to solve collisions among readers with same priority.

Analysis of the probability of transmitting

The improvement in fairness of NFRA+ with respect to NFRA is proved comparing the probability of querying tags in the two protocols. A harsh environment, where every reader interferes with each other of the network, is considered. Let $P_m(V, M, l, n)$ be the probability of querying tags for a reader that extracted number m, with priority l out of n different priority levels, and in presence of V neighbors $v_1, v_2, ..., v_V$. For every number k, $1 \leq k \leq M$, that is selected by a generic reader i, one of the following cases occurs:

1. k is not selected by any neighbors: $\forall v_j\ m_j \neq k$
2. at least two neighbors select k: $\exists v_j, v_l : m_j = m_l = k$
3. k is chosen by only one neighbor: $\exists! v_j : m_j = k$

After selecting number m_i, reader i queries tags if:

Condition 1. For $k = m_i$, case 1 is satisfied;

Condition 2. $\forall k$: $1 \leq k < m_i$, at least one between case 1 and case 2 is satisfied.

In NFRA, all the M numbers are equally probable, thus:

$$Pr(\text{cond. } 1) = \left(\frac{M-1}{M}\right)^V \tag{5.2}$$

Condition 2 is always true for $m_i = 1$, as in this case no OF can be received. As the initial selections of the readers are independent events, the number of identical choices follows a binomial distribution. The probability for an event with success probability p to occur k times in t trials is given by the probability mass function $f(k;t,p) = \binom{t}{k}p^k(1-p)^{t-k}$, thus:

$$Pr(\text{cond. } 2,\ m_i = 2) = \sum_{h=0;h\neq 1}^{V} f\left(h; V, \frac{1}{M-1}\right) \tag{5.3}$$

When $m_i > 2$, the probability of condition 2 depends on how many readers have chosen the previous values from 1 to m_i - 1. In order to consider the contribution of all the cases, we define the recursive function $Q(V, r, m_i)$ as the conditional probability that, in presence of V neighbors, $\forall k : 1 \leq k \leq m_i - r$ condition 2 is satisfied, given that $\forall k : m_i - r < k < m_i$ condition 2 is satisfied *and that* for $k = m_i$ condition 1 is satisfied. Thus, $Pr(\text{cond. } 2) = Q(V, 1, m_i)$. The probability is evaluated as follows:

$$Q(V, r, m_i) = \sum_{h=0;h\neq 1}^{V} Q(V-h, r+1, m_i) \cdot f\left(h; V, \frac{1}{M-r}\right) \tag{5.4}$$

where $Q(V, m_i, m_i)$ is defined as 1.

After selecting value m_i, the probability to identify tags is:

$$P_{m_i}(V, M, 1, 1) = Pr(\text{cond. } 1) \cdot Pr(\text{cond. } 2) = \left(\frac{M-1}{M}\right)^V \cdot Q(V, 1, m_i) \tag{5.5}$$

In NFRA, since all the values are equally probable, a reader has the same probability of querying tags at every round:

$$P(V, M, 1, 1) = \frac{1}{M}\sum_{h=1}^{M} P_h(V, M, 1, 1) = \frac{1}{M} \cdot \left(\frac{M-1}{M}\right)^V \cdot \sum_{h=1}^{M} Q(V, 1, h) \tag{5.6}$$

In NFRA+, this probability depends on the waiting times of the reader and of its neighbors. The number of neighbors with priority l_i ranges from a minimum of 0, if none of them identified any tags in the related interval, to a maximum of u. Let V_i be the set of neighbors with priority i. The probability of querying tags for a reader with the highest priority is:

$$P(V, M, 1, n) = \frac{n}{M}\left(\frac{\lceil \frac{M}{n} \rceil - 1}{\lceil \frac{M}{n} \rceil}\right)^{V_1} \sum_{h=1}^{\lceil \frac{M}{n} \rceil} Q(V_1, 1, h) = P(V_1, \lceil \frac{M}{n} \rceil, 1, 1) \tag{5.7}$$

With a proper setting of n and u, the readers are equally distributed among the priority levels, and V_1 approaches the minimum value $V - (n-1)u$. $P(V, M, 1, n)$ is similar to the probability of querying tags in the original version of NFRA with a reduced number of neighbors V_1. It advantages readers that have not been communicating with tags for the longest time, and it results in a fairer network.

A reader with priority 2 can query tags only if all the highest priority readers collide; the probability of this event is:

$$P_c(1) = \sum_{f=1}^{V_1} \left((-1)^{f-1} \binom{V_1}{f} \left(\frac{\lceil \frac{M}{n} \rceil - f}{\lceil \frac{M}{n} \rceil} \right)^{V_1 - f - 1} \cdot \prod_{g=1}^{f} \frac{\lceil \frac{M}{n} \rceil - g}{\lceil \frac{M}{n} \rceil} \right) \tag{5.8}$$

The probability that a reader with a priority level equal to l queries tags is obtained multiplying (5.7) and (5.8):

$$P(V, M, l, n) = P(V, M, 1, n) \cdot \prod_{e=1}^{l-1} P_c(e) \tag{5.9}$$

In NFRA+, the probability of transmitting is maximum for the readers with the highest priority, then sharply decreases, according to (5.9). This avoid long delays in tags identification and guarantees a similar performance of the readers.

5.1.2 Maximizing throughput in NFRA

The throughput attained by NFRA is affected by the random choice of m. Even if a collision is detected at the beginning of the round, it could be no longer valid at the end, as one of the readers may have received an OF in the meantime. Fig. 5.1 provides an example. After the first OC, only reader 4 can identify tags, since readers 1 and 2 mutually exchange beacons. After the second OC, readers 3 and 5 don't detect any collision and start the interrogation of their tags. At the end of the round, 3 readers out of 5 identify their tags. However, in the example reader 1 has no active neighbor, so it can communicate with tags without generating a collision.

Algorithm 6 Pseudocode of proposed approach NFRA++

loop
  while a signal is not received from the server **do**
    No operation
  end while
  if the signal is AC **then**
    Decode the number M from AC
    set $l_i = max(1, n - \lfloor \frac{w_i}{u} \rfloor)$
    set $m_i = random\big(\lfloor \frac{M}{n} * (l_i - 1) \rfloor + 1, \lceil \frac{M}{n} * l_i \rceil\big)$
  else if signal is OC **and** no OFs received since last AC **then**
    Decode the number j from OC
    if $(j == m_i)$ **then**
      Broadcast a beacon to neighbors
      if a beacon collision is not detected **then**
        Broadcast OF to neighbors
        Query tags
      end if
    else if $(j == M + 1)$ **and** *random(0, 1)* $\leq T$ **then**
      Broadcast a second beacon to neighbors
      if *a new beacon collision is not detected* **then**
        Broadcast OF to neighbors
        Query tags
      end if
    end if
  end if
end loop

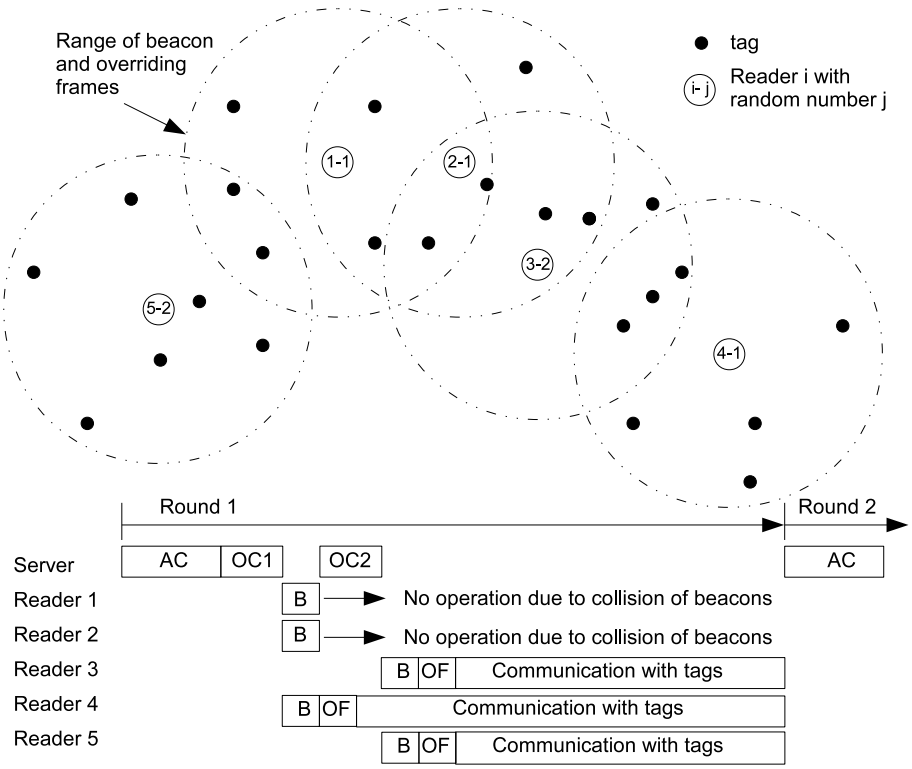

Figure 5.1. An example of critical network for NFRA ($M = 2$)

The proposed improvement concerns the possibility of sending a second beacon. This further signal can resolve collisions detected during the first slots, but no more valid at the end of the round. In detail, after the ordinary OCs, the server broadcasts an additional one. According to NFRA specifications, the length of a slot is negligible compared to the average time requested by a reader to query tags [12]. Thereby, an additional OC does not introduce a significant overhead. This signal can only be detected by active readers that have experienced a collision of beacons and that have not received any OF. Then, if no beacon is received, the reader can query tags.

The pseudocode of the proposed approach, henceforth denoted as NFRA++, is reported in Algorithm 6, highlighting in italic the differences with respect to NFRA. The correctness of the protocol has been formally proved by means of an automatic model checker tool, called Spin [84]. First, the finite-state model of Algorithm 6 has been implemented through the Promela process modeling language [84]. The Promela model is composed of two concurrent processes, i.e. Server and Reader. Several instances of the Reader process are simultaneously executed to simulate a dense RFID network. AC and OF signals are broadcast by the Server process to all the Reader instances via a synchronous message channel. Other channels are used by the Reader instances to exchange beacons and OFs. At the end, the Promela model

has been exhaustively verified by Spin for the absence of deadlocks and invalid final states. Moreover, Spin has verified that the property of anticollision always holds among neighbors.

In Fig. 5.1, when the server broadcasts the $(M+1)^{th}$ OC, reader 1 is the only one which experienced a beacon collision without receiving any OF. It sends a second beacon to its neighbors, but this time no beacon collisions occur, because reader 2 was previously disabled by an OF received by reader 3. Thus, after sending an OF, reader 1 can interrogate tags, improving the network throughput with respect to NFRA.

While some previously detected beacon collisions disappear, the second generation of beacons could generate new collisions among readers that have initially selected different numbers. This case is shown in Fig. 5.2. After the first OC, readers 1 and 5 mutually exchange beacons, so neither of them could query tags. Another collision occurs after the second OC, involving readers 2 and 3. When the server broadcasts the third OC, reader 4 does not notice any interference and sends an OF to readers 3 and 5. Now, only readers 1 and 2 are able to detect the last OC. When they try to broadcast a new beacon, they experience a collision, even if it did not happened before.

In order to minimize the number of collisions caused by the second beacon, the proposed approach only grants a subset of readers the right to broadcast beacons for the second time. After detecting the last OC, the reader sends the beacon with a probability T. In the example of Fig. 5.2 four cases can happen:

1. both reader 1 and 2 extract a value higher than T and do not send any more beacon, as in NFRA;
2. only reader 1 generates a value lower than T, sends its second beacon and queries tags;
3. only reader 2 generates a value lower than T, so it can communicate with tags;
4. readers 1 and 2 extract a value lower than T and collide.

Only cases 2 and 3 ensure an improvement in throughput.

Quantitative analysis of readers sending a second beacon

This section quantifies how many readers per round experience a beacon collision but do not receive an OF in the following slots. These readers can send a second beacon in the additional slot, as described above.

Let us consider a network of N readers, uniformly randomly located, with an average neighborhood of V readers. Let N_i indicate the number of idle readers at slot i, i.e. readers which neither send an OF nor received one. Given a generic idle

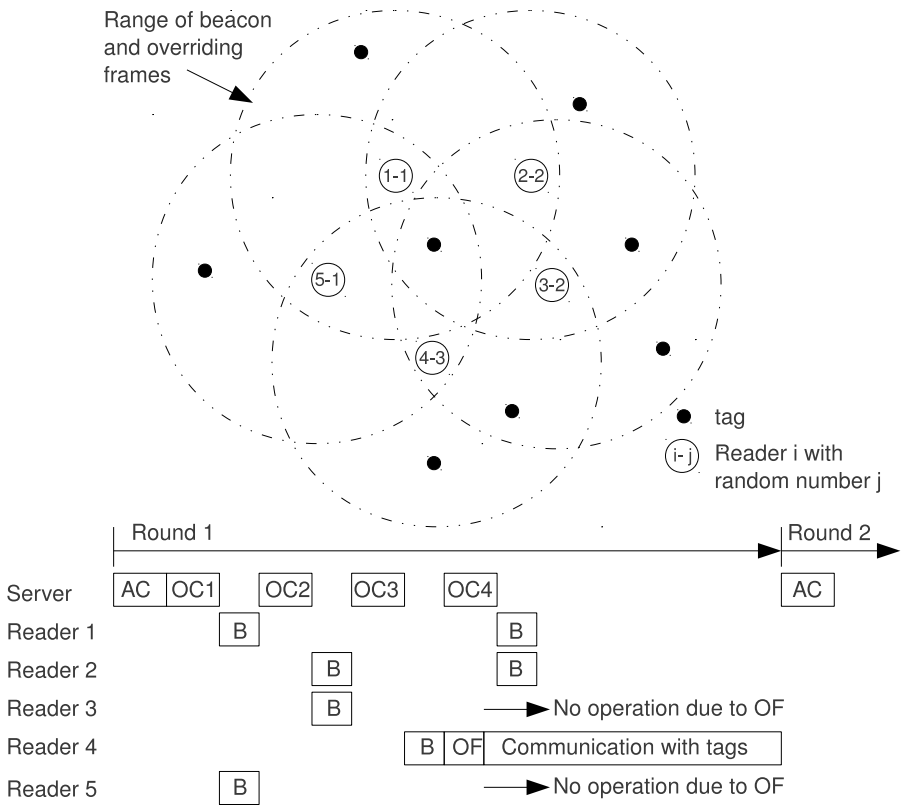

Figure 5.2. A beacon collision in the additional slot of NFRA++ ($M = 3$) between two readers that selected different numbers at the beginning of the round

reader, its average idle neighborhood at slot i is denoted as V_i. Obviously, when the server broadcasts the first OC, $N_1 = N$ and $V_1 = V$. On the average there are $\frac{N_1}{M}$ readers sending beacons. A reader, which has selected value 1 at the beginning of the round, can communicate with tags only if none of its neighbors extracted the same value. Since $N_1 - V_1 - 1$ readers are located outside its interference range, the probability that all the readers sending beacons are out of its neighborhood is:

$$P_{B1} = \frac{\binom{V_1}{0}\binom{N_1-V_1-1}{\frac{N_1}{M}-1}}{\binom{N_1-1}{\frac{N_1}{M}-1}} = \frac{\Gamma(N_1-V_1)\Gamma(N_1-\frac{N_1}{M}+1)}{\Gamma(N_1)\Gamma(N_1-V_1-\frac{N_1}{M}+1)} \tag{5.10}$$

where $\Gamma(n)$ is the Gamma function.

On the average, after the first OC, $\frac{N_1 P_{B1}}{M}$ readers do not notice any interference and broadcast an OF. Since there are $N_1 - \frac{N_1}{M}$ readers that have chosen a value

higher than 1, the probability of receiving an OF from readers with value 1 is:

$$P_{OF1} = 1 - \left(1 - \frac{V_1}{N_1 - \frac{N_1}{M}}\right)^{\frac{N_1 P_{B1}}{M}} \tag{5.11}$$

Consequently, $P_{OF1}\left(N_1 - \frac{N_1}{M}\right)$ readers receive an OF.

When the second OC is sent, the number of idle readers is:

$$N_2 = N_1 - \frac{N_1 P_{B1}}{M} - P_{OF1}\left(N_1 - \frac{N_1}{M}\right) \tag{5.12}$$

After the first OC, the average neighborhood is V_1; in this set of readers, on average $\frac{V_1}{M}$ readers have selected value 1 and, among them, $\frac{P_{B1}V_1}{M}$ do not experience a beacon collision and send an OF. All the neighborhoods that contain a transmitting readers are isolated. Since the readers are uniformly deployed, when the server broadcasts the second OC, an idle reader shares on average $\frac{V_1}{2}$ neighbors with a reader that has sent an OF. Therefore, the average neighborhood reduces to:

$$V_2 = V_1 - \frac{P_{B1}V_1^2}{M} \tag{5.13}$$

In general, at the i^{th} OC, the number of idle readers is:

$$N_i = \frac{N_{i-1}}{M}\left(M - P_{Bi-1} - P_{OFi-1}\left(M - 1\right)\right) \tag{5.14}$$

The average neighborhood is:

$$V_i = V_{i-1} - \frac{P_{Bi-1}V_{i-1}^2}{M} \tag{5.15}$$

At slot i, there are $\frac{N_i}{M}$ readers that send a beacon; the number of those that avoid a beacon collision and send an OF is:

$$P_{Bi} = \frac{\Gamma(N_i - V_i)\Gamma(N_i - \frac{N_i}{M} + 1)}{\Gamma(N_i)\Gamma(N_i - V_i - \frac{N_i}{M} + 1)} \tag{5.16}$$

The remaining idle readers may receive an OF with probability

$$P_{OFi} = 1 - \left(1 - \frac{V_i}{N_i - \frac{N_i}{M}}\right)^{\frac{N_1 P_{Bi}}{M}} \tag{5.17}$$

After the M^{th} OC, some readers have detected a beacon collision but do no received any OF; their number is:

$$N_M = \frac{N_{M-1}}{M}\left(M - P_{BM-1} - P_{OFM-1}\left(M - 1\right)\right) \tag{5.18}$$

(5.18) gives the sum of readers that can send a second beacon.

5.1.3 Evaluation

This section presents the results of the simulations performed in order to measure the improvements in fairness and throughput of the proposed approach, compared to DCS, PDCS, Colorwave, Pulse and NFRA. The interrogation range is set to 2 m and the interference range is 8 m, as in [12]. Different networks was sampled, fixing the number of uniformly randomly deployed readers to 500 and varying the number of neighbors, from a minimum of 10 to a maximum of 50 readers. The chosen interval covers the majority of the supply chain scenarios: according to Section 1.7, the corresponding deployment surfaces range from 40 x 40 m^2 to 100 x 100 m^2. For each deployment surface, 5 different network configurations were tested, and each one was simulated 4 times.

The identification time is 0.46 s, as in [12]. In [85], the authors point out that 100 tags can be read during this time. However, the number of identified tags strongly depends on the technology, e.g. an experiment reported in [86] shows that an EPC Class 1 Gen 2 UHF reader working in Dense Reader Mode can read about 7 tags in 0.46 s at a distance of 2 m.

The exchanged signals in DCS, PDCS and Colorwave requires 1 ms [12, 79]: the length of a slot is 0.461 s and 0.462 s, respectively. In Pulse, the length of the signals is longer: the beacon interval is set to 5 ms, as specified in [78]. However, this does not disadvantage Pulse with respect to the other protocols, because authors point out that its throughput is not significantly affected by the length of the beacon interval. In NFRA, the length of an OC is 1 ms, while beacons and OFs are shorter (0.3 ms) [12]. The AC is 2.83 ms, thus the round length is lower than 0.5 s (0.46283 s + 0.0016 s $\cdot M$).

For each protocol, the possible configurations were tested, and the best one is used as benchmark. In DCS, the optimal number of colors depends on the size of the neighborhood: the experimental analysis have shown that the best configuration is close to 1.35 times the number of neighbors. In PDCS, this ratio decreases to 1.2. The probability of changing color after a collision is set to 70%, as specified in Section 4.1. Since DCS performs always worse than or equal to PDCS, only the results of PDCS are displayed. In Colorwave, the thresholds for varying the number of colors are set according to the first test input in [10]. The initially available colors are 4; the minimum time to spend with the same number of colors is 500 slots. For Pulse, the maximum backoff time is not specified in [78]. The simulations were performed adopting a value equal to 50 times the beacon interval: this means that, before sending a beacon, every reader waits in the Contend state a period up to 250 ms, nearly the half of the identification time. In NFRA, M is related to the size of the neighborhood V, ranging from 14 (for $V = 10$) to 20 (for $V = 50$). In the proposed approach, the available values are divided in 4 priority levels. Fixing the number of priority levels, the granularity for the evaluation of the waiting time is

proportional to V. Simulations show that, with 4 priority levels, its optimal setting is about $\frac{V}{4}$ rounds.

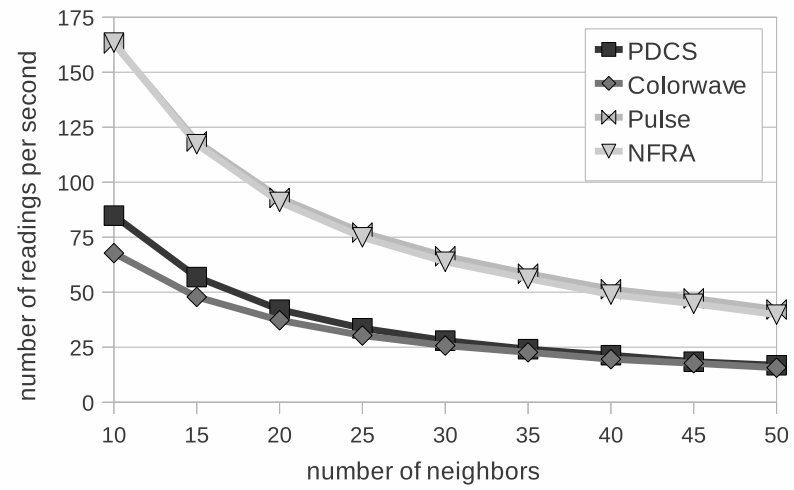

Figure 5.3. Throughput of the state-of-the-art protocols, in static networks

Fig. 5.3 reports the throughput for the state-of-the-art protocols, in case of fixed readers. Pulse and NFRA achieve the highest values, as their lines overlap in Fig. 5.3. The throughput of PDCS is strongly affected by the number of used colors. Using few colors, many collisions occur, with low performances. With too many colors, there are no collisions, but the channel is underloaded. Fig. 5.3 plots the highest throughput attained by PDCS, adopting the optimal number of colors. The performance of Colorwave is lower than PDCS, but independent of the initial configuration.

The main scope of the proposed protocol is to provide high fairness. Fig. 5.4 shows the fairness of the protocols, considering static networks and varying the number of neighbors. The fairness of PDCS is strongly affected by the number of used colors. The optimal results plotted in Fig. 5.4 are achieved only if the number of colors is higher than the number of neighbors, in order to allow communication without collisions. However, this configuration results in long rounds and limits the overall throughput. In Colorwave each reader can vary the number of used colors. As a consequence, there is a significant difference of the frequency used by the readers to query tags. This fact dramatically impacts on fairness. In Pulse it happens frequently that the performance of a reader is dramatically reduced by two neighbors that take turns with each other at querying tags. In order to increase the fairness of the protocol, the only countermeasure is to enlarge the maximum backoff time. This prolong the time that a reader spent in the Contend state after completing a transmission. However, readers that have received a beacon have a lower delay, because they use the residual backoff time when they return again to the Contend

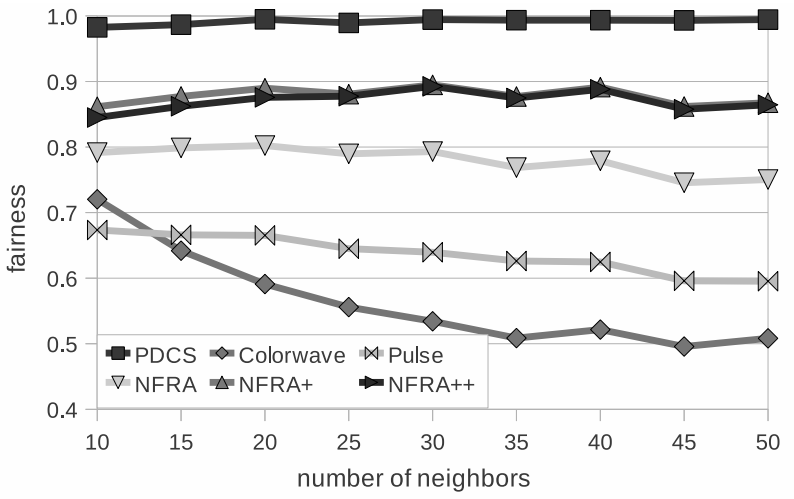

Figure 5.4. Fairness of the evaluated protocols, in static networks

state. The higher the backoff time is, the fairer the protocol is, but to the detriment of throughput. The fairness of NFRA is affected by the absence of a mechanism for managing the heterogeneous distribution of the readers in the network, as explained in section 5.1.1. The introduction of the priority in the proposed approaches increase the fairness of about 10%.

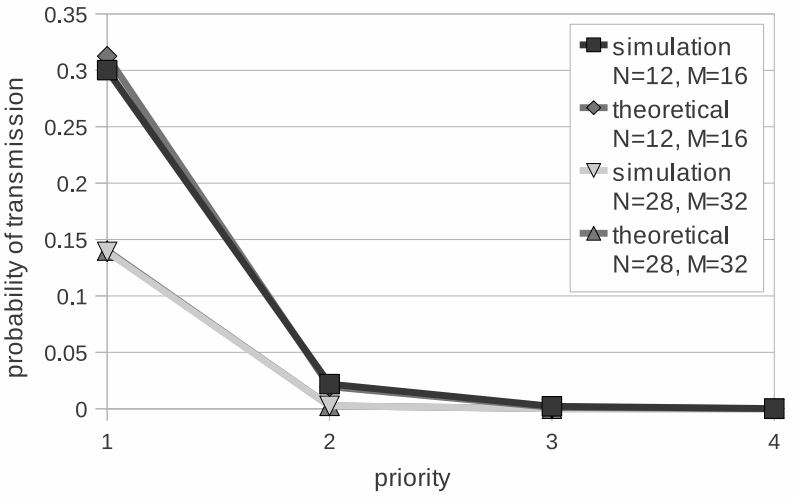

Figure 5.5. Probability of transmitting in NFRA+, in function of the priority

The effectiveness of the priority levels is demonstrated in Fig. 5.5. Two networks are considered: the first one is constituted by 12 readers, the second one by 28. In both networks, every reader interferes with all the others. The NFRA+ algorithm

is adopted, setting it up with 4 priority levels. Each level contains 4 colors in the first network and 8 in the second one. Fig. 5.5 shows the probability of querying tags, in function of the priority. A reader with the highest priority can interrogate tags quite often, whereas a reader with the lowest priority seldom can do it. Since the highest priority is reserved to readers that have not completed any transmission from the longest time, this guarantees the fairness of the NFRA+ proposal. Fig. 5.5 shows also the results obtained from equation (5.9), demonstrating that they match the simulation data.

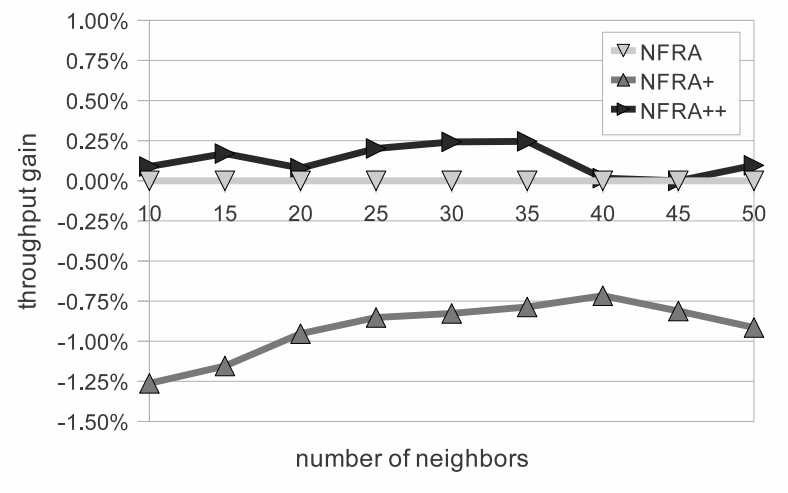

Figure 5.6. Throughput gain of the proposed protocols, with respect to NFRA

As a side effect, the priority management decreases the overall throughput, as shown in Fig. 5.6. However, this reduction is completely compensated by the NFRA++ approach, detailed in section 5.1.2. The fairness of NFRA++ remains the same as NFRA+, as shown in Fig. 5.4.

The throughput increase provided by the additional slot is analyzed in Fig. 5.7. 5 different networks of 500 readers, with an average neighborhood equal to 10, have been simulated. The server broadcasts 12 OCs, plus another one in which readers can send a second beacon. The average statistics are compared with the theoretical analysis of Section 5.1.2. At the beginning of each slot, the number of readers that neither did not send an OF nor receive anyone decreases sharply. As a consequence the number of readers that send a beacon follows the same trend. However, a significant amount of them experiences a beacon collision, since the readers sending an OF are roughly the half. After a beacon collision, many readers do not receive an OF in the next slots. Therefore, the number of readers that can send a second beacon in the additional slot is higher than in the previous ones, providing a throughput improvement.

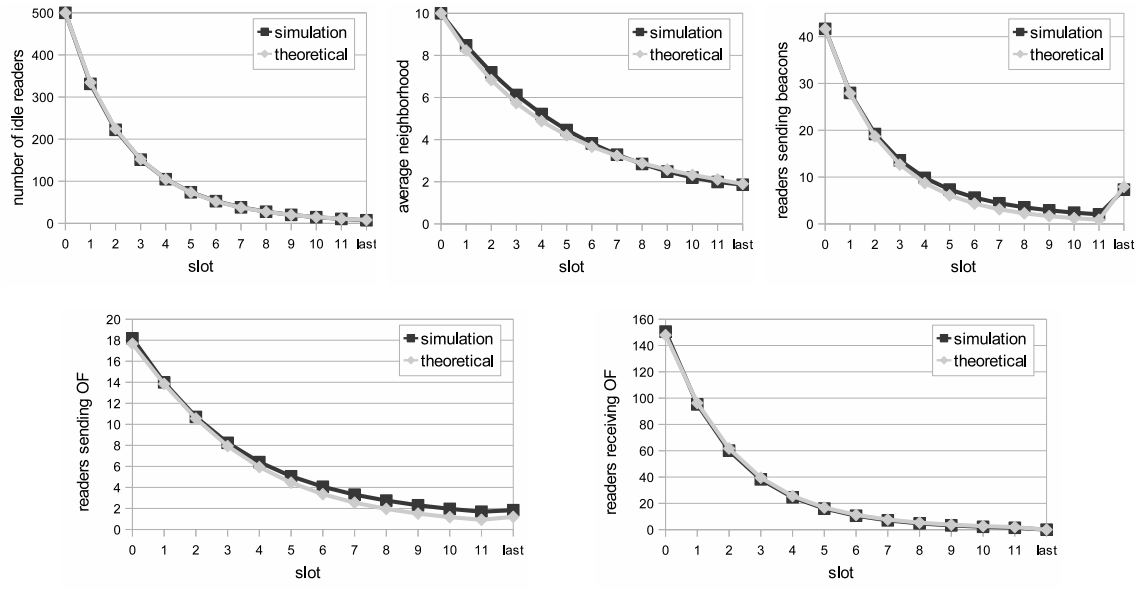

Figure 5.7. Analysis validation, for a network with N = 500, V = 10, M = 12

The behavior of the considered approaches in a dynamic situation is reported in Fig. 5.8 and 5.9. In general, the throughput of a mobile network is lower than the one of a static network, because readers need to adapt to the changing neighborhood. This reduction is particularly evident in Pulse, as it is less likely the case of two readers that alternate with each others in querying tags to the detriment of another reader. This causes a fairer network, even with a shorter backoff time, but also a higher number of collisions and therefore a lower throughput. In PDCS, the optimal number of colors is lower in a mobile environment than in a static one: the initial differences in the layout are regulated by the mobility of the readers, generating a smaller average neighborhood that requires fewer colors. However, the variation of the neighborhood prevents the network from reaching a stable state without collisions, penalizing the throughput. Despite the flexibility of the number of colors used by a reader, in Colorwave, after an increment or a decrement, this number is kept constant for a fixed period. Therefore the variation may be not fast enough to adapt to the quickly changing neighborhood. NFRA is less affected by the mobility of the readers, because a variation of the neighborhood can be immediately detected. This greater adaptability to mobile networks is kept in the proposed approach, as shown in Fig. 5.8.

The mobility increases the fairness of the protocols, because it reduces the differences in the deployment of the readers. As stated previously, Pulse gets the greater benefit in fairness. Although in a mobile network the fairness of NFRA increases, the management of the priority introduced by the proposed approach can raise further

the fairness of the protocol.

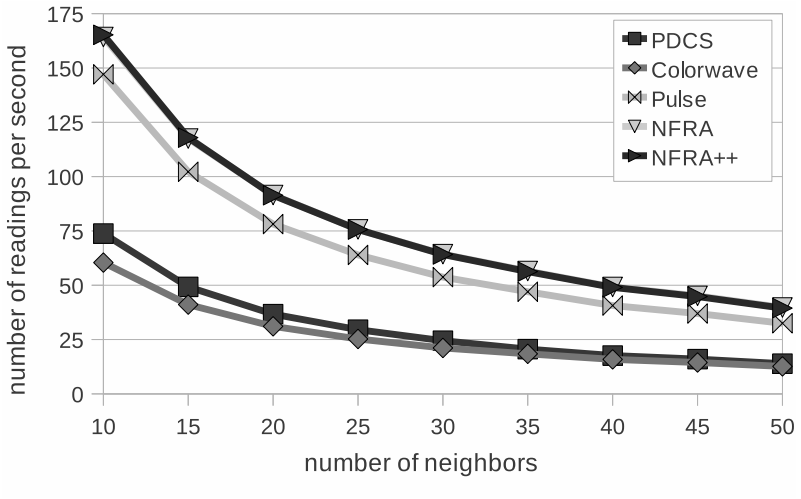

Figure 5.8. Throughput of the evaluated protocols, in mobile networks

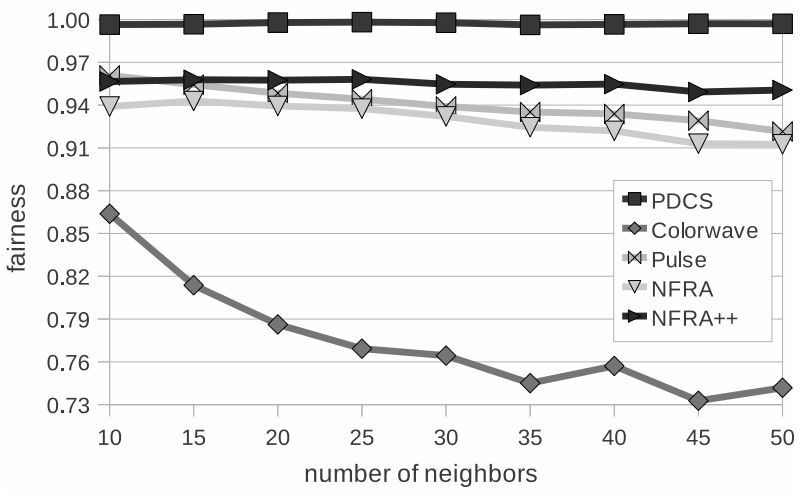

Figure 5.9. Fairness of the evaluated protocols, in mobile networks

5.2 Geometric Distribution Reader Anticollision (GDRA)

The protocol Geometric Distribution Reader Anticollision (GDRA) has been developed in order to regulate the activities of a dense RFID system placed in a

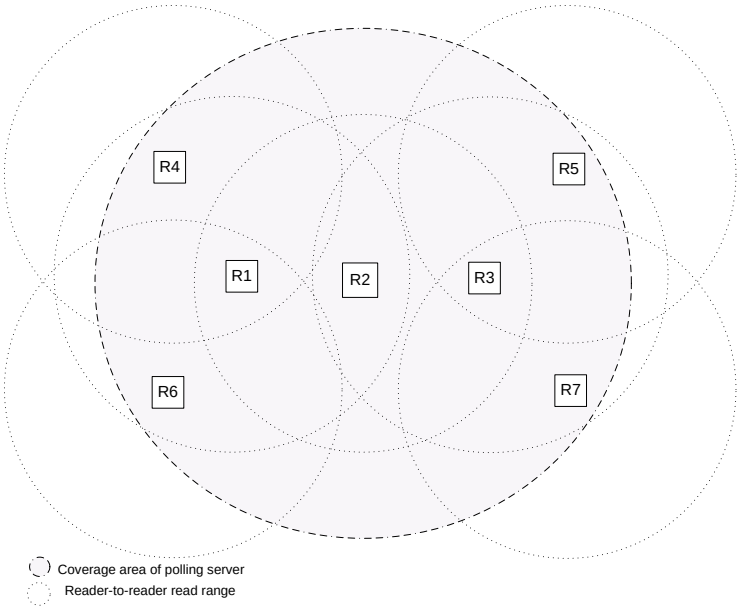

Figure 5.10. Example of dense reader environment with $R = 7$

European location. The RFID system is composed of a set of R fixed and/or mobile commercial readers connected to a central server by means of a wired (e.g. Ethernet infrastructure) or wireless connection (e.g. Wifi), as the network depicted in Fig. 5.10. Readers are provided by two bi-static antennas [87]: one for transmitting and the other for being continuously receiving. This hardware allows readers to detect if other readers are using the same channel while they are transmitting. Readers are working under the EPCglobal Class-1 Gen-2 standard, in particular at UHF Europe band, allocated at 868 MHz. They collect information from tags identified in their target region and send it back to the central server periodically, following the LLRP. Finally, they operate in any of the four frequencies recommended by EPC-ETSI.

The proposed approach is based on a TDMA scheme, but it also combines the FDMA scheme of ETSI-EN 302 208. When readers start working in the network, they randomly select one out of four available frequencies to start the communication, both among them (through the GDRA mechanism) and with tags in their range. Hence, from R readers in the network, there will be up to four sets of readers working under the same frequency. In every frequency, a TDMA scheme is addressed like in NFRA. A central server synchronizes readers in every set, and divides the time in identification rounds of fixed or variable length (T). The identification rounds are formed by a contention round and a reader-to-tag communication phase (see Fig. 5.11). The central server determines the beginning of every identification round sending an AC packet which contains the length of the contention round expressed

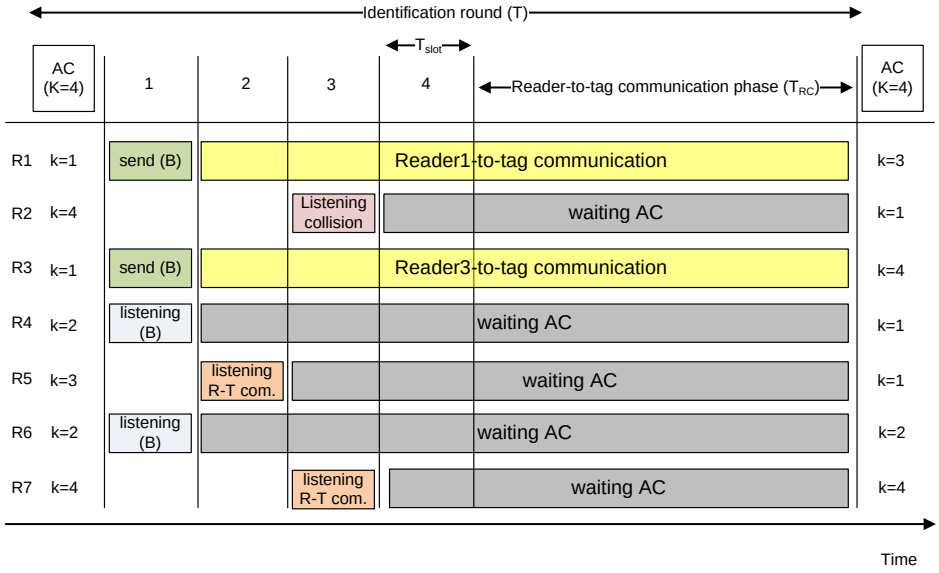

Figure 5.11. Example of GDRA procedure. Readers work at the same frequency and listen to the central server by an Ethernet or wireless link. The central server announces an identification round with length K=4.

in number of slots (K). A slot is defined as the minimum time required by a reader to determine if a channel is busy or not. EPC-ETSI [9, 18] sets this time to $t_{slot} = 5$ ms. In every identification round readers randomly select one out of the K slots. The reader that wins the contention in a set is the only one able to transmit in that frequency, during the reader-to-tag communication phase. The length of the reader-to-tag communication phase (T_{RC}) is given by:

$$T_{RC} = T - T_{slot} \cdot k_{r-wins} \tag{5.19}$$

T_{RC} depends on the slot where the reader wins the contention (k_{r-wins}), as discuss in Section 5.2.

An example of GDRA procedure is shown in Fig. 5.11, according to the network configuration of Fig. 5.10. In this scenario, all readers are working under the same frequency, that is, they are in the same set s. Although the central server determines a TDMA scheme for every frequency, there will be as many *virtual* identification rounds as readers working under the same frequency overlapping their reader-to-reader read ranges. Those readers under that condition are considered readers belonging the same subset. For example, in Fig. 5.10 there are seven readers working at the same frequency. Hence, there will be up to seven *virtual* identification rounds (one per each set or readers overlapping: (s_1=$\{R1, R2, R4, R6\}$,

s_2=$\{R1, R4\}$, s_3=$\{R1, R6\}$, s_4=$\{R1, R2, R3\}$, s_5=$\{R2, R3, R5, R7\}$, s_6=$\{R3, R5\}$, s_7=$\{R3, R7\}$). If $R1$ and $R3$ transmit simultaneously, as stated in Fig. 5.11, only readers belonging to the same subset listen them, that is, readers in $P = s_1 \bigcup s_2 \bigcup s_3 \bigcup s_4$ listen $R1$ and readers in $Q = s_4 \bigcup s_5 \bigcup s_6 \bigcup s_7$ listen $R3$. Readers in $P \bigcap Q$, like $R2$, notice only collisions of $R1$ and $R3$.

Algorithm procedure

Every identification round starts when the central server broadcasts an AC packet by a wired or wireless link (line 4 in Algorithm 7). The AC packet contains the value of K. Readers receive the AC packet, extract K value (line 7) and randomly select one slot k, being $k \in 1,2,\ldots,K$. In contrast to NFRA, where readers use the uniform distribution function for selecting slots, in GDRA the readers use *Sift* probability (lines 8-16), a geometric distribution function [19] that minimizes collision probability between contending readers, maximizing the probability that a single reader takes a slot, winning the channel for reader-to-tag communication. The *Sift* distribution function is detailed in Section 5.2.

In contrast to NFRA, the beginning of the slots in the contention round is not announced by the central server, because readers know the length of the slots and can determine when a slot finishes using a synchronous clock (e.g. an internal clock) (line 32).

Readers, after selecting a slot k, keep waiting for $k-2$ slots without listening the channel for saving energy (see Fig. 5.11). Those readers that selected $k = 1$ send a beacon packet B directly and keep listening the channel to detect beacon collisions (lines 17-19 and lines 26-28). After $k - 2$ slots, readers listen the channel selected (lines 29-31). When slot k starts:

- If the channel was busy in the $(k - 1)$-th slot (due to collisions or successful reader transmissions), those readers that selected slot k leave the contention, randomly select a new frequency and keep waiting a new AC packet (lines 37-41).

- If the channel was *idle* (free channel) in the $(k - 1)$-th slot, those readers that selected slot k consider that the channel is not busy. Hence, at the beginning of slot k, these readers send a beacon packet B, requiring the channel for reader-to-tag communication (lines 26-28 and lines 47-49).

When readers send a B packet in slot k, two actions can occur:

- If only a single reader transmits a B packet in its set, the reader wins the contention and takes the channel in slot $k + 1$, starting the reader-to-tag communication phase (lines 43-46). Hence, the reader uses the subsequent slots

Algorithm 7 GDRA protocol for every reader r_i

set frequency f_i = (int) random(1,4)
loop
  r_i listens the central server connection
  while AC packet is not received **do**
    no operation
  end while
  r_i extracts the K value from AC packet
  set $\alpha_i = M^{\frac{-1}{K-1}}$
  set l_i = random(0,1)
  set $k_i = K$
  for $z = 1$ to K **do**
    if $p_z = \frac{(1-\alpha)\alpha^K}{1-\alpha^K}\alpha^{-z} > l_i$ **then**
      set $k_i = z$
      break
    end if
  end for
  if $k_i == 1$ **then**
    set b_i = true
    set $listen_i$ = true
  else
    set b_i = false
    set $listen_i$ = false
  end if
  set $query_i$ = false
  for $c = 1$ to K **do**
    if $b_i ==$ true **then**
      r_i broadcasts B packet in f_i
    end if
    if $k_i == c{+}1$ **then**
      set $listen_i$ = true
    end if
    while r_i does not receive an internal clock signal **do**
      if $listen_i ==$ true **then**
        r_i keeps listening f_i
      end if
    end while
    if $listen_i ==$ true **AND** $query_i ==$ false **then**
      if f_i is busy **then**
        set f_i = (int) random(1,4)
        set b_i = false
        set $listen_i$ = false
      else
        if $b_i ==$ true **then**
          set b_i = false
          set $query_i$ = true
          r_i starts reader-to-tag communication in f_i
        else
          set b_i = true
        end if
      end if
    end if
  end for
end loop

and the reader-to-tag communication phase for tag identifications (see reader $R1$ in Fig. 5.11).

- If two or more neighboring readers transmit a B packet simultaneously, a collision occurs (lines 38-41). These readers (assumed to be bi-static [87]) detect their own collisions. Then, they leave the contention, select a new frequency and keep waiting a new AC packet. The remaining readers keep waiting the internal clock signal, except those readers that selected slot $k+1$, which also leave the contention because they could be suffering collisions due to being in range of two sets, like $R2$ in Fig. 5.11. Hence, to avoid further collisions, these readers must leave the contention round, select a new frequency and keep waiting a new AC packet.

After transmitting in the reader-to-tag communication phase, the reader keeps the same frequency, waiting a new AC packet and the subsequent contention procedure.

Sift: a geometric probability distribution function

The design of the new approach GDRA started in the contention procedure. The uniform distribution is the typical distribution probability used for dense RFID proposals, as NFRA, where the probability to collide in any slot is the same for all contenders. However, since RFID readers can sense the environment, readers could use this ability to reduce collisions in some way, like MAC protocols in wireless sensor networks. For example, the *Carrier Sense Multiple Access/p** protocol (CSMA/p^*) [19] exploits a non-uniform probability distribution p* that nodes use for randomly selecting contention slots, minimizing collisions between contending nodes. CSMA/p* is considered as the optimal distribution in a MAC protocol, and several works in the literature have referenced it.

In a network of transmitting nodes, if a set of R nodes are contending in a frame of K slots, using CSMA, there is an optimal probability distribution for selecting the contending slots which minimizes collisions between contending nodes, maximizing the probability that a node takes a slot alone [19]. This probability distribution is denoted as

$$p_k^* = \frac{1 - f_{K-k}(R)}{R - f_{K-k}(R)}(1 - p_1^* - p_2^* - \ldots - p_{k-1}^*) \tag{5.20}$$

for $k = 1,2,\ldots,K$. $f_{K-k}(R)$ is a recursive function given by

$$f_{K-k}(R) = \left(\frac{R-1}{R - f_{K-k-1}(R)}\right)^{R-1} \tag{5.21}$$

for $2 \leq k \leq K$, $R \geq 2$ and $f_1(R) = 0$.

To apply CSMA/p^* in a dense RFID protocol, every reader has to know (or estimate) the number of neighbors, a data which is not available in practice. But, if the number of neighbors is unknown, the *Sift* geometric probability distribution function is proposed in [19] as an approximation to CSMA/p*. With *Sift* the probability (p_k) that a node selects a slot K is denoted as a truncated geometric distribution

$$p_k = \frac{(1-\alpha)\alpha^K}{1-\alpha^K}\alpha^{-k} \tag{5.22}$$

for $k = 1, \ldots, K$, $0 < \alpha < 1$ and $\alpha = M^{\frac{-1}{K-1}}$. M is the maximum number of contenders. Note that when $M = 1$ then $\alpha = 1$ and $lim_{\alpha \to 1} p_k = \frac{1}{K}$, being the uniform probability distribution.

In Fig. 5.12 the uniform and *Sift* probabilities distribution are compared for a contention frame with $K = 8$ slots. Uniform distribution shows the same probability p_k for every slot in the contention round whereas with *Sift* distribution the probability increases in every higher slot. This mechanism increases the probability that a unique node selects a slot in a low position, winning the contention quickly. Fig. 5.12 also shows how the M value affects to the p_k. As M increases, the probability of selecting one of the last slots in the frame increases. This mechanism provokes that if a high quantity of nodes are competing, many of them will select the last slots, and only a few will select the first slots, decreasing the probability of collision, and increasing the probability that a reader wins the contention in one of the first slots of the frame.

The probability that a node wins the contention when R neighboring nodes select a contention slot using *Sift* probability distribution is denoted as

$$P_c(R) = R \sum_{k=1}^{K-1} p_k \left(1 - \sum_{z=1}^{k} p_z\right)^{R-1} \tag{5.23}$$

Fig. 5.13 shows this probability when $R = 50$ and $K = 8$ using uniform and *Sift* distribution at different M values. The uniform distribution shows a low probability when the number of nodes is high. Instead, *Sift* distribution shows a good response, for different M values. The best performance is achieved with M closest to R. Hence, *Sift* works better than uniform distribution, and also has the desirable property it scales linearly as the maximum number of contenders raises.

In GDRA, the *Sift* distribution is the probability distribution function used to select a slot in a contention frame. Contending nodes are RFID readers and CSMA procedure is the LBT strategy.

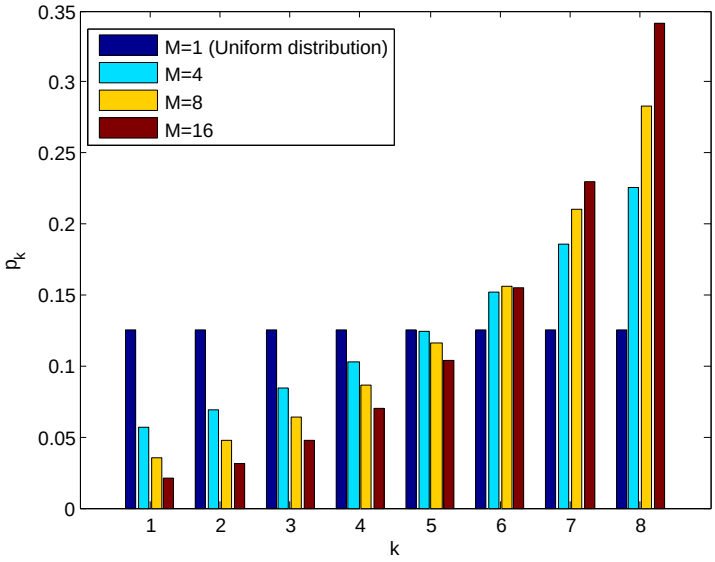

Figure 5.12. Probability of selecting every slot $k \in 1, ..., K$ under Sift and Uniform distribution. $R = 50$ and $K = 8$.

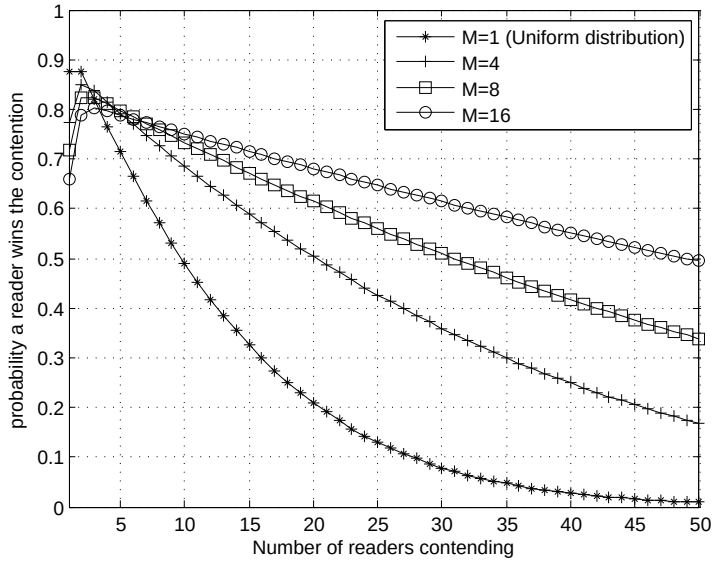

Figure 5.13. Probability a reader wins the contention under Sift and Uniform distribution. $R = 1, \ldots, 50$ and $K = 8$.

5.2.1 Evaluation

The performance of GDRA has been compared with the most relevant state-of-the-art mechanisms: the distributed protocols DCS, Colorwave and PDCS; the centralized protocol NFRA, and the European standard and regulation Listen Before

Mechanism	Parameters
EPC-ETSI	LBT = 5 ms Reader-to-tag communication length = 0.46 s Waiting time = 100 ms
Colorwave	Reader exchange signals = 1 ms UpSafe = 93 % DnSafe = 90 % UpTrig = 2 % DnTrig = 1 % MinTimeInColor = 100 slots Reader-to-tag communication length = 0.46 s
DCS	Reader exchange signals = X ms MinTimeInColor = 100 slots Reader-to-tag communication length = 0.46 s
PDCS	Reader exchange signals = X ms MinTimeInColor = 100 slots Reader-to-tag communication length = 0.46 s Probability of changing color P= 0.70
NFRA	AC packet = 2.83 ms OC packet = 1 ms OF packet = 0.3 ms B packet = 0.3 ms Reader-to-tag communication length (CRT) = 0.46 s
GDRA	AC packet = 2.83 ms B packet = 0.3 ms Reader-to-tag communication length (CRT) = 0.46 s T_{slot} = 5 ms $T = CRT + K * T_{slot}$ $T_{RC} = T - T_{slot} * k_{r-wins}$

Table 5.2. Parameters of the mechanisms simulated

Talks (EPC-ETSI). The performance evaluation has been carried out by means of an in-house developed discrete-event simulator with a modular structure: 6 classes represent the basic entities (i.e., reader, protocol, simulation) and specify the common actions (e.g. network deployment, readers movement, interference detection, etc.); each protocol inherits from a common superclass and it is implemented with a specific class. The total number of lines of code is 4300.

In a typical scenario in Europe, an RFID system works at UHF band (868MHz) and it is composed by a set of bi-static RFID readers randomly placed in a square areas of different sizes. Readers output power is set at the maximum value permitted in Europe, P_{tx} = 3.2 Watts EIRP [9]. This value limits the reader read distance (reader-to-tag read range) and the reader interference range to a maximum of 10 and 1000 m in indoor scenarios respectively [67]. At P_{tx} = 3.2 Watts EIRP, a reader-to-tag collision occurs when readers are placed at less than 20 m each other ($< 2 * d_{RT}$) and a reader-to-reader collision at less than 1000 m each other ($< d_{RR}$) [67].

The parameters of the evaluated approaches are summarized in Table 5.2. EPC-ETSI recommends a maximum length of reader-to-tag communication phase of 4 s, but this value is not mandatory. Since NFRA first adopted 0.46 s, in order to

obtain a fair comparison, the same communication length is set for all the evaluated protocols. In PDCS, the probability of selecting a new color is set to $P = 0.70$.

During the reader-to-tag communication phase, it is assumed that readers identify tags and handle/avoid collisions using the Frame Slotted Aloha (FSA) procedure suggested by EPCglobal Class-1 Gen2 [18]. With the standard configuration parameters enumerated in [60], 100 tags are queried in 0.46 s, on the average.

Four different scenarios have been sampled to show the performance of the new proposal and to compare it with the other strategies in different environments. Scenario 1 is an usual situation with a moderate quantity of readers R, $R \in [25, 50, 75, 100]$, in an area of 1000x1000 m. In the second scenario the size of the area is the same but the number of readers is increased $R \in [100, \ldots, 1000]$, provoking that the evaluated network has higher number of neighboring readers than the previous scenario. The third scenario is a very harsh environment. The size of the area is reduced to 250x250 m and the number of readers placed in that area is $R \in [100, \ldots, 500]$. Finally, scenario 4 evaluates the effect of the size of the neighborhood. In this case, only R=50 readers are placed in different areas to obtain a size of neighborhood from 5 to 45 in steps of 5, that is, the percentage of neighboring readers varies from 10% to 90%.

In order to provide a fair comparison, for every scenario two different kinds of tests was conducted. In the first one, a single channel version of GDRA was compared with the protocols that use only one channel: DCS, Colorwave and NFRA. In the second group, the proposed multi-channel protocol was compared with the standard EPC-ETSI and with PDCS.

For every scenario and set of tests, the approaches have been simulated for different values of frame-length K (*colors* in Colorwave, DCS and PDCS) and M (only for GDRA). The configurations that show the best performance for every protocol are summarized in Tables 5.3 and 5.4.

Since GDRA has been designed to work as a multi-channel strategy, its performance in a single-channel configuration is plotted for only one scenario. The performance of the best configurations of single-channel protocols in scenario 1 is compared in Fig. 5.14. As can be seen, GDRA improves all the other strategies, increasing the NFRA throughput due to the use of Sift distribution, instead of Uniform. Note that the time spent by the reader listening the channel to check if it is busy is 5 ms, whereas in NFRA it is only 0.3 ms (B packet length). Hence, if both mechanisms work with the same time for listening the channel, the difference in throughput between them would be still higher. Note that the performance of GDRA in the other evaluated scenarios with single-channel protocols shows the same tendency, being always higher than the other strategies.

The performance of the best configurations of multi-channel protocols are compared as follows. In Fig. 5.15 scenario 1 is plotted. GDRA improves all the other strategies and the performance results are higher than with single-channel strategy,

Scenario	Range of evaluated values	Protocols	Best values
1	K=2^x, $4 \leq x \leq 7$ M=2^x, $3 \leq x \leq 6$	Colorwave DCS NFRA GDRA	K=64 K=32 K=32 K=16, M=16
2	K=2^x, $4 \leq x \leq 10$ M=2^x, $4 \leq x \leq 10$	Colorwave DCS NFRA GDRA	K=512 K=512 K=256 K=256, M=512
3	K=2^x, $4 \leq x \leq 9$ M=2^x, $4 \leq x \leq 9$	Colorwave DCS NFRA GDRA	K=32 K=128 K=128 K=128, M=128
4	K=2^x, $3 \leq x \leq 8$ M=2^x, $2 \leq x \leq 8$	Colorwave DCS NFRA GDRA	K=16 K=16 K=16 K=16, M=16

Table 5.3. Evaluated values in tests with single channel protocols

Scenario	Range of evaluated values	Protocols	Best values
1	K=2^x, $3 \leq x \leq 7$ M=2^x, $3 \leq x \leq 6$	PDCS GDRA	K=16 K=16, M=16
2	K=2^x, $4 \leq x \leq 10$ M=2^x, $4 \leq x \leq 10$	PDCS GDRA	K=64 K=256, M=512
3	K=2^x, $4 \leq x \leq 8$ M=2^x, $4 \leq x \leq 7$	PDCS GDRA	K=256 K=32, M=32
4	K=2^x, $2 \leq x \leq 6$ M=2^x, $2 \leq x \leq 6$	PDCS GDRA	K=8 K=16, M=16

Table 5.4. Evaluated values in tests with multi-channel protocols

due to the use of four frequencies. If multi-channel GDRA is compared with NFRA in this scenario, the performance is increased in almost 400%.

The best results of the multi-channel approaches in the second scenario are compared in Fig. 5.16. GDRA shows the best performance for all the R values except for R=100 and R=200, where EPC-ETSI and PDCS reach the highest performance respectively. The low performance of GDRA in these points comes from the use of the *Sift* distribution in a scenario where K and M values are higher than R (number of contenders due to almost all readers are neighbors). The *Sift* distribution shows a good response when K and M values are equal or lower than the number of neighbors (see Section 5.2).

Fig. 5.17 shows the results with the best configurations of the evaluated multi-channel mechanisms in the third scenario. Also in this scenario GDRA presents better performance than the other protocols, even if PDCS is a bit better with R=200. In this case, GDRA is negatively affected by the M value, which is much lower than the real number of readers competing. The lower performance of EPC-ETSI is caused by its inefficient mechanism to select the transmission frequency in

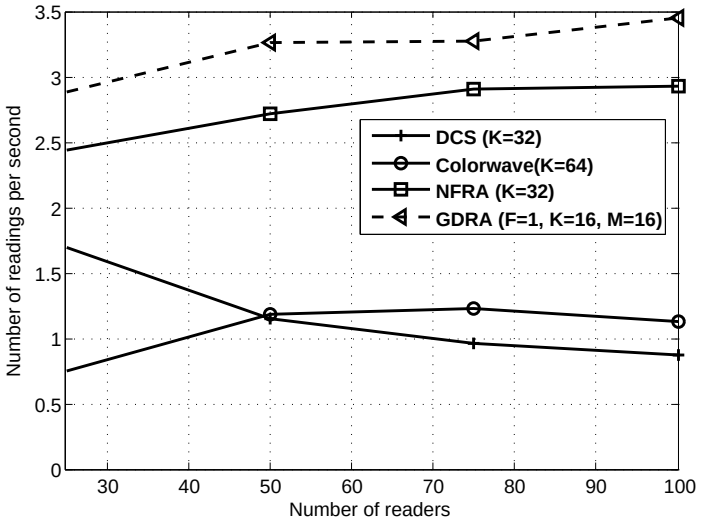

Figure 5.14. Throughput of the evaluated single-channel protocols in 1000x1000 m area with a low number of neighboring readers

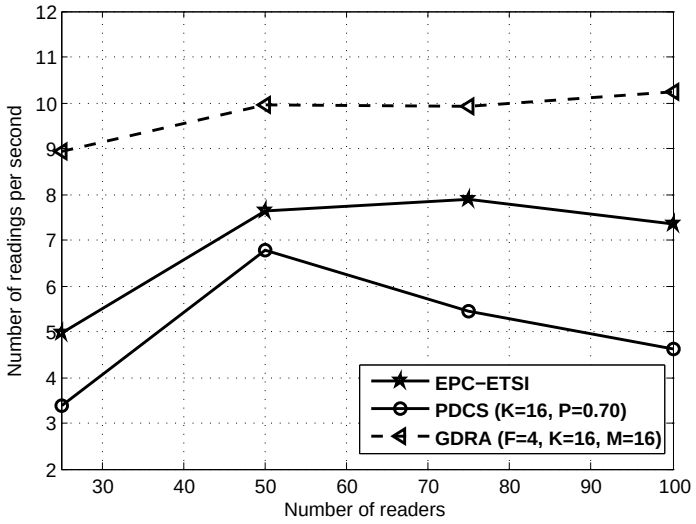

Figure 5.15. Throughput of the evaluated protocols in 1000x1000 m area with a low number of neighboring readers

case of contention.

Finally, the best performances of the multi-channel approaches in scenario 4 are shown in Fig. 5.18. Again GDRA strategy shows the best throughput, resulting in more than four times throughput of PDCS and more than two times throughput of EPC-ETSI in the point with the highest neighboring readers percentage (90%).

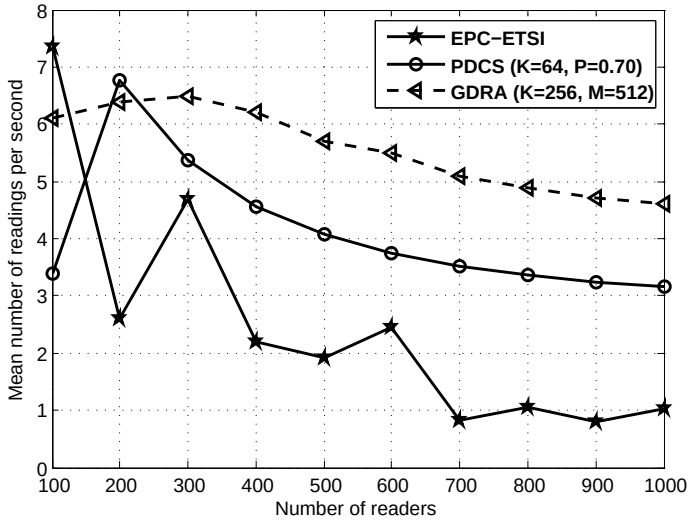

Figure 5.16. Throughput of the evaluated protocols in a 1000x1000 m area with a high number of neighboring readers

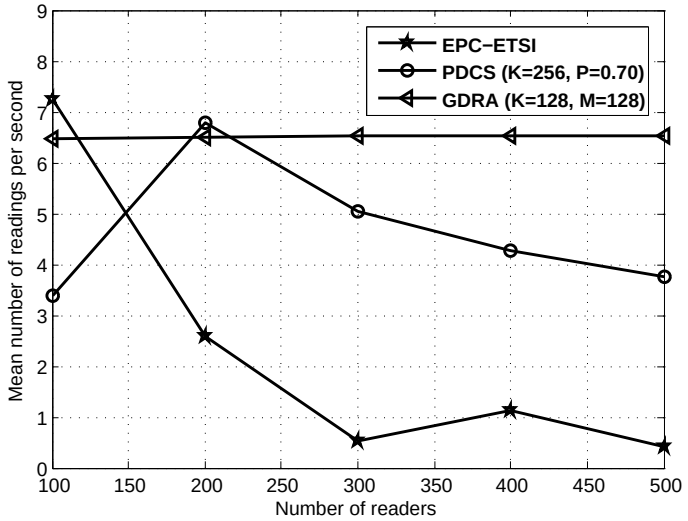

Figure 5.17. Throughput of the evaluated protocols in 250x250 m area

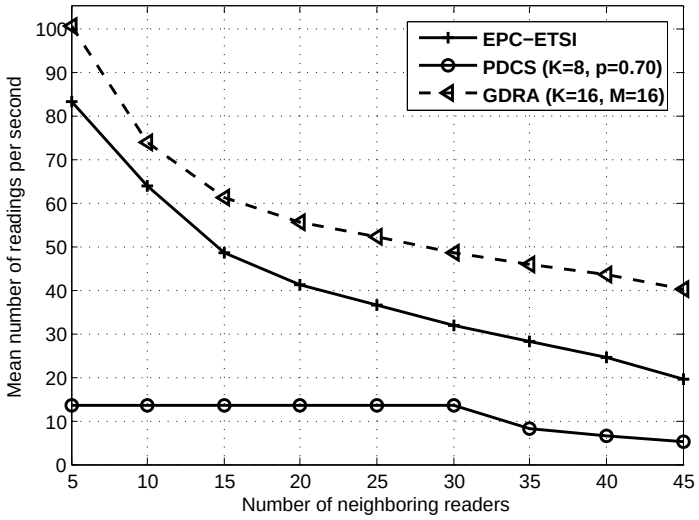

Figure 5.18. Throughput of the evaluated protocols in 30000x30000 m area and R=50

Conclusion

In Chapter 1 a new degree distribution of UDGs for uniformly randomly deployed nodes on rectangular surfaces has been presented. This kind of graph is used in computer science to model wireless networks, and it corresponds to a typical simulation setting, where nodes are uniformly randomly deployed on a rectangular surface. Several state-of-the-art papers have proposed approximations of degree distribution, characterized by low accuracy. The main issue in finding an accurate distribution is how to manage border effects.

The main contribution of Chapter 1 corresponds to a careful geometric analysis of the intersection between the deployment surface and the neighborhood surface. The results of this analysis are used to derive the probability mass function of the degree distribution and the mean. The evaluation section validates the theoretic analysis, and shows that the proposed formulas provide a greater accuracy than state-of-the-art approaches.

In Chapter 2, the single and additive reader-to-reader interference models are analyzed and compared in various scenarios. In particular, the ring deployment scenario is analyzed to get the relationship between the radius of the circle area and the number of interfering readers. The interaction between two interfering readers is also investigated. Numerical evaluation results have shown how the minimum distance between readers is influenced by the number of interfering readers, according to different path loss exponents and SIR threshold requirements. Compared with the reader-to-reader collision range in the unit disk graph model, the distance in the radio propagation model is quite larger. However, in an environment with a higher path loss with a low required SIR, the collision distance of the two models are very close and the unit disk graph model is preferred.

Chapter 3 describes the state-of-the-art solutions for the reader-to-reader interference, identifies the protocol requirements and discusses the criteria that are used to evaluate the performance of a protocol.

Chapter 4 presents three different techniques in order to address the reader-to-reader collision problem without exploiting an additional control channel. The first proposal is PDCS, a multichannel anticollision protocol, compliant to the international regulation for UHF RFID. Thanks to the parameter p, representing the

probability to change color after a collision, the number of collisions is lower, and PDCS reaches a steady state with a lower number of timeslots in a round. A theoretical analysis demonstrates that the correct configuration of p can provide over 30% reduction of second generation collisions. An evaluation approach based on waiting time has been adopted. A theoretical analysis justifies the reduction of the waiting time. Experimental simulations validate the theoretical analysis, showing that PDCS can reach a time reduction about 10%, compared to the best DCS configuration. According the analysis, the best configuration of PDCS requires $p \cong 0.7$. For all the analyzed networks, values close to 0.7 provide optimal performances.

The second proposal provides two contributions: the Killer configuration and the DCNS protocol. The Killer configuration can be applied both to Colorwave and DCNS. Its goal is to generate a selfish behavior similar to the natural selection in the network, in order to reduce the unused timeslots and to increase throughput. DCNS is a new protocol based on Colorwave, particularly suitable for the Killer configuration. Like Colorwave, it does not require deployment knowledge, and it is appropriate for low-cost RFID readers. Its main innovations are: reduced channel control overhead; a new color update mechanism; dynamic priority management; and the introduction of a dynamic reader state, which acts as a starvation countermeasure. The simulation analysis has shown that the Killer configuration applied to Colorwave strongly increases throughput. Moreover, the simulations have shown the validity of the theoretical basis of DCNS. The proposed protocol has been compared with state-of-the-art RFID reader-to-reader anti-collision ones. DCNS provides the best throughput, which is 18% higher than NFRA, the best protocol as far as throughput is concerned. Furthermore, the priority management analysis has shown that selected readers can reach even higher throughput, when it is required by the application.

The third proposal studies the effects of the introduction of the probabilistic parameter p in the collision resolution routine of Colorwave. A new version of the protocol, called PCW, has been proposed. Benefits can be achieved both in throughput and in fairness. Two different configuration of Colorwave have been studied. The first one, which was proposed in [11], reaches a good fairness. The second one is the killer configuration and privileges the network throughput, evetually to the detriment of fairness. PCW generally achieves a higher fairness than Colorwave: lower the value of p is, higher the gain is. The only exception regards networks where the average size of the neighborhood is lower than 10: if PCW is adopted in conjunction with the configuration proposed in [11], it achieves a higher throughput than Colorwave, but a lower fairness. Together with the fairness gain, a throughput improvement is achieved by PCW in conjunction with the killer configuration if the average number of neighbor in the networks is equal to or higher than 10.

Chapter 5 investigates two solutions to the reader-to-reader interference problem that exploit an additional control channel in order to improve their performance.

The first proposal, based on NFRA and called NFRA++, guarantees high throughput and similar opportunities to query tags to all the readers in a network. Among the existing protocols, NFRA achieves the highest network throughput. It suitably manages mobile networks, while performance of other protocols, like DCS, Colorwave and Pulse, decreases. However NFRA intrinsically advantages readers with fewer neighbors, as they have lower probability to collide. This causes low fairness, i.e., significant differences in throughput among readers. The proposed NFRA++ ensures good fairness by means of the mechanism of priority. The highest priority is assigned to readers that have not identified their tags from the longer time. The correlation between priority and waiting time increases the probability of querying tags for readers with many neighbors. A throughput improvement is obtained recognizing collisions, detected at the beginning of the round, that are no longer valid when a reader becomes inactive. The removal of out-of-date constraints grants more readers the right to query tags. The new proposal has been compared to NFRA and to state-of-the-art protocols, by analyzing throughput and fairness. The analysis has shown that the priority management makes the performance of the readers uniform, increasing the fairness of the network, and providing a throughput similar or better than NFRA, both in static and dynamic configurations.

The second proposal is a mechanism based on NFRA and called GDRA.It minimizes the interference in dense reader environments, providing higher throughput than the state-of-the-art proposals. GDRA is compatible with European standards and regulations and does not require extra hardware in readers. Besides, GDRA implements the *Sift* geometric probability distribution function as the mechanism to select a slot in a contention frame. The *Sift* distribution provides, in those scenarios where the number of neighbors per reader is not known, a quasi optimal distribution probability that minimizes collision probability between contending readers, maximizing the probability that a single reader takes a slot, and increasing the throughput. Different scenarios have been evaluated. The results show that GDRA outperforms single-channel proposals, like Colorwave, DCS or NFRA, as well as multi-channel proposals, as PDCS and Listen Before Talk. This holds even for those harsh environments where the percentage of neighboring readers is close to 100%.

Bibliography

[1] A. Sen and M. Huson, "A new model for scheduling packet radio networks," *Wireless Networks*, vol. 3, pp. 71–82, 1997.

[2] B. N. Clark, C. J. Colbourn, and D. S. Johnson, "Unit disk graphs," *Discrete Mathematics*, vol. 86, no. 1-3, pp. 165–177, Dec. 1990.

[3] J. Kim, J. Lim, and K. Chae, "Energy-efficient code dissemination using minimal virtual backbone in sensor networks," in *International Conference on Broadband, Wireless Computing, Communication and Applications (BWCCA)*, Nov. 2010, pp. 149 –154.

[4] R. Ferrero and F. Gandino, "Degree distribution of unit disk graphs with uniformly deployed nodes on a rectangular surface," in *6th International Conference on Broadband and Wireless Computing, Communication and Applications*, Oct. 2011, pp. 255–262.

[5] A. Papapostolou and H. Chaouchi, "RFID-assisted indoor localization and the impact of interference on its performance," *Journal of Network and Computer Applications*, vol. 34, no. 3, pp. 902–913, 2011.

[6] W. Yoon and N. H. Vaidya, "RFID reader collision problem: performance analysis and medium access," *Wireless Communications and Mobile Computing*, 2010.

[7] J. Choi and C. Lee, "An MILP-based cross-layer optimization for a multi-reader arbitration in the UHF RFID system," *Sensors*, vol. 11, no. 3, pp. 2347–2368, 2011.

[8] L. Zhang, R. Ferrero, F. Gandino, and M. Rebaudengo, "A comparison between single and additive contribution in RFID reader-to-reader interference models," in *The Sixth International Conference on Innovative Mobile and Internet Services in Ubiquitous Computing (IMIS)*, July 2012.

[9] "ETSI EN 302 208-1 v1.4.1," Nov. 2011. [Online]. Available: www.etsi.org

[10] J. Waldrop, D. Engels, and S. Sarma, "Colorwave: an anticollision algorithm for the reader collision problem," in *IEEE International Conference on Communications*, vol. 2, May 2003, pp. 1206–1210.

[11] ——, "Colorwave: a MAC for RFID reader networks," in *IEEE Wireless Communications and Networking*, vol. 3, March 2003, pp. 1701–1704.

[12] J.-B. Eom, S.-B. Yim, and T.-J. Lee, "An efficient reader anticollision algorithm in dense RFID networks with mobile RFID readers," *IEEE Trans. Ind. Electron.*, vol. 56, no. 7, pp. 2326–2336, July 2009.

[13] F. Gandino, R. Ferrero, B. Montrucchio, and M. Rebaudengo, "Introducing probability in RFID reader-to-reader anti-collision," in *8th IEEE International Symposium on Network Computing and Applications*, July 2009, pp. 250–257.

[14] ——, "Probabilistic DCS: An RFID reader-to-reader anti-collision protocol," *Journal of Network and Computer Applications*, vol. 34, no. 3, pp. 821–832, 2011.

[15] ——, "Increasing throughput in RFID multi-reader environments avoiding reader-to-reader collisions," in *IEEE International Conference on Consumer Electronics (ICCE)*, Jan. 2011, pp. 37–38.

[16] R. Ferrero, F. Gandino, B. Montrucchio, and M. Rebaudengo, "Fair anticollision protocol in dense RFID networks," in *Third International EURASIP Workshop on RFID Technology*, Sept. 2010, pp. 101–105.

[17] ——, "A fair and high throughput reader-to-reader anticollision protocol in dense RFID networks," *IEEE Trans. Ind. Informat.*, 2012.

[18] EPCGlobal, "EPC radio-frequency identity protocols Class-1 Generation-2 UHF RFID," Oct. 2008.

[19] Y. Tay, K. Jamienson, and H. Balakrishnan, "Collision-minimizing CSMA and its applications to wireless sensor networks," *IEEE Journal on Selected Areas in Communications*, vol. 22(6), pp. 1048–1057, 2004.

[20] T. Arampatzis, J. Lygeros, and S. Manesis, "A survey of applications of wireless sensors and wireless sensor networks," in *Mediterrean Conference on Control and Automation*, June 2005, pp. 719–724.

[21] I. F. Akyildiz, X. Wang, and W. Wang, "Wireless mesh networks: a survey," *Computer Networks*, vol. 47, no. 4, pp. 445–487, March 2005.

[22] M. Burkhart, P. von Rickenbach, R. Wattenhofer, and A. Zollinger, "Does topology control reduce interference?" in *Proceedings of the 5th ACM international symposium on Mobile ad hoc networking and computing*, ser. MobiHoc '04. New York, NY, USA: ACM, 2004, pp. 9–19.

[23] M. Fussen, R. Wattenhofer, and A. Zollinger, "Interference arises at the receiver," in *International Conference on Wireless Networks, Communications and Mobile Computing*, vol. 1, June 2005, pp. 427–432.

[24] P. von Rickenbach, S. Schmid, R. Wattenhofer, and A. Zollinger, "A robust interference model for wireless ad-hoc networks," in *Proceedings of the 19th IEEE International Parallel and Distributed Processing Symposium*, April 2005.

[25] I. Kanj, A. Wiese, and F. Zhang, "Local algorithms for edge colorings in UDGs," in *Graph-Theoretic Concepts in Computer Science*, ser. Lecture Notes in Computer Science. Springer Berlin / Heidelberg, 2010, vol. 5911, pp. 202–213.

[26] A. Grf, M. Stumpf, and G. Weienfels, "On coloring unit disk graphs," *Algorithmica*, vol. 20, pp. 277–293, 1998.

[27] T. Moscibroda and R. Wattenhofer, "Coloring unstructured radio networks," *Distributed Computing*, vol. 21, pp. 271–284, 2008.

[28] T. Moscibroda, P. von Rickenbach, and R. Wattenhofer, "Analyzing the energy-latency trade-off during the deployment of sensor networks," in *Proceedings of the 25th IEEE International Conference on Computer Communications (INFOCOM)*, April 2006, pp. 1–13.

[29] T. Nieberg, J. Hurink, and W. Kern, "A robust PTAS for maximum weight independent sets in unit disk graphs," in *Graph-Theoretic Concepts in Computer Science*, ser. Lecture Notes in Computer Science. Springer Berlin / Heidelberg, 2005, vol. 3353, pp. 214–221.

[30] J. Aspnes, D. Goldenberg, and Y. R. Yang, "On the computational complexity of sensor network localization," in *Algorithmic Aspects of Wireless Sensor Networks*, ser. Lecture Notes in Computer Science. Springer Berlin / Heidelberg, 2004, vol. 3121, pp. 32–44.

[31] F. Kuhn, R. Wattenhofer, and A. Zollinger, "Worst-case optimal and average-case efficient geometric ad-hoc routing," in *Proceedings of the 4th ACM international symposium on Mobile ad hoc networking & computing*, ser. MobiHoc '03. New York, NY, USA: ACM, 2003, pp. 267–278.

[32] K. M. Alzoubi, P.-J. Wan, and O. Frieder, "Message-optimal connected dominating sets in mobile ad hoc networks," in *Proceedings of the 3rd ACM international symposium on Mobile ad hoc networking & computing*, ser. MobiHoc '02. New York, NY, USA: ACM, 2002, pp. 157–164.

[33] C. Bettstetter, "On the minimum node degree and connectivity of a wireless multihop network," in *Proceedings of the 3rd ACM international symposium on Mobile ad hoc networking & computing*, ser. MobiHoc '02. New York, NY, USA: ACM, 2002, pp. 80–91.

[34] R. Hekmat and P. Van Mieghem, "Degree distribution and hopcount in wireless ad-hoc networks," in *11th IEEE International Conference on Networks (ICON)*, Sept. 2003, pp. 603–609.

[35] L. Guo, K. Harfoush, and H. Xu, "Distribution of the node degree in manets," in *4th International Conference on Next Generation Mobile Applications, Services and Technologies (NGMAST)*, July 2010, pp. 162–167.

[36] L.-H. Yen and C. W. Yu, "Link probability, network coverage, and related properties of wireless ad hoc networks," in *IEEE International Conference on Mobile Ad-hoc and Sensor Systems*, Oct. 2004, pp. 525–527.

[37] K. Li, "Topological characteristics of random multihop wireless networks," in *23rd International Conference on Distributed Computing Systems Workshops*, May 2003, pp. 685–690.

[38] S. Kullback and R. Leibler, "On information and sufficiency," *Annals of Mathematical Statistics*, vol. 22, no. 1, p. 7986, June 1951.

[39] R. Tesoriero, J. Gallud, M. Lozano, and V. Penichet, "A location-aware system using RFID and mobile devices for art museums," in *4th International Conference on Autonomic and Autonomous Systems (ICAS)*, March 2008, pp. 76–81.

[40] S. Nishiyama, H. Fukuoka, M. Ohashi, and H. Murakami, "Combining RFID tag reader with mobile phone: An approach to realize everyone's ubiquitous appliances," in *International Symposium on Intelligent Signal Processing and Communications (ISPACS)*, Dec. 2006, pp. 87 –90.

[41] R. Xue, L. Wang, and J. Chen, "Using the IOT to construct ubiquitous learning environment," in *2nd International Conference on Mechanic Automation and Control Engineering (MACE)*, July 2011, pp. 7878–7880.

[42] P.-Y. Chen, W.-T. Chen, Y.-C. Tseng, and C.-F. Huang, "Providing group tour guide by RFIDs and wireless sensor networks," *IEEE Trans. Wireless Commun.*, vol. 8, no. 6, pp. 3059–3067, June 2009.

[43] P. Bernardi, C. Demartini, F. Gandino, B. Montrucchio, M. Rebaudengo, and E. Sanchez, "Agri-food traceability management using a RFID system with privacy protection," in *21st International Conference on Advanced Information Networking and Applications (AINA)*, May 2007, pp. 68–75.

[44] F. Gandino, E. Sanchez, B. Montrucchio, and M. Rebaudengo, "Opportunity and constraints for wide adoption of RFID in agri-food," *International Journal of Advanced Pervasive and Ubiquitous Computing*, vol. 1, no. 2, pp. 49–67, July 2009.

[45] F. Gandino, B. Montrucchio, M. Rebaudengo, and E. Sanchez, "On improving automation by integrating RFID in the traceability management of the agri-food sector," *IEEE Trans. Ind. Electron.*, vol. 56, no. 7, pp. 2357–2365, July 2009.

[46] ——, "Analysis of an RFID-based information system for tracking and tracing in an agri-food chain," in *RFID Eurasia, 1st Annual*, Sept. 2007, pp. 1–6.

[47] F. Gandino, E. Sanchez, B. Montrucchio, and M. Rebaudengo, "Rfid technology for agri-food trafficability management," in *Auto-identification and Ubiquitous Computing Applications: Rfid and Smart Technologies for Information Convergence*, J. A. S. D. P. J. Ayoade, Ed. Information Science Publishing, 2009, pp. 54–73.

[48] ——, "New perspectives on adoption of RFID technology for agrifood traceability," *Emerging Pervasive and Ubiquitous Aspects of Information Systems: Cross-Disciplinary Advancements*, pp. 112–131, 2011.

[49] R. Martí, S. Robles, A. Martín-Campillo, and J. Cucurull, "Providing early resource allocation during emergencies: The mobile triage tag," *Journal of Network and Computer Applications*, vol. 32, pp. 1167–1182, Nov. 2009.

[Online]. Available: http://dl.acm.org/citation.cfm?id=1598089.1598476

[50] W. Yao, C.-H. Chu, and Z. Li, "Leveraging complex event processing for smart hospitals using RFID," *Journal of Network and Computer Applications*, vol. 34, no. 3, pp. 799–810, 2011.

[51] P. Najera, J. Lopez, and R. Roman, "Real-time location and inpatient care systems based on passive RFID," *Journal of Network and Computer Applications*, vol. 34, no. 3, pp. 980–989, 2011.

[52] D. C. Ranasinghe, M. Harrison, K. Frmling, and D. McFarlane, "Enabling through life product-instance management: Solutions and challenges," *Journal of Network and Computer Applications*, vol. 34, no. 3, pp. 1015–1031, 2011.

[53] C. Kao and P. Hung, "A systematical approach to improve supply chain: An application of RFID technology on cargo transportation," in *IEEE International Conference on Industrial Engineering and Engineering Management*, Dec. 2009, pp. 1484–1488.

[54] X. Zhang and X. Lian, "Design of warehouse information acquisition system based on RFID," in *IEEE International Conference on Automation and Logistics*, Sept. 2008, pp. 2550–2555.

[55] J. Wang, Z. Luo, E. Wong, and C. Tan, "RFID assisted object tracking for automating manufacturing assembly lines," in *IEEE International Conference on e-Business Engineering*, Oct. 2007, pp. 48–53.

[56] G. M. Gaukler, "Item-level RFID in a retail supply chain with stock-out-based substitution," *IEEE Trans. Ind. Informat.*, vol. 7, no. 2, pp. 362–370, May 2011.

[57] C. Wang, M. Daneshmand, K. Sohraby, and B. Li, "Performance analysis of RFID Generation-2 protocol," *IEEE Trans. Wireless Commun.*, vol. 8, no. 5, pp. 2592–2601, May 2009.

[58] D.-H. Shih, P.-L. Sun, D. C. Yen, and S.-M. Huang, "Taxonomy and survey of RFID anti-collision protocols," *Computer Communications*, vol. 29, no. 11, pp. 2150–2166, 2006.

[59] N. Abramson, "The ALOHA system: another alternative for computer communications," in *Proceedings of Fall Joint Computer Conference*, 1970, pp. 281–285.

[60] M. Bueno-Delgado and J. Vales-Alonso, "On the optimal frame-length configuration on real passive RFID systems," *Journal of Network and Computer Applications*, vol. 34, no. 3, pp. 864–876, 2011.

[61] I. Onat and A. Miri, "DiSEL: A distance based slot selection protocol for framed slotted ALOHA RFID systems," in *IEEE Wireless Communications and Networking Conference*, April 2009, pp. 1–6.

[62] J. Kim, "A combined polling and random access technique for enhanced anti-collision performance in RFID systems," *IEICE Transactions on Communications*, vol. E92-B, no. 4, pp. 1357–1360, April 2009.

[63] Y.-C. Lai and C.-C. Lin, "Two blocking algorithms on adaptive binary splitting: Single and pair resolutions for RFID tag identification," *IEEE/ACM Transactions on Networking*, vol. 17, no. 3, pp. 962–975, June 2009.

[64] Y.-H. Chen, S.-J. Horng, R.-S. Run, J.-L. Lai, R.-J. Chen, W.-C. Chen, Y. Pan, and T. Takao, "A novel anti-collision algorithm in RFID systems for identifying passive tags," *IEEE Trans. Ind. Informat.*, vol. 6, no. 1, pp. 105–121, Feb. 2010.

[65] D. Engels and S. Sarma, "The reader collision problem," in *IEEE International Conference on Systems, Man and Cybernetics*, vol. 3, Oct. 2002.

[66] G. Joshi and S. Kim, "Survey, nomenclature and comparison of reader anti-collision protocols in RFID," in *IETE Tech Rev*, vol. 25, no. 5, 2008, pp. 285–292.

[67] K. Leong, M. Ng, and P. H. Cole, "The reader collision problem in RFID systems," in *Proc. of IEEE International Symposium on Microwave, Antenna, Propagation and EMC Technologies for Wireless Communications*, 2005, pp. 658–661.

[68] C. Wang, B. Li, M. Daneshmand, K. Sohraby, and R. Jana, "On object identification reliability using RFID," *Mobile Networks and Applications*, vol. 16, pp. 71–80, Feb. 2011.

[69] S. Ramanathan and E. L. Lloyd, "Scheduling algorithms for multi-hop radio networks," *SIGCOMM Comput. Commun. Rev.*, vol. 22, pp. 211–222, Oct. 1992.

[70] D.-Y. Kim, B.-J. Jang, H.-G. Yoon, J.-S. Park, and J.-G. Yook, "Effects of reader interference on the RFID interrogation range," in *37th European Microwave Conference*, Oct. 2007, pp. 728–731.

[71] D.-Y. Kim, J.-G. Yook, H.-G. Yoon, and B.-J. Jang, "Interference analysis of UHF RFID systems," *Progress In Electromagnetics Research B*, vol. 4, pp. 115–126, 2008.

[72] D.-Y. Kim, H.-G. Yoon, B.-J. Jang, and J.-G. Yook, "Effects of reader-to-reader interference on the UHF RFID interrogation range," *IEEE Trans. Ind. Electron.*, vol. 56, no. 7, pp. 2337–2346, July 2009.

[73] H. Seo and C. Lee, "A new GA-based resource allocation scheme for a reader-to-reader interference problem in RFID systems," in *IEEE International Conference on Communications (ICC)*, May 2010, pp. 1–5.

[74] K. Whitehouse, A. Woo, F. Jiang, J. Polastre, and D. Culler, "Exploiting the capture effect for collision detection and recovery," in *The Second IEEE Workshop on Embedded Networked Sensors (EmNetS-II)*, May 2005, pp. 45–52.

[75] M. Zuniga and B. Krishnamachari, "Analyzing the transitional region in low power wireless links," in *First Annual IEEE Communications Society Conference on Sensor and Ad Hoc Communications and Networks (SECON)*, Oct. 2004, pp. 517–526.

[76] M. Bueno-Delgado, J. Vales-Alonso, C. Angerer, and M. Rupp, "A comparative study of RFID schedulers in dense reader environments," in *IEEE International Conference on Industrial Technology (ICIT)*, 2010, pp. 1373–1378.

[77] S. Birari and S. Iyer, "PULSE: a MAC protocol for RFID networks," in *Embedded and Ubiquitous Computing EUC Workshops*, ser. Lecture Notes in Computer Science, 2005, vol. 3823, pp. 1036–1046.

[78] ——, "Mitigating the reader collision problem in RFID networks with mobile readers," in *13th IEEE International Conference on Networks*, vol. 1, Nov. 2005, pp. 463–468.

[79] J.-B. Eom and T.-J. Lee, "RFID reader anti-collision algorithm using a server and mobile readers based on conflict-free multiple access," in *Performance, Computing and Communications, IEEE International Conference on*, Dec. 2008, pp. 395–399.

[80] K. C. Shin, S. B. Park, and G. S. Jo, "Enhanced TDMA based anti-collision algorithm with a dynamic frame size adjustment strategy for mobile RFID readers," *Sensors*, vol. 9, no. 2, pp. 845–858, 2009.

[81] J. Ho, D. Engels, and S. Sarma, "HiQ: a hierarchical Q-learning algorithm to solve the reader collision problem," in *International Symposium on Applications and the Internet Workshops (SAINT)*, Jan. 2006, pp. 88–91.

[82] C. Galiotto, K. Cetin, S. Frattasi, N. Marchetti, N. Prasad, and R. Prasad, "High fairness reader anti-collision protocol in passive rfid systems," in *RFID, IEEE International Conference on*, April 2011, pp. 113–120.

[83] R. Jain, D.-M. Chiu, and W. Hawe, "A quantitative measure of fairness and discrimination for resource allocation in shared computer systems," *DEC Technical Report 301*, vol. cs.NI/9809099, Sept. 1984.

[84] G. Holzmann, "The model checker SPIN," *IEEE Trans. Softw. Eng.*, vol. 23, no. 5, pp. 279–295, May 1997.

[85] G. Khandelwal, A. Yener, K. Lee, and S. Serbetli, "ASAP : a MAC protocol for dense and time constrained RFID systems," in *IEEE International Conference on Communications*, June 2006, pp. 4028–4033.

[86] M. Buettner and D. Werherall, "An empirical study of UHF RFID performance," in *Proceedings of the 14th ACM international conference on Mobile computing and networking*, Sept. 2008, pp. 223–234.

[87] R. Drodi, "RFID white paper," 2005, available on line at:http://www.mtiwe.com.